2006

PETROFABRIC AND GEOCHEMICAL ANALYSIS OF THE GREAT SMOKY -- SNOWBIRD GROUP CONTACT, WESTERN BLUE RIDGE, NORTH CAROLINA AND TENNESSEE

Kristopher M. Clemons
University of Kentucky, k.clemons@utah.edu

ABSTRACT OF THESIS

PETROFABRIC AND GEOCHEMICAL ANALYSIS OF THE GREAT SMOKY – SNOWBIRD GROUP CONTACT, WESTERN BLUE RIDGE, NORTH CAROLINA AND TENNESSEE

Detailed structural and petrographic analysis of the Greenbrier Fault (GBF) reveal different fold and fabric styles and generations preserved in the Great Smoky Group (GSG) hanging wall and Snowbird Group (SG) footwall. Four planar fabrics (S_0, S_1, S_2, and S_3) are completely overprinted within meters of the contact by shear zone-related fabrics. Bedding (S_0) is defined by planar laminations in the SG siltstones. S_1 is weak, not associated with folding of S_0, and defined locally by sub-parallel alignment of biotite. S_2 (slaty cleavage) is deflected into a disjunctive planar (in GSG) or continuous planar (in SG) S_3 foliation characterized by mica formation and dynamic recrystallization of quartz. Metamorphic microstructures indicate lower greenschist to upper amphibolite facies Taconian metamorphism is syn- to post-S_2, and pre-S_3. Local lower greenschist facies retrograde metamorphism precedes S_3 formation. A meter scale, ductile mesoscopic shear zone in SG at the GSG-SG contact is characterized by S/C fabric; this is the youngest deformational event and postdates retrograde mineral assemblages indicating postmetamorphic motion along the contact. Premetamorphic fault fabrics indicative of GSG thrusting onto the SG were absent or completely reconstituted during metamorphism and deformation. The Metcalf phyllite and Pigeon siltstone were also compared to test the hypothesis that the Metcalf phyllite is tectonized Pigeon siltstone. Major and trace element abundances are similar between the lithologies, with the exception of depletion of Ca, Na and Zr in the Metcalf. The system appears to have been open with respect to these elements. It is concluded that the Metcalf phyllite is the tectonized equivalent of the Pigeon siltstone based on lateral continuity, the strong macroscopic and microscopic resemblance of weakly deformed Metcalf to the Pigeon, similar mean values and ranges in major, minor, and trace elements, and identical rock densities.

KEYWORDS: Great Smoky Mountains, Greenbrier Fault, Metamorphism, Structure, Tectonics

Kristopher M. Clemons
August 16, 2006

PETROFABRIC AND GEOCHEMICAL ANALYSIS OF THE GREAT SMOKY – SNOWBIRD GROUP CONTACT, WESTERN BLUE RIDGE, NORTH CAROLINA AND TENNESSEE

By

Kristopher M. Clemons

David P. Moecher
Director of Thesis

Susan Rimmer
Director of Graduate Studies

August 16, 2006

THESIS

Kristopher M. Clemons

The Graduate School

University of Kentucky

2006

PETROFABRIC AND GEOCHEMICAL ANALYSIS OF THE GREAT SMOKY – SNOWBIRD GROUP CONTACT, WESTERN BLUE RIDGE, NORTH CAROLINA AND TENNESSEE

THESIS

A thesis submitted in partial fulfillment of the
Requirements for the degree of Master of Science in the
College of Arts and Sciences
at the University of Kentucky

By

Kristopher M. Clemons

Lexington, Kentucky

Director: David P. Moecher, Associate Professor of Geology

Lexington, Kentucky

2006

MASTER'S THESIS RELEASE

I authorize the University of Kentucky
Libraries to reproduce this thesis in
whole or in part for purposes of research.

Kristopher M. Clemons
August 16, 2006

ACKNOWLEDGMENTS

First and foremost, I would like to thank my Thesis Advisor, Prof. David P. Moecher, who believed in me and who has challenged and inspired me to become a better scientist. I owe him a huge debt of gratitude providing me a great opportunity to learn and develop my analytical skills while working on a truly challenging and enjoyable project.

I would also like to thank my Thesis Committee members, Prof. Kieran O'Hara, who kept me on my toes by questioning my interpretations, offered new points of view, and who provided assistance in interpreting microstructures and isochon analysis and Prof. Michael Handke, whose office I visited often for advice and instruction.

In addition, I would like to thank my loving wife Amy without whose support and encouragement, none of this would have been possible, Jeremy Burns and Mary Ann Hollingshead for their outstanding field assistance, David and Helen Brumfield, Danny and Anna Lee Albertson, Dan and Melissa Hillis, Sarabeth Burns, Tom Compton, Jason Heck, and my family for their support and encouragement. Last but not least, Phoebe and Gretchen for the comic relief.

TABLE OF CONTENTS

LIST OF TABLES

LIST OF FIGURES

Chapter 1

The Blue Ridge province of the southern Appalachian Mountains is a composite orogen formed by multiple collisional events that progressed westward toward Laurentia during the Paleozoic (Hatcher 1981, 1987, 1989, 2000, 2001). Metamorphism and deformation affecting the Laurentian basement and metasedimentary cover assemblages began in the late Cambrian Penebscot collisional event and continued through the Pennsylvanian-Permian Alleghanian event. (Adams et al., 1995; Drake et al., 1989; Goldberg et al., 1989; Hatcher 1981, 1987, 1989; Rast and Kohles, 1986).

The Great Smoky Mountains region of the Western Blue Ridge province is dominated by a series of thrust sheets comprised of predominantly thick-bedded metasandstones, interbedded metasiltstones, slates, and phyllites, each sheet having varying tectonic histories. These lithologies are assigned to the Ocoee Supergroup, subdivided into the Chilhowee (CG), Walden Creek (WCG), Great Smoky (GSG), and Snowbird (SG) Groups. (Hadley and Golsdmith, 1963; King, 1964; Hatcher, 1978, 1987).

The nature of the contact between the Great Smoky group (GSG) and Snowbird (SG) group has long posed a problem for interpretation of the tectonic evolution of the southern Appalachian Western Blue Ridge province. The contact has been interpreted as a premetamorphic fault with more than 20 km of lateral displacement (Hadley and Goldsmith 1963), a premetamorphic fault with an unspecified amount of displacement (Montes and Hatcher, 1999), or a faulted contact (Southworth et al. 2006). Folding and faulting were interpreted to precede high-grade Taconian regional metamorphism and folding and post-metamorphic (Acadian or Alleghanian) deformation obscures possible interpretations. Further complication is caused by uncertainty in stratigraphic relationships between units along the contact. One such relationship is between the Metcalf phyllite and Pigeon siltstone. The Metcalf has been proposed to be the tectonized equivalent of the Pigeon siltstone (King, 1964; Neuman and Nelson, 1965). Hadley and Goldsmith (1963) and King (1964) recognized that the Metcalf phyllite (pCm) shared lithologic characteristics with the Pigeon Siltstone (pCp). King (1964) suggested that the rocks were most likely equivalent, despite the fact the Metcalf is foliated, folded, and penetratively sheared over most of its extent. Primary sedimentary structures have been obliterated over most of the exposed area of the Metcalf phyllite.

King's preliminary chemical analyses of the Metcalf Phyllite and Pigeon Siltstone are geochemically similar, and the two units were differentiated based primarily on the greater degree of deformation of the Metcalf phyllite (King, 1964) (Appendix II, Table 1 King geochemistry). Shearing is the proposed mechanism for deformation and recrystallization of mineral assemblages within the Pigeon siltstone to form the Metcalf phyllite (King, 1964). The equivalency of the two is further suggested by their spatial distribution along strike.

Structural and petrofabric analysis along the GSG/ SG contact provide first order constraints on the deformation history and models for assembly of the present architecture of the Great Smoky Mountain region. The contact ranges from gently to isoclinally folded. Foliations are defined macroscopically by a variety of schistosities in the GSG and SG. Samples collected along and across the contact reveal a complex polydeformational history and several generations of both static and dynamic metamorphism, foliation formation, and phyllonitization of SG that strongly overprint regional metamorphic assemblages and foliations. The purpose of this study is two fold:

1. To examine GSG/SG units along the contact from lower greenschist facies to upper amphibolite facies, documenting fabrics and relationships between the two groups by employing petrologic, petrofabric and field relationships to test the hypothesis that the Greenbrier fault is a premetamorphic fault. This is the subject of Chapter 1.
2. Test the hypothesis that the Metcalf phyllite is the deformed equivalent of the Pigeon siltstone by employing geochemical, petrologic, petrofabric and field relationships to demonstrate that the two units can be correlated and are the same original sedimentary deposit. This is the subject of Chapter 2.

The chapters are written for the intent of ultimately being published as separate journal articles.

Chapter 2
Kinematic and Petrofabric Analysis of the Greenbrier Discontinuity, Great Smoky Mountains, North Carolina and Tennessee.

2.1 Introduction

The southern Appalachian Mountains are a composite orogen produced by episodic collisional events that progressed westward toward Laurentia during the Paleozoic (Hatcher 1981, 1987, 1989, 2000, 2001). Metamorphic and deformational processes affecting the Laurentian basement and metasedimentary assemblages began in the late Cambrian Penebscot collisional event and continued through the middle Ordovician Taconian Orogeny, late Devonian/early Missippian Acadian orogeny, and the Pennsylvanian-Permian Alleghanian event (Adams et al., 1995; Drake et al., 1989; Goldberg et al., 1989; Hatcher 1981, 1987, 1989; Rast and Kohles, 1986).

The Great Smoky Mountains region of the Blue Ridge province, one of the more inboard provinces in the southern Appalachians, is dominated by a series of thrust sheets comprised of predominantly thick-bedded metasandstones with interbedded metasiltstones, slates and phyllites, each sheet having varying tectonic histories. These lithologies are assigned to the Ocoee Supergroup, which is further subdivided into the Chilhowee (CG), Walden Creek (WCG), Great Smoky (GSG), and Snowbird (SG) Groups. (Hadley and Golsdmith, 1963; Hatcher, 1978, 1987; King, 1964). The Greenbrier fault (GBF) separates the Neoproterozoic Great Smoky Group and Snowbird Group (King, 1964; Hadley and Goldsmith 1963). The Greenbrier fault is proposed to be a premetamorphic, multiply-deformed fault formed during the Taconian orogeny (King, et al, 1958; Hadley and Goldsmith, 1963). The initial folding of GSG/SG and thrusting of GSG upon SG faulting occurred prior to peak Taconian metamorphism (King, et al, 1958; Hadley and Goldsmith, 1963). Subsequent Acadian and/or Alleghanian deformation complicates the current interpretation that the contact between these two distinct lithologic groups is a fault.

Timing of metamorphism in the Western Blue Ridge is still the subject of much debate, but recent studies indicate a Barrovian progression developed in GSG in the

Taconian (~460 Ma: Moecher et al., 2005). The ^{40}Ar-^{39}Ar ages (360-380 Ma) of Connelly and Dallmeyer (1993) most likely represent closure ages for Ar diffusion in muscovite during cooling from peak kyanite grade metamorphic temperatures (not the time of *attainment* of peak thermal conditions: Connelly and Dallmeyer, 1993), consistent with Taconian tectonometamorphism, and not Acadian or Alleghanian.

Despite the fact that the GBF has been widely accepted as a major tectonic boundary in the Western Blue Ridge there are many questions pertaining to specific events such as the relative ages of deformation and formation of petrofabrics and mineral assemblages along this contact. Based on the inherent problems of: (1) limited exposure; (2) steep and remote terrain; (3) uncertainties in Ocoee stratigraphy; (4) the changing metamorphic character and deformational styles of the contact between the GSG/SG along its length; and (5) lack of widespread fault rocks, a contemporary re-examination of the characteristics of this contact is warranted. The purpose of this study is to examine GSG and SG units along the contact from lower greenschist facies to upper amphibolite facies documenting fabrics and relationships between the two groups. The study will employ petrologic, petrofabric, structural and field relationships to characterize the contact separating the Great Smoky and Snowbird groups in order to test whether the GBF is a premetamorphic fault.

2.2 Geologic Setting

The Blue Ridge Province is a regional anticlinorium associated with large scale, west directed thrust faulting. The basement complex in the Great Smoky Mountain/ Western Blue Ridge terrane (Figure 2.1– Regional geologic map) consists of Mesoproterozoic (Grenville) gneisses, meta-granitic rocks, amphibolites and Paleozoic gneisses and schists. Overlying the basement is a series of unfossiliferous, clastic-metasediments comprising the Ocoee Supergroup. Ocoee rocks were subjected to Paleozoic metamorphism ranging from greenschist facies in the western Great Smoky Mountain region to upper amphibolite facies in the eastern Great Smoky Mountain region (Hadley and Goldsmith, 1963; Moecher et al., 2005). The Ocoee is subdivided into three major units: the Snowbird, the Great Smoky, and the Walden Creek Groups, with total thickness of approximately 12 km (Hadley and Goldsmith, 1963). The Snowbird Group

(SG) is characterized by fine- to medium-grained feldspar- and quartz-rich metasiltstone, metasandstone, slate, and phyllite. The thickness of the Snowbird Group decreases to the south and east (Hadley and Goldsmith, 1963; Montes and Hatcher, 1999). The Great Smoky Group (GSG) includes meta-conglomerate, meta-arkose, feldspathic meta-sandstones, and shale (now slate) interbeds. The highest stratigraphic members are characterized by graphitic slates, phyllites, and schists. To the south of the Great Smoky Mountains the GSG was originally interpreted by Hadley and Goldsmith (1963) to lie unconformably on the basement. More recently this has been interpreted as a fault contact (Southworth et al. 2005). The Walden Creek Group (WCG) is interpreted to be the youngest group in the Ocoee Supergroup (Hadley and Goldsmith, 1963; Southworth et al. 2005). The WCG consists of meta-quartzite, slate, dolomitic marble, and meta-conglomerate. The WCG is exposed as an isolated thrust sheet and may be (at least partially) equivalent to the Great Smoky Group (Hadley and Goldsmith, 1963; King, 1964; Southworth et al., 2005). To the southwest of the Great Smoky Mountains, the GSG is conformably overlain by the Murphy Belt in a synclinal structure and may be correlative to the Cambrian Chilhowee Group in the foothills belt (Figure 2.2). The rocks of the Great Smoky Mountains experienced multiple deformational events and consequently display a complex range of folds, faults, and metamorphic fabrics. Basement complex unit structural features have been obscured by later deformation to the point that little about their origin and nature is known other than they are of Grenville affinity (Hadley and Goldsmith, 1963). Deformation and metamorphism in the Ocoee series reached peak intensity in the Ordovician (Moecher at al. 2005), during which, an early period of folding was followed by low angle faulting (GBF?), and then by continued folding and peak regional metamorphism. Peak deformation and metamorphism were followed by successive periods of northwest vergent Paleozoic faulting and folding (Hadley and Goldsmith, 1963; King, 1964; Southworth et al., 2005; Moeche et al., 2005). This polydeformational history manifests itself on the surface as large anticline/syncline pairs and faults with smaller scale folds, various cleavages, foliations, lineations, and joints with a wide and complexly overlapping distribution. Major structural elements consist of ENE trending folds and reverse faults in the Valley and Ridge, and low angle thrust faults which moved basement and Ocoee units

northwestward over other Ocoee units (Hadley and Goldsmith, 1963; King, 1964), and a series of overprinting younger folds and thrust faults (e.g. Gatlinburg fault, Dunn Creek Fault, and the Miller Cove fault).

2.3 Previous Work

The Greenbrier fault is traditionally interpreted as the contact between the Snowbird and Great Smoky groups in the Great Smoky Mountains. The contact is inferred from structure sections to truncate map scale folds in the overlying Great Smoky Group hanging wall, and over wider areas (~ 20 km) is inferred to cut off as much as 7 km of both Great Smoky Group and Snowbird Group sequences in the footwall (Hadley and Goldsmith, 1963; Southworth et al., 2005). The contact was originally interpreted to be tectonic and not a stratigraphic contact (King et. al., 1958). Unlike the Great Smoky

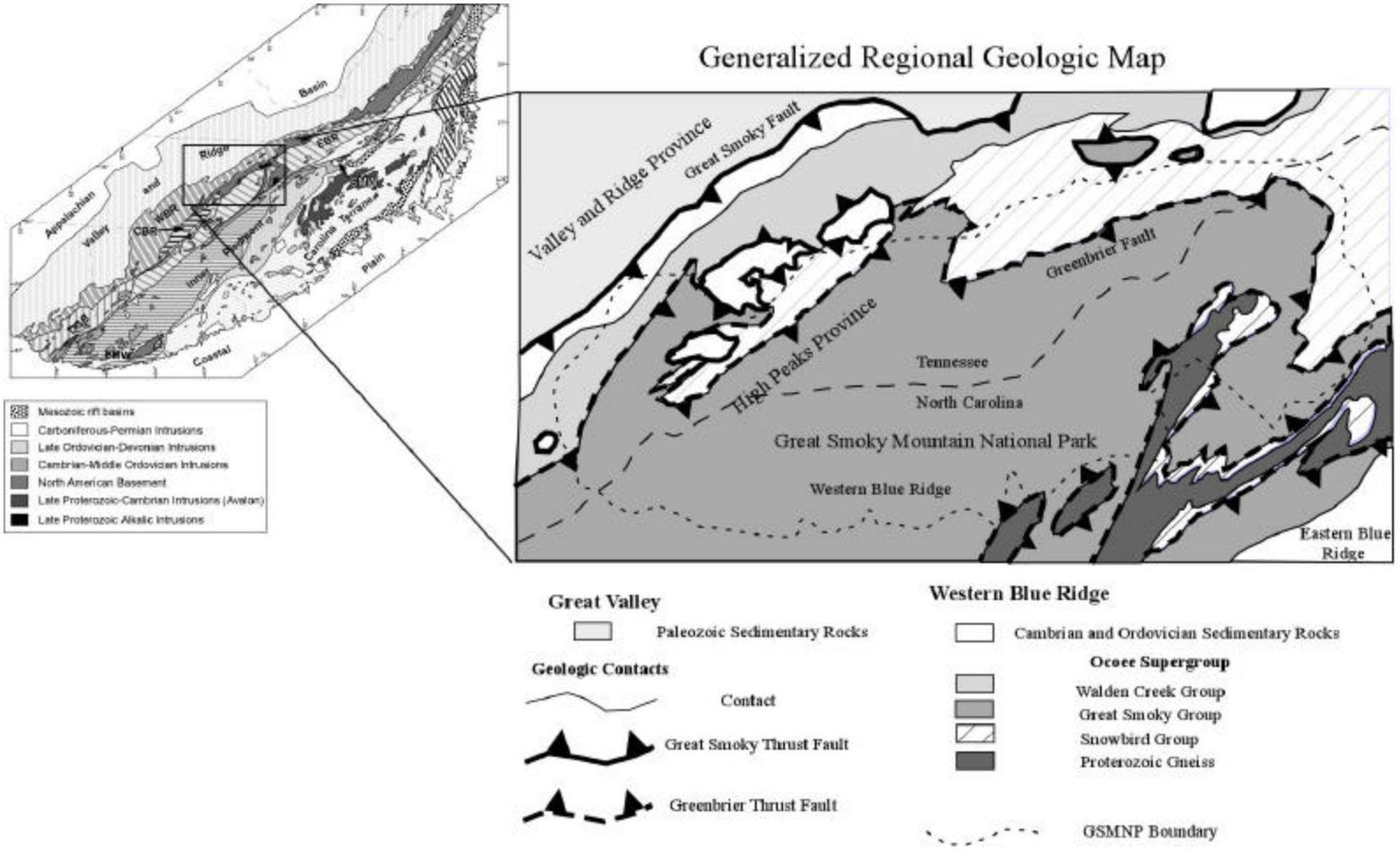

Figure 2.1 - Regional geologic map.

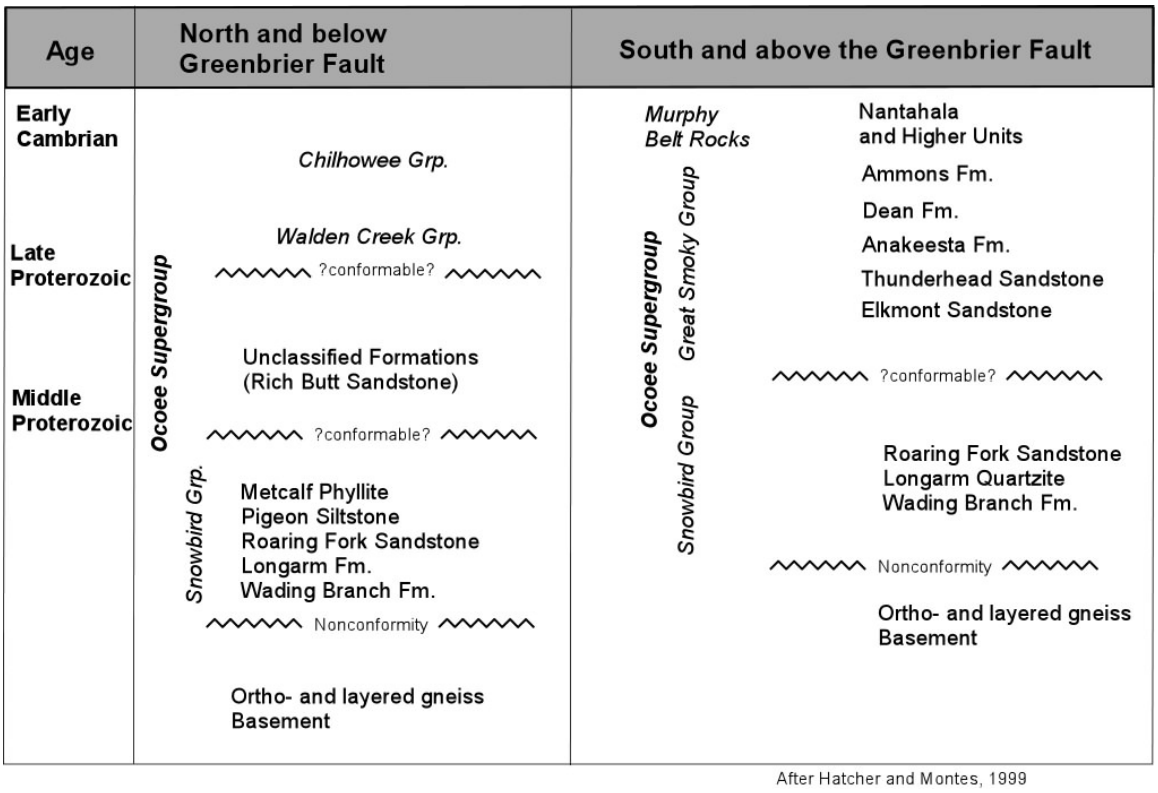

Figure 2.2 - Ocoee Supergroup Stratigraphy. Questionable conformable relations may also be faults.

fault, the actual surface on which the Greenbrier fault has moved is rarely (if ever) exposed, presumably because the GBF is a much older feature and has experienced one or two additional phases of deformation than younger structures such as the Alleghanian Great Smoky fault. The early mappers further inferred that the fault was premetamorphic because the regional metamorphic isograds and cleavages trend northeastward across it without any offset (Hadley and Goldsmith, 1963). However, this lack of offset would be the case for a lithologic contact as well. King hypothesized that the GBF is probably the oldest major structural feature in the Great Smoky Mountains. Faulting was distinct from the development of the post-Mississippian (Alleghanian) Great Smoky fault and related features, but it has not been determined whether all these events were part of a single orogeny, or whether some of them, including emplacement of the Greenbrier fault, took place during an earlier orogeny (Taconian). The Greenbrier fault was inferred to have developed early in Taconic history and to precede folding of strata in the hanging wall and footwall (Hadley and Goldsmith 1963). The fault was first documented and named on the north slope of the Greenbrier Pinnacle in Great Smoky Mountain National Park. The GBF is interpreted to cut through the large northeastward trending Alum Cave syncline of the Great Smoky Group, truncating the higher stratigraphic units in the hinge and the lower units in the limbs (Hadley and Goldsmith, 1963). The current interpretation was shaped by field work and mapping in the 1950's and 1960's and presumes the structure is a fault that extends along the north slope of the Great Smoky Mountain front in the eastern, central and western parts of the range. In the east, the fault's trace curves southward (Figure 2.3). On the southeast side of the structure, the fault slices through the Great Smoky, Snowbird, and basement lithologies. The southeast side is interpreted to be the overriding block.

The Greenbrier Fault is an easily traceable contact, defined by an abrupt lithologic contrast between the Snowbird Group, which is a fine-grained metasiltstone in its upper sections and thick, massive beds of feldspathic sandstone and conglomerate of the Great Smoky Group. The contrast between the GSG and SG lithologies is emphasized where tight folding and staurolite–kyanite grade metamorphism has affected the GSG and SBG in the Cove Creek Region. In this area a fault is unrecognizable due to tight isoclinal folding and kyanite grade metamorphism.

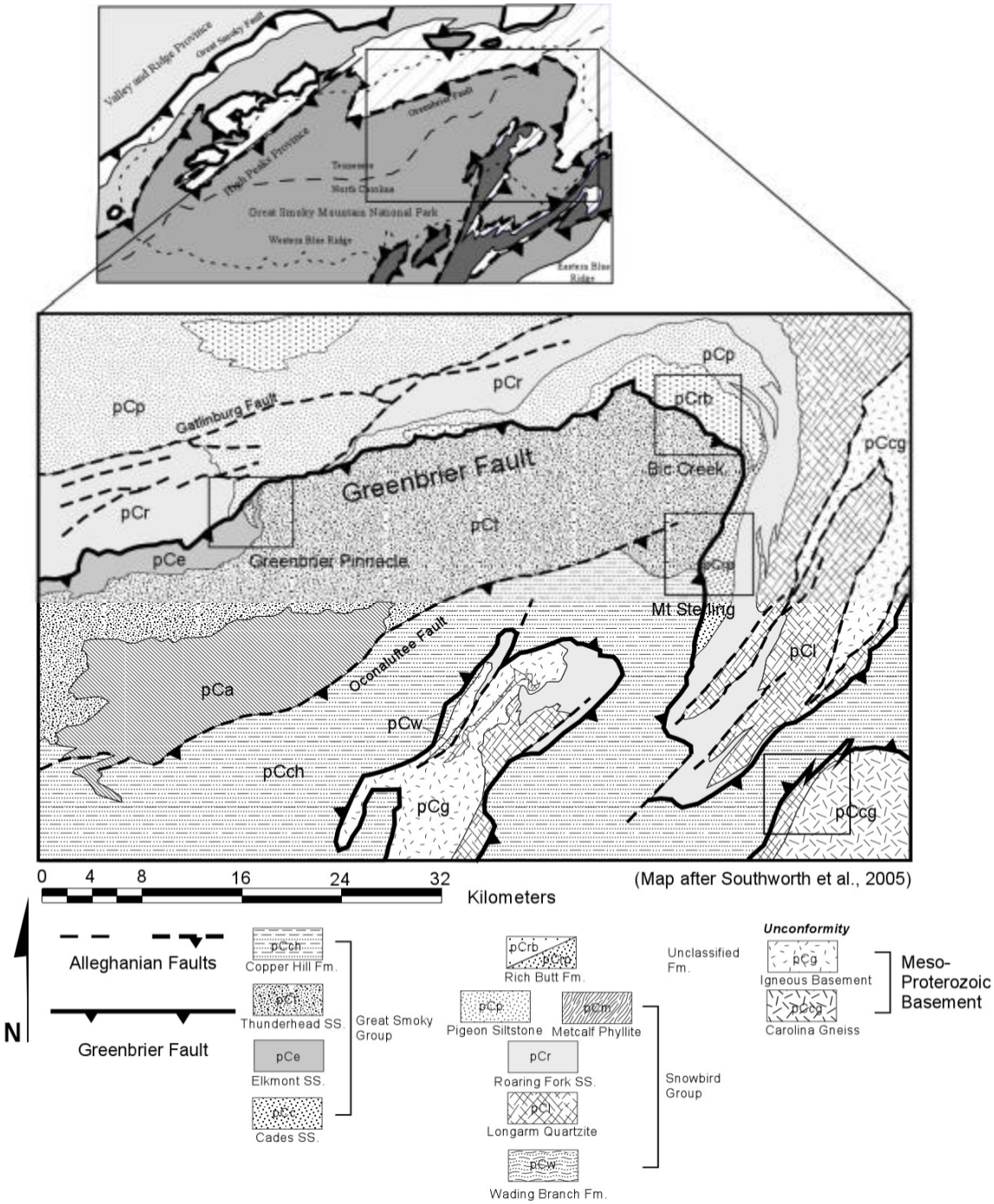

Figure 2.3 – Location of Study Area. Sample localities 1) Greenbrier Pinnacle, 2) Big Creek, 3) Mount Sterling, and 4) Cove Creek.

2.4 Outstanding Questions and Problems

The accepted interpretation of stratigraphic relationships (Hadley and Goldsmith, 1963) has inherent problems because stratigraphy is not continuous anywhere in the Great Smoky Mountains area and almost all contacts are faults. Because of this the key interpretations that the GF is an (A) 'premetamorphic' (pre-Taconian), (B) thrust fault that (C) places the younger GSG over older Snowbird Group in an unconventional thrust relationship produce questions or potential problems that may be investigated in detail with modern concepts of structural and petrologic analysis that geologists were not cognizant of in the 1950's and 1960's. Questions arise from examination of the geologic maps from the Central and Eastern Great Smoky Mountains (U.S.G.S. Professional Papers, 349B [Hadley and Goldsmith, 1963] and 349C [King, 1964]) and cross sections: Figure 1.4). The contact truncates folds in bedding (S_0) in the footwall (Pigeon and Roaring Fork Fm.) and folds in the hanging wall (Elkmont and Thunderhead Fms.). If the fault is premetamorphic, it implies the following:

1. Displacement along the fault involved transport of lithified sedimentary rocks (assuming the Ocoee is late Proterozoic in age and was lithified by early Paleozoic time); preservation of soft sediment deformation structures throughout the Snowbird group supports this inference.
2. Tectonic transport of the amount inferred by Hadley and Goldsmith (23 km) during faulting should have produced brittle or ductile fault structures and/or fabrics in hanging wall and footwall rocks. Possible structures and fabrics include cataclasite, gouge, breccia, and mylonites that would have overprinted, to varying degrees, the original sedimentary structures, textures, and detrital clasts.

Metamorphic grade is lowest in the type area of the Greenbrier fault (compared to more deeply exposed areas to the east and south), so overprinting would be weakest there and fault related features should be best preserved at this locality. Examination of rocks along the GSG/SG contact near the type locality is the most favorable area for examining this potential relationship (Area 1, Figure 2.3). The cross- sections of Hadley and

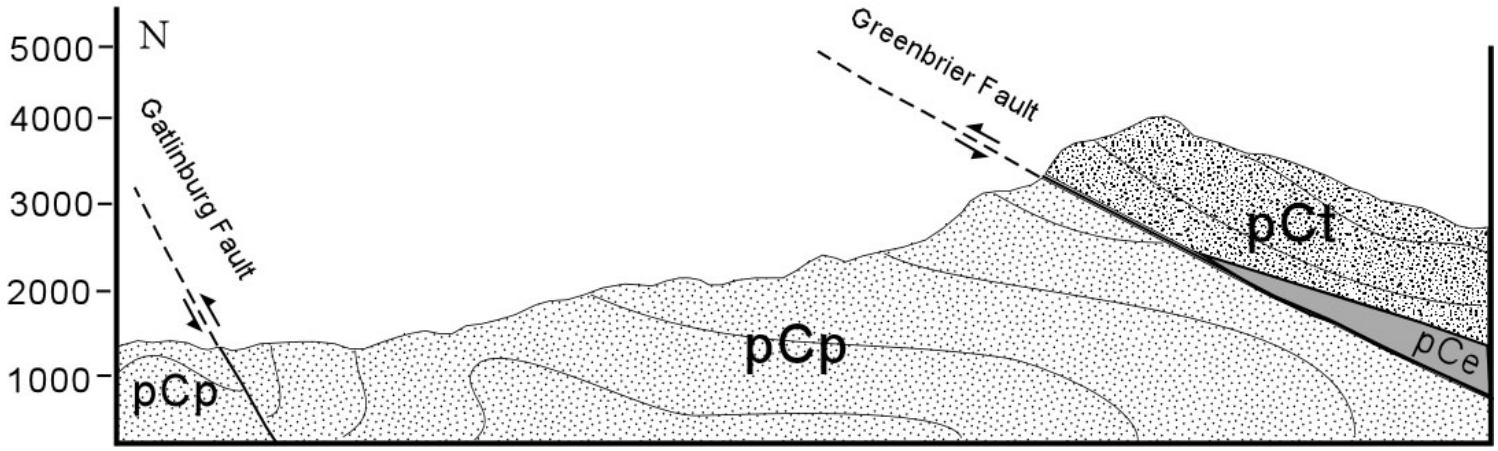

Figure 2.4 – Cross section across Greenbrier Pinnacle showing map scale F_1 folds inferred at map scale. S_0 orientations (solid lines). (after Hadley and Goldsmith, 1964).

Goldsmith (1963) and King (1964) (e.g. Figure 2.4) imply the Greenbrier fault post-dates folding. The Greenbrier fault also places Great Smoky Group on top of Walden Creek Group rocks north of Gatlinburg. This is a true thrust relationship, if the inferred Ocoee stratigraphy is correct. Here again, however, the same problems arise regarding timing of metamorphism relative to thrusting as it does for the GBF in the type locality on the north slope of Greenbrier Pinnacle. Also, through most of the extent of the GBF, the younger Great Smoky group (GSG) is thrust over older Snowbird group (SBG) and related formations. This is a non-traditional thrust relationship. Did the initial fracture, at least in the forward part of the structure, developed along the stratigraphic contact between the two groups (King, 1964, p. 121)? This is possible due to the competency differences between the two groups. The thick, massive, quartz-rich Great Smoky Group strata are highly competent, and the thin-bedded, micaceous Snowbird Group less competent. In the southeastern part of the Great Smoky Mountains the Greenbrier fault is interpreted to descend into basement rocks (Hadley and Goldsmith, 1963) (Figure 2.3).

The idea that a thrust fault can place a package of younger rocks over older by the GBF is problematic when attempting to use stratigraphy to understand the contact. The usual criteria which would indicate the displacement of a low angle fault are not applicable, and the amount of its displacement is uncertain. An estimate of 23 km (Hadley and Goldsmith, 1963) of displacement has been made on the basis of differences in stratigraphy and thickness of the SG above and below the fault in the eastern Great Smoky Mountains (Hadley and Goldsmith, 1963), but the actual displacement may be less or greater. Relative displacement between originally adjacent rocks above and below the fault may vary considerably from place to place. King (1964) states "*As younger rocks are thrust over older on the GBF, many of the usual criteria which would indicate the displacement is uncertain…*" (p. 121). In many areas "*the relationship (of hanging wall and footwall units) is deceptive because beds above and below the fault are nearly parallel*" (Hadley and Goldsmith, 1963, p B79), implying there is no stratigraphic evidence for a fault relationship. Truncations of both the units above and below the fault vary considerably and this relationship is only apparent over wider areas (Hadley and Goldsmith, 1963; King, 1964). The base of the overriding GSG rocks is truncated to a greater extent, especially toward the northwest along the front of the Great Smoky

Mountains. Based on the interpretation that the folding of the SG preceded faulting, emplacement of the Greenbrier thrust sheet occurred by forward movement of the upper plate (GSG) and by shortening of the lower plate (SG) by folding, and faulting, either immediately before or during the time when it was overridden (Hadley and Goldsmith, 1963, King, 1964). *"Relative displacement along the fault may vary considerably throughout its trace…* (p.B79)" (Hadley and Goldsmith, 1963). The 23 km displacement may be greatly overestimated.

The fault has also been mapped on top of Rich Butt Sandstone (pCrb) (Figure 1.3), a lithology which was interpreted to be a vertical transitional unit between the GSG and SG and was not assigned to either group by Hadley and Goldsmith (1963) or King (1964). Recently the pCrb has been assigned to the SG by Southworth et al. (2005). *"The boundary between the Rich Butt sandstone and the underlying (SG) is gradational and indefinitely located in most places…* (p.B49) (Hadley and Goldsmith, 1963). *"The (pCrb) seems to have been deposited on the (SG) without important interruption, but accessory minerals, type of bedding, and intraformational arkosic conglomerates indicate a closer affinity to the (GSG) …. and suggests a vertical transition between (SG) and (GSG)* (p.B49)" (Hadley and Goldsmith, 1963). If the pCrb is a transitional unit that separates GSG and SG, relative displacement of the fault is not known, and is accepted to vary greatly across its trace, it would seem to imply a conformable lithologic relationship between the GSG and SG, and not a fault.

2.5 Data Collection and Methods

Data collection and analysis were two fold; the field-oriented aspect consisted of outcrop descriptions and orientation measurements of structural elements along and across the fault zone. This entailed measuring foliations and lineations, outcrop description and the collection of oriented and unoriented samples. Laboratory analysis consisted of petrographic examination and analysis of samples from rock units across and along the GSG/ SG contact. Petrographic examinations were made of microstructures, especially quartz and feldspar relationships, fabrics, and shear sense asymmetry in the oriented samples. These samples were prepared in the department's rock prep lab and thin sections will be prepared by the University of Oregon. Documentation of the

relationship of metamorphic index minerals to matrix fabrics permits determination of pre, syn, or post-metamorphic deformation. Macro-, meso-, and microscopic structural analysis of the Snowbird- Great Smoky Mountain boundary, in this study, was based primarily on detailed field mapping along the contact at the Greenbrier fault's type locality on Greenbrier Pinnacle (biotite grade), and at three other localities of successively increasing metamorphic grade. Measurement and description of structural and fabric elements focused on resolving and comparing the evolution of folding, faulting, and the development of planar and linear features across the boundary. Ninety-four oriented hand samples from sixty-two different data localities (see figures in following sections) were collected for subsequent oriented thin-section analysis concentrating on development and relative timing of petrofabrics.

2.6 Results

Fabric Relationships at Greenbrier Pinnacle

A detailed field map (Figure 2.5) of the Greenbrier Cove study area shows bedding (S_0) (Figure 2.6) with a predominant NE strike (Figure 2.7, and 2.8). Weakly foliated Pigeon siltstone from localities ~5 km northwest of the contact were used as a frame of reference in describing S_0/ F_1, M_1/ S_1, and M_2/S_2 relationships (Figures 3.5). Bedding (S_0) in the argillaceous SG units is defined by laminated planar beds that alternate in color from dark to light. The lighter-colored, more feldspathic and quartzose layers are typically thicker (0.1-0.8 cm) and coarser-grained than the darker layers (0.05-0.5 cm) which were presumably more argillaceous and are now chlorite- and muscovite-rich. S_0 and its orientations are visible on the macroscopic and mesoscopic scale (Figure 1.6). S_0 in the GSG is characterized by medium- to coarse-grained feldspathic metasandstone with interbedded metaconglomerate (Figure 1.6). Bedding in GSG is not well developed and defined by undulating bedding plane partings (Figure 2.6). S_0 can be seen in a variety of orientations in the Greenbrier Cove area, ranging from horizontal to vertical (Figure 2.6 and 2.7).

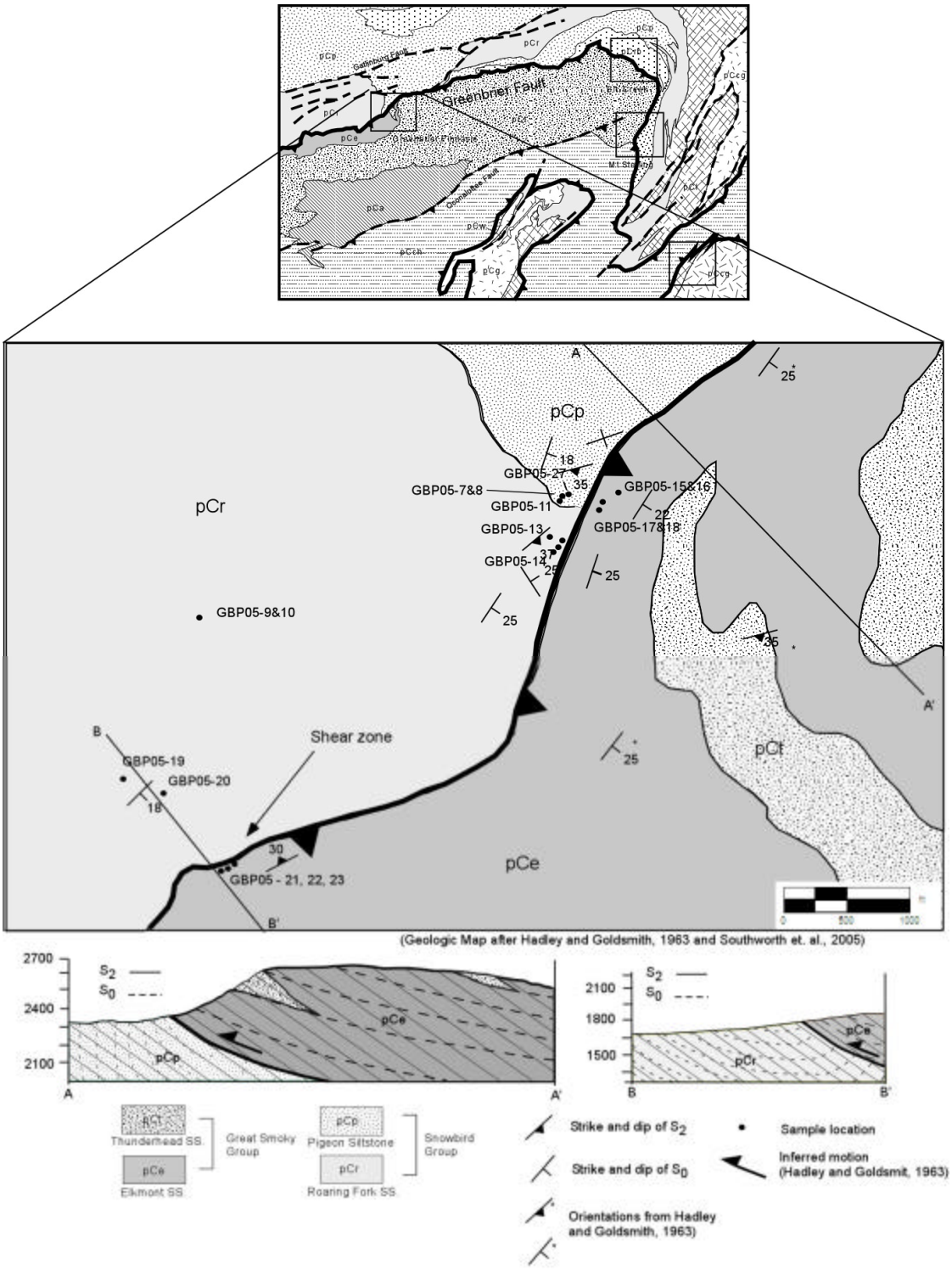

Figure 2.5 – Greenbrier Pinnacle area geologic and sample location map.

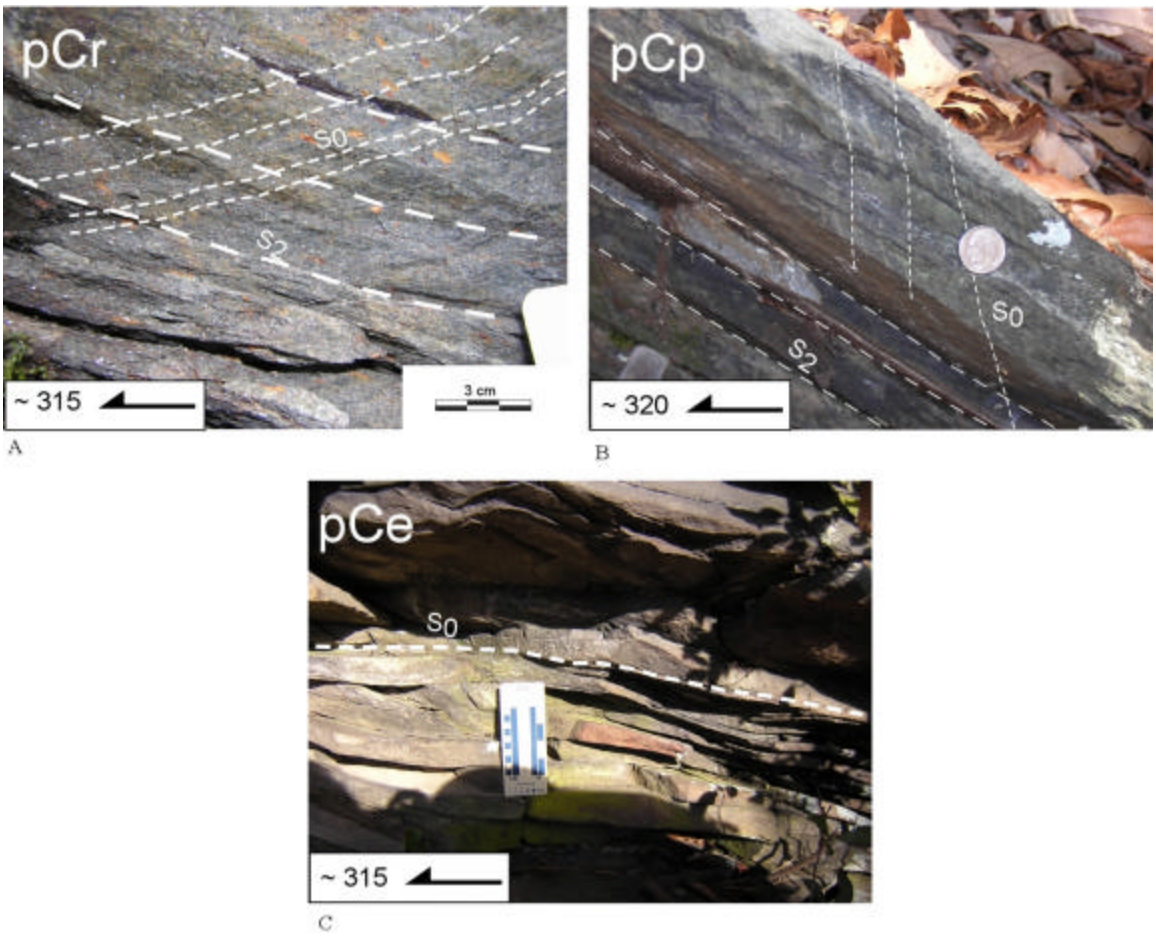

Figure 2.6 - Outcrop photos displaying bedding orientations (folding styles inferred from map) and their relationship to the S_2 cleavage in (A) Roaring Fork sandstone - tight to isoclinal folds, (B) Pigeon siltstone – tight to isoclinal folds, and (C) GSG hanging wall Elkmont sandstone - open folds. S_2 is easily seen in outcrop in footwall units and not identifiable in coarse-grained hanging wall units.

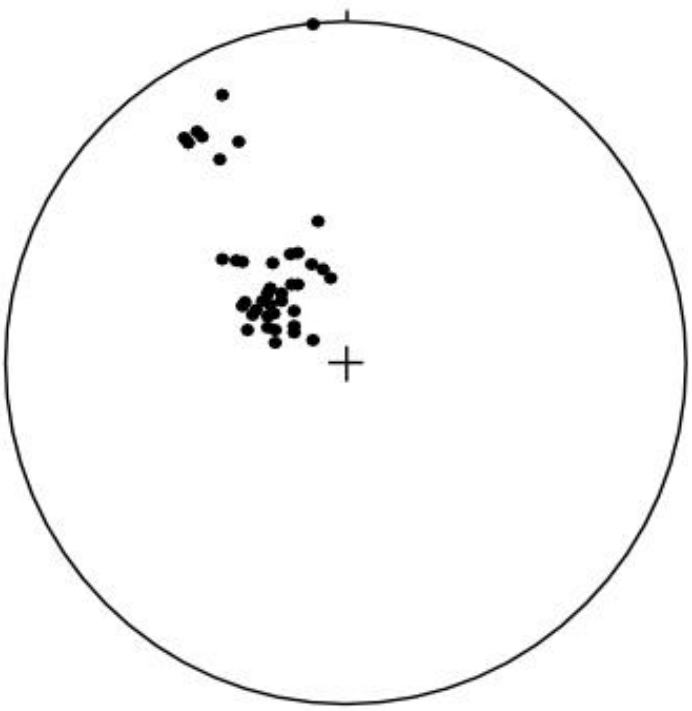

Figure 2.7 - Equal area net of poles to bedding (S_0) throughout the Greenbrier Pinnacle study area (area 1).

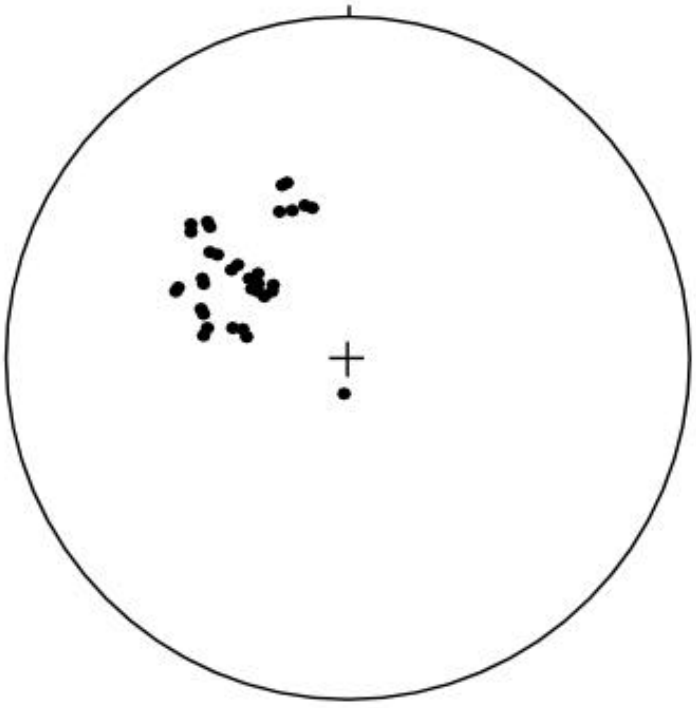

Figure 2.8 - Equal area net of poles to S_2 throughout the Greenbrier Pinnacle study area (area 1).

An axial plane foliation related to map scale folds throughout the study area (S_1) is weak to non-existent and is characterized by M_1 biotite with a weak preferred orientation and occurring at oblique angles to S_0. Microstructures associated with peak metamorphic (M_1/S_1) biotite are weakly or rarely associated with a preferred fabric (Figure 2.9).

S_2 (parallelism of chlorite and muscovite) is the dominant cleavage/foliation and is defined mesoscopically by spaced fractures and appears at varying angles to bedding (S_0) but with a similar strike, most notably in the SG. Muscovite and chlorite are preferentially oriented parallel to the axial planes of regional F_2 folds and define the continuous (SG) (Figure 2.10) and disjunctive (GSG) cleavage (S_2) (Figure – 2.11). S_2 is more strongly developed in the fine-grained to argillaceous SG footwall units and weakly in the coarse-grained to conglomeratic GSG hanging wall units. S_2 is characterized by dynamic recrystallization of quartz, formation of retrograde (M_2) chlorite, and mica fish. S_2 is manifested as a continuous cleavage in the fine grained- argillaceous (SG) and a disjunctive cleavage in the massive quartzo-feldspathic GSG. Post-metamorphic F_2 regional folds are inferred from the orientation of S_2.

A non-penetrative shear band cleavage (slip-cleavage of Hadley and Goldsmith 1963) makes up a third fabric (S_3). S_3 is always steep and characterized by deflection of micas and recrystallized quartz along spaced shear bands (Figure 2.12).

A late ductile shear zone developed at the SG-GSG contact (presumably the "Greenbrier fault") seems to be unrelated to the prevailing regional trends and overprints, obscures and/or obliterate earlier folding, cleavage formation and peak metamorphic regional foliation. This ductile shear zone, observed 0.5 km southwest of Greenbrier Pinnacle (Figure 2.13), clearly overprints both peak and retrograde mineral assemblages. A ductile S/C fabric (Figure 2.14, 2.15, and 2.16) associated with the mesoscopic shear zone is the youngest fabric and postdates both prograde and retrograde metamorphic assemblages indicating post metamorphic motion along the boundary. Samples from this outcrop-scale shear zone southwest of Greenbrier Pinnacle reveal phyllonitic SG displaying ductile S/C microstructures that overprint regional metamorphic assemblages and foliations. The phyllonitic fabric obliterates bedding (S_0) and overprints early foliations (S_1 and S_2), and obliterates the disjunctive shear band cleavage (S_3).

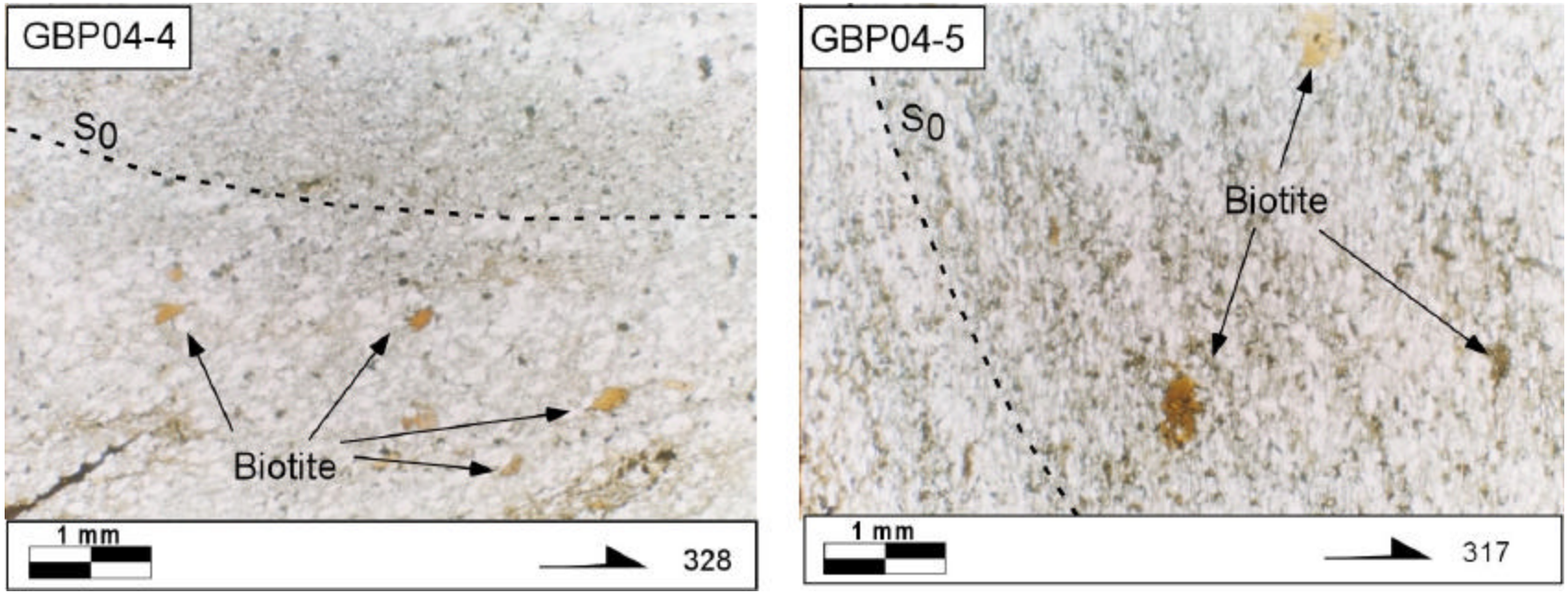

Figure 2.9 – M_1/S_1 biotite in SG Roaring Fork sandstone. M_1 biotite displaying a weak preferential alignment of long axes. Orientation indicated at the bottom is the strike of the vertical thin-section. Plane polars.

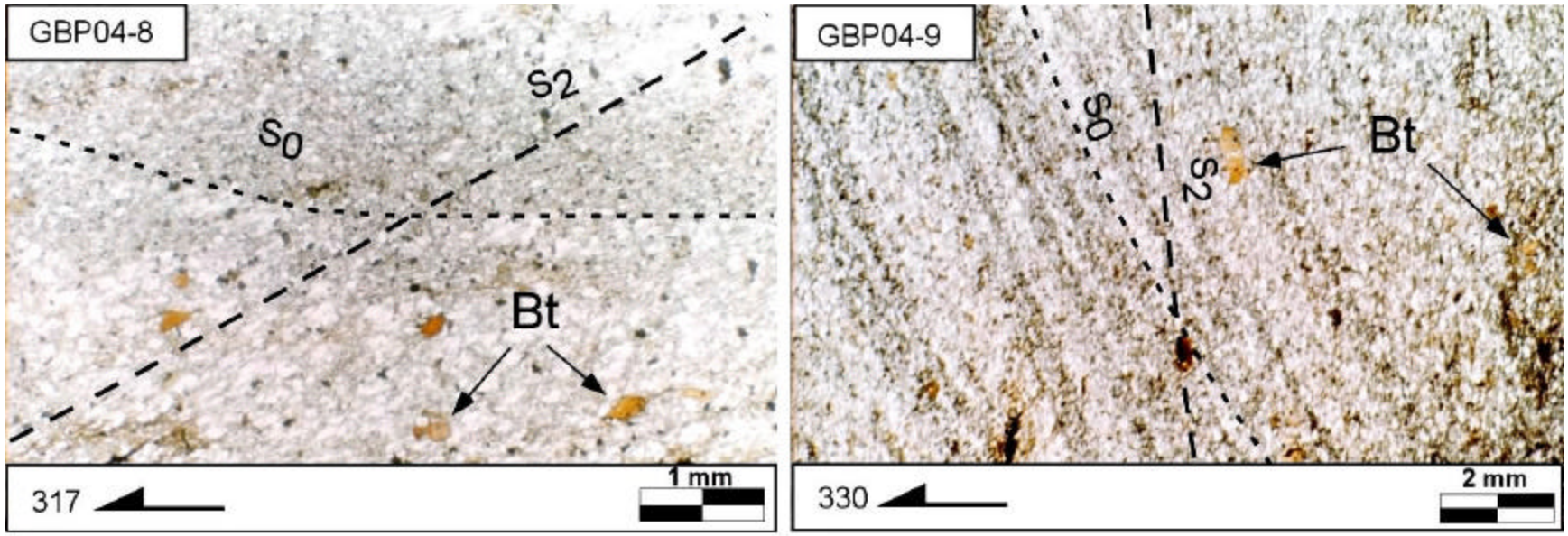

Figure 2.10 – A) and B) Pigeon siltstone (SG) displaying the relationship between folded S_0 and S_2 continuous cleavage. Orientation indicated at the bottom is the strike of the vertical thin-section. Plane light.

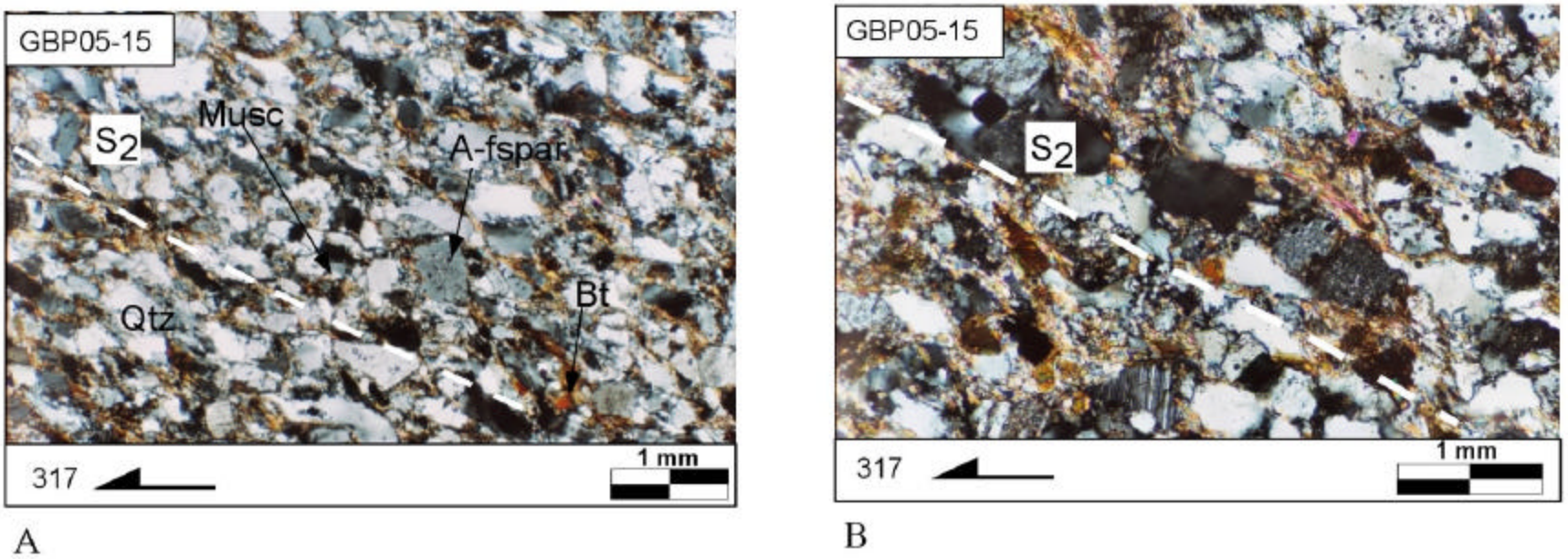

Figure 2.11 A) and B) Elkmont sandstone (GSG) displaying weak disjunctive S_2. Orientation indicated at the bottom is the strike of the vertical thin-section. Crossed polars.

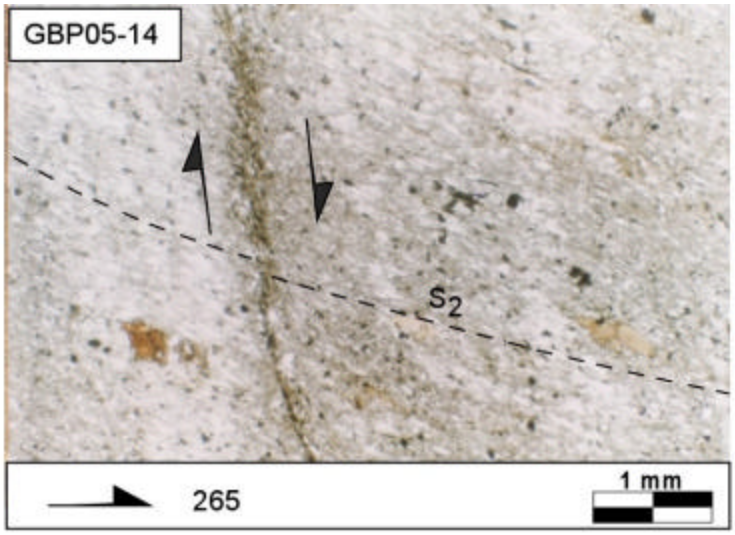

A

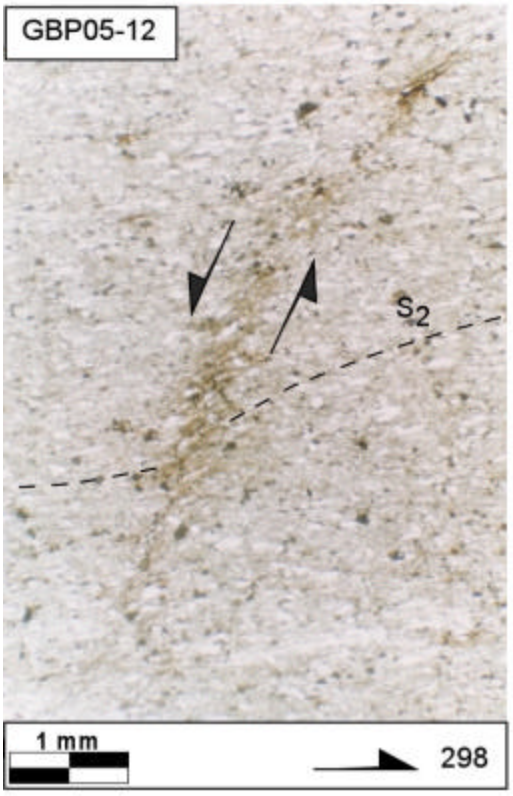

B

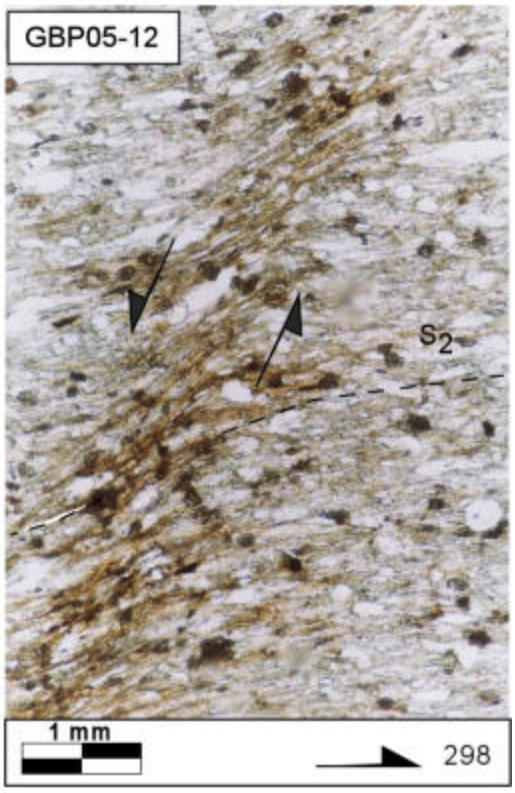

C

Figure 2.12 – A), B) and C) examples of S_3 shear band cleavage in pCp (SG) and its relationship to S_0 and S_2. Shear band cleavage in these samples exhibits A) dextral shear (top to the SW) and B) and C) sinistral shear, top to the SE. Orientation indicated at the bottom is the strike of the vertical thin-section. Plane light

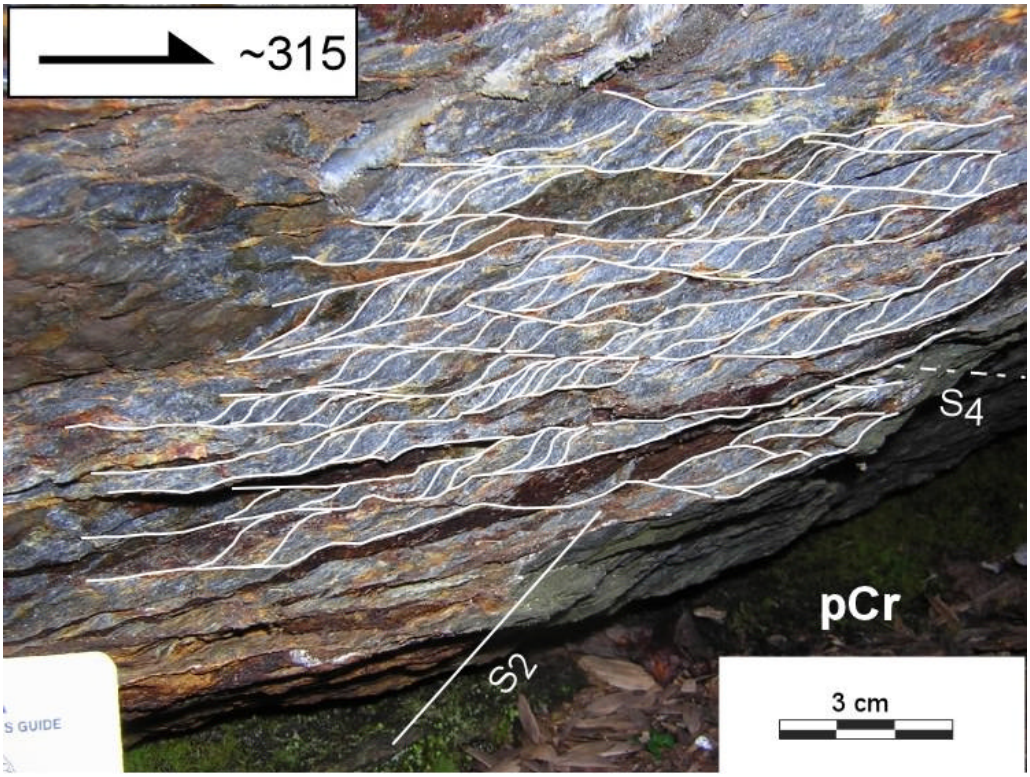

Figure 2.13 - Outcrop photo displaying shearing in Roaring Fork (SG footwall). S_2 has been deflected into parallelism with S_4.

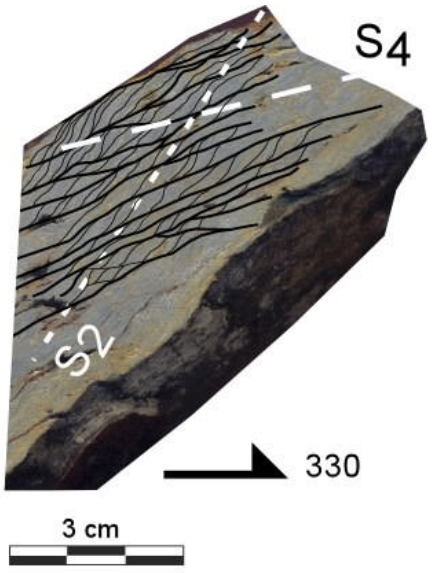

Figure 2.14 - Hand sample from Greenbrier Cove shear zone displaying the relationship between S_2 and S_4.

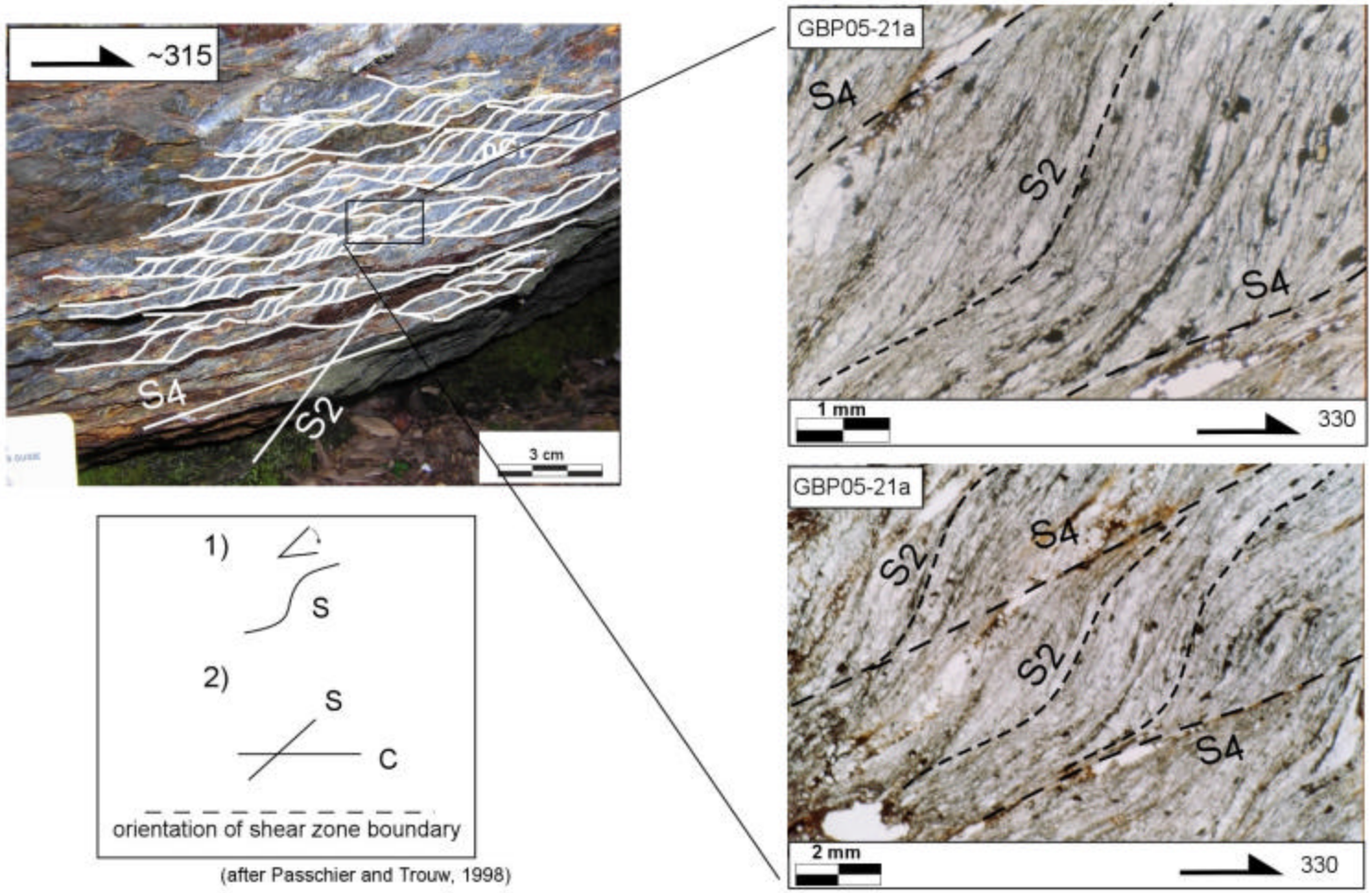

Figure 2.15 – Sheared pCr (SG) displaying S/C fabric. Mica preferred orientation (S_2) is transected by sub parallel shear zones. S_2 is deflected into parallelism with S_4. Shear sense is dextral; top to the NW. Orientation indicated at the bottom is the strike of the vertical thin-section. Plain light.

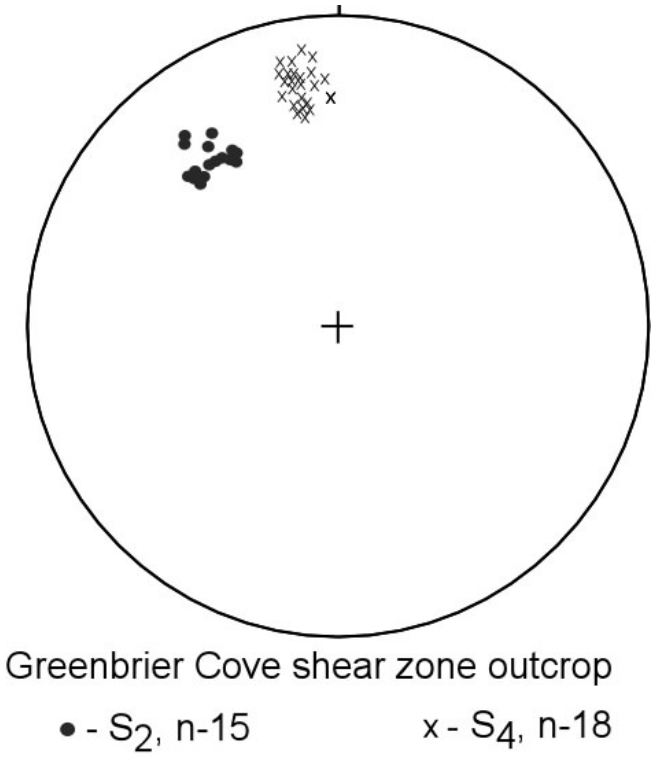

Figure 2.16 - Equal area net of poles to cleavage (S_2) and S/C (S_4) fabric at the shear zone southwest of Greenbrier Pinnacle (area 1).

Shear zone SG microstructures include S/C fabric, boudinage and dynamic recrystallization of vein quartz, and mica fish. Sense of shear based on asymmetry of these microstructures indicate reverse, top to the northwest motion (Figure – 2.15).

Great Smoky group (pCe and pCt) characteristics near the shear zone at Greenbrier Pinnacle include a weak foliation defined by parallelism of biotite, muscovite, and chlorite (Figure -2.11). These lithologies consist largely of fine- to medium- grained, variably recrystallized quartz, with lobate grain boundaries and undulose extinction, and medium- to coarse-grained feldspar (mostly plagioclase, some alkali-feldspar) porphyroclasts.

Fabric Relationships at Big Creek

A detailed field map shows the east end of the study area near Big Creek (Area 2, Figure 2.17). The SG in this area is comprised of Rich Butt sandstone (metasiltstone in this locality), a unit whose character appears to be one of transition between Snowbird and Great Smoky Groups and is conformable with both the Snowbird Group and Great Smoky Group (Hadley and Goldsmith, 1963; Southworth et al., 2005). Because the Rich Butt contains characteristics of both the SG/GSG, its appearance in this locality contradicts the interpretation of the contact in this area as a premetamorphic fault.

Bedding (S_0) in the SG at Big Creek is characterized by alternating quartzo-feldspathic and argillaceous layers. S_0 in the argillaceous SG units is defined by planar laminae that alternate in color from dark to light beds. Bedding (S_0) is visible on the macroscopic and mesoscopic scale in the SG, ranges from horizontal to vertical, and can be seen in a variety of orientations in the Big Creek area.(Figure 2.18, 2.19, 2.21, and 2.22). S_0 in the GSG is characterized by medium- to coarse-grained feldspathic metasandstone, angular rip-up clasts of dark gray argillite (Figure – 2.20), and quartz pebble conglomerate lenses. Orientation of GSG bedding is weak or not apparent in macroscopic or mesoscopic scale.

The contact at this locality has been folded and forms the nose of a plunging-regional scale syncline (Figure-2.3) and metamorphic isograds (Bt to Grt) cross the

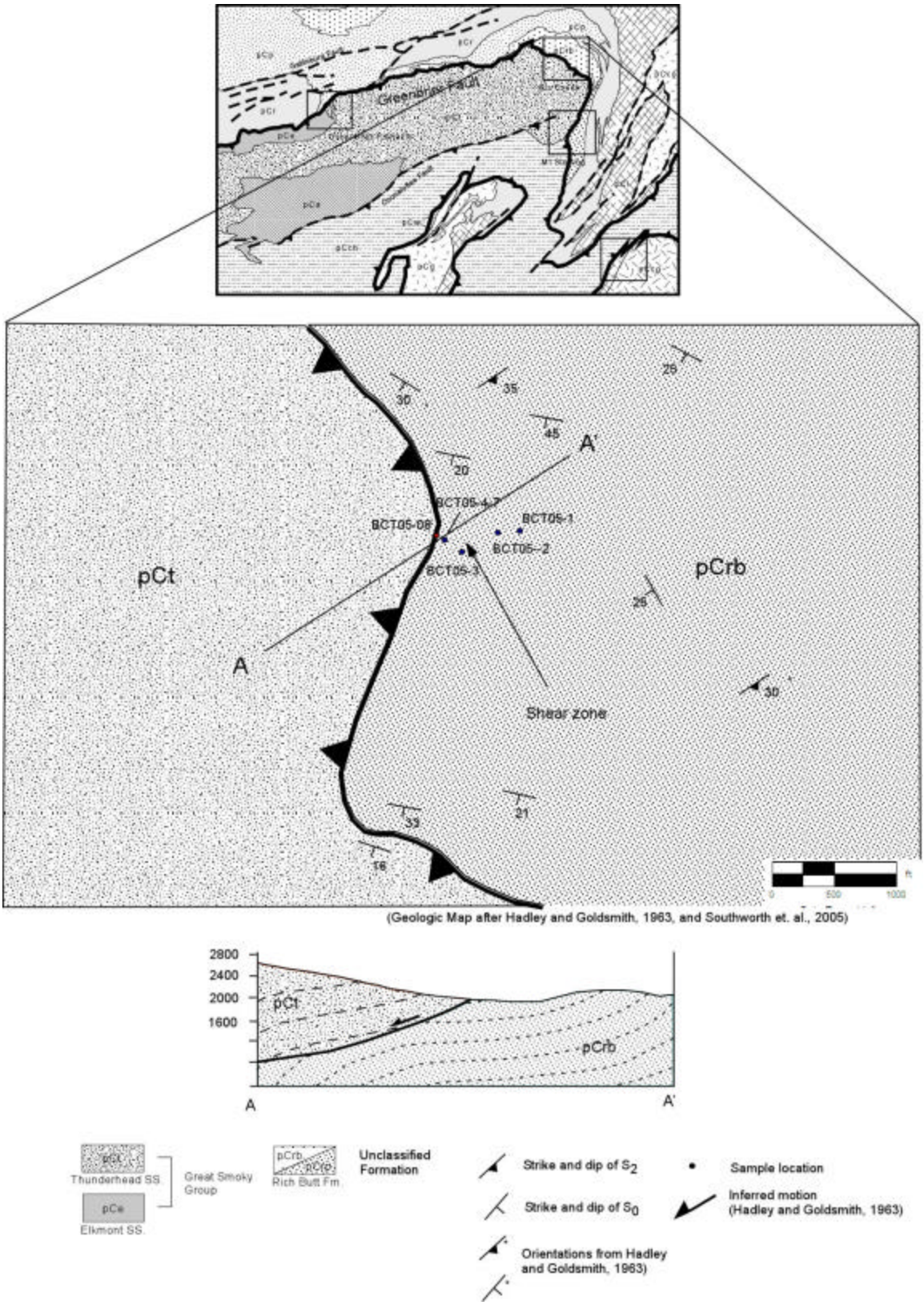

Figure 2.17 Big Creek area geologic and sample map. Thrust motion inferred from the traditional interpretation of the GBF by Hadley and Goldsmith (1963).

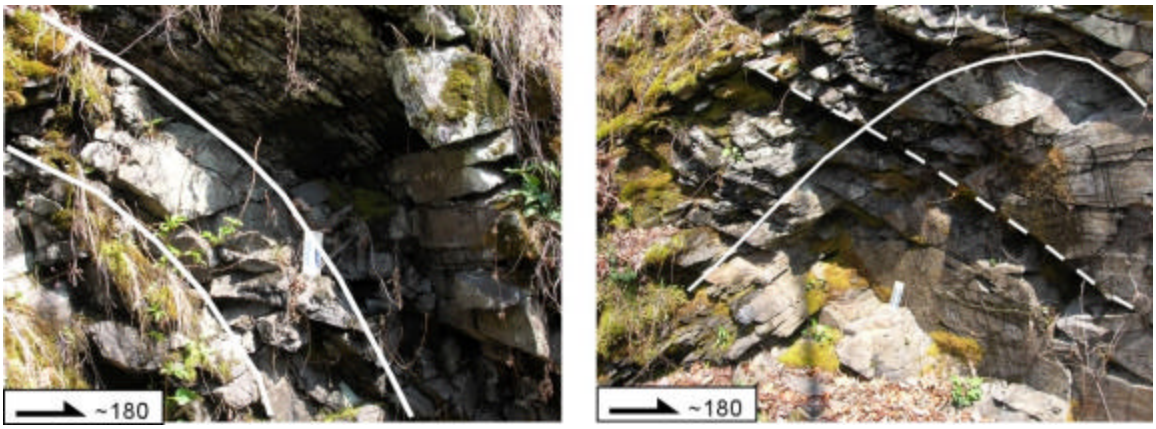

Figure 2.18 - Rich Butt sandstone, S_2 cleavage (dashed line) visible as a fracture cleavage in outcrop, cutting S_0 (solid line) folds in the Rich Butt formation.

Figure 2.19 - Relationship between S_0 and S_2 in the Rich Butt sandstone. S_0 is defined by thin laminae of alternating quartz-rich and argillaceous layers. S_2 in outcrop is defined by fracture cleavage.

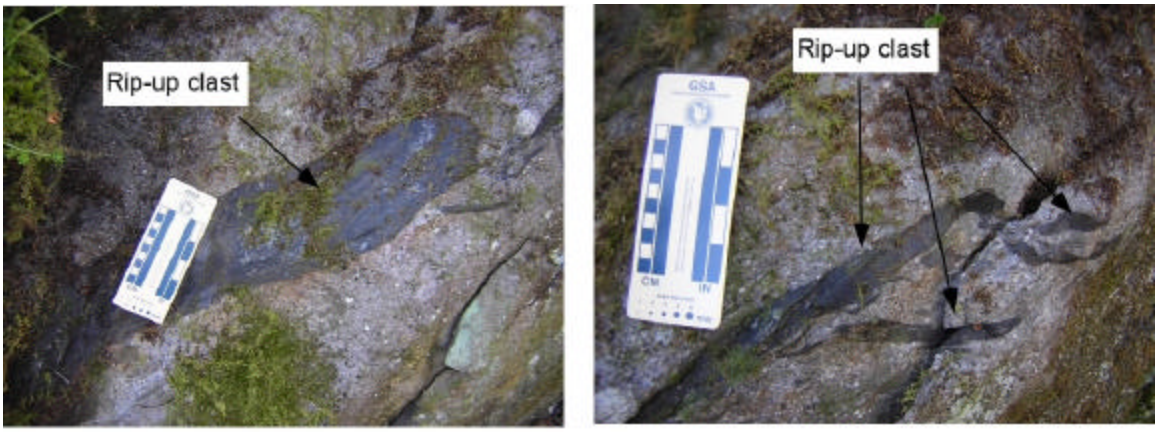

Figure 2.20 A) and B) Rip-up clasts in the Thunderhead sandstone (GSG)

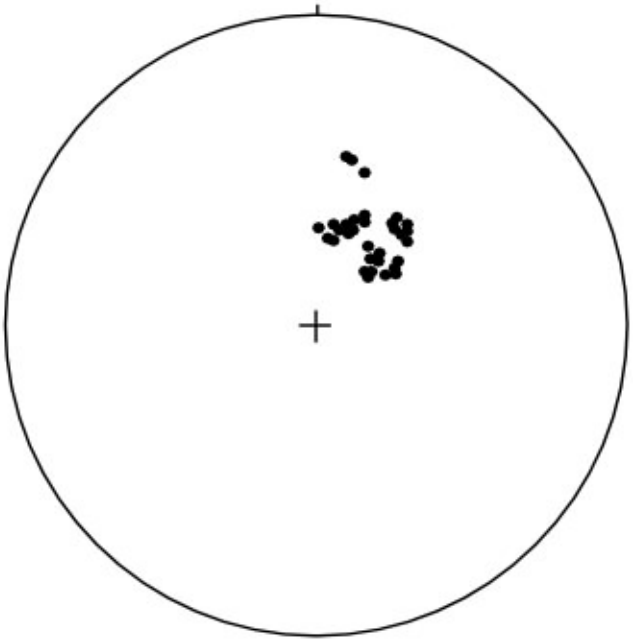

Figure 2.21 - Equal area net of poles to bedding (S_0) throughout the Big Creek study area (area 2). Strike of S_0 in this area is oriented WNW in this locality as bedding begins to wrap around the nose of the Waterville syncline.

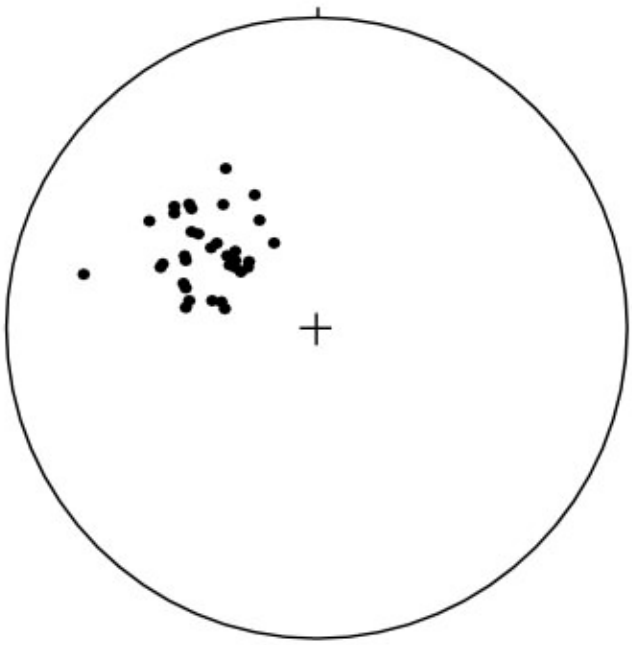

Figure 2.22 - Equal area net of poles to S_2 foliation throughout the Big Creek study area (area 2).

contact without deflection or truncation. Outcrop scale folds (F_1) lacking an axial plane cleavage (S_1) in the SG are transected by S_2 (Figure 2.18). The contact at Big Creek displays many of the same characteristics seen at the Greenbrier Pinnacle: secondary S_2 (chlorite and muscovite) is the dominant cleavage/foliation, is defined mesoscopically by spaced fractures that appear at varying angles to bedding (S_0) (Figure 2.21 and 2.22) and is most identifiable in the footwall. S_3 was not observed at this locality.

Microscopically, primary S_1 is weak to non-existent and is characterized by M_1 biotite with a weak preferred orientation at oblique angles to S_0. Microstructures associated with peak metamorphic M_1/S_1 biotite are weakly or rarely associated with a preferred fabric. Retrograde muscovite and chlorite are preferentially oriented parallel to and define the continuous (SG) and disjunctive (GSG) cleavage (S_2) (Figure – 2.26). S_2 is more strongly developed in the fine-grained to argillaceous SG footwall units and weakly developed in the coarse-grained to conglomeratic GSG hanging wall units. Hanging wall characteristics in this locality included a weak foliation (S_2) defined by biotite, muscovite and chlorite. S_2 is characterized by dynamic recrystallization of quartz, formation of retrograde (M_2) chlorite, and mica fish. S_2 is manifested as a continuous cleavage in the SG and a disjunctive cleavage in the massive quartzo-feldspathic GSG.

A second shear zone, similar to the one documented at Greenbrier Pinnacle, north of Big Creek (Figure – 2.23) also exhibits fabric orientations (Figure 2.24) that overprint those of the earlier foliations and regional trends. These fabrics include transposed S_2 foliation and boudinaged quartz veins. The contact at this locality revealed similar multi-deformational events in mapped units as the fault's footwall near the type locality (Hadley and Goldsmith, 1963; Southworth et al. 2005). Samples of sheared Rich Butt sandstone (pCrb) at this locality (biotite grade) (Figure 2.23) reveal Rich Butt displaying S/C microstructures that overprint the regional metamorphic assemblages and foliations (Figure 2.24 and 2.25). The phyllonitic S/C fabric overprints the bedding (S_0) and the continuous cleavage (S_2). Shear zone footwall microstructures include crenulation cleavage, dynamic recrystallization of quartz, and mica fish. Sense of shear based on asymmetry of footwall

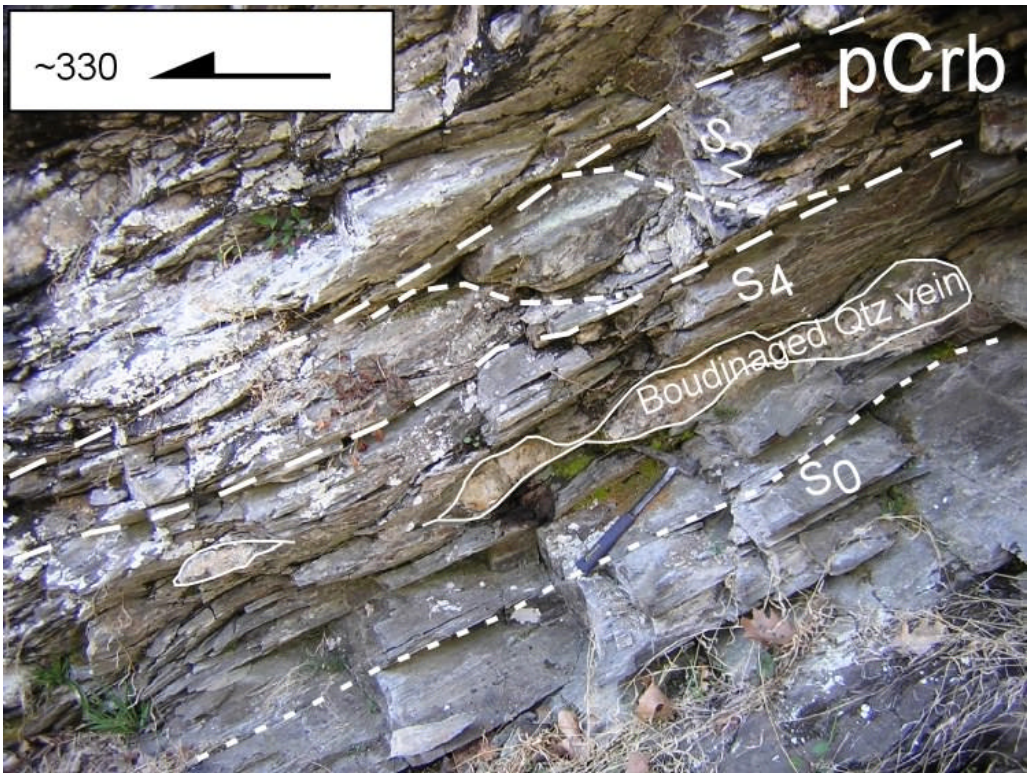

Figure 2.23 - Outcrop photo displaying sheared Rich Butt sandstone (Big Creek). S_2 is deflected into parallelism with S_4. Quartz vein has been boudinaged by S_4.

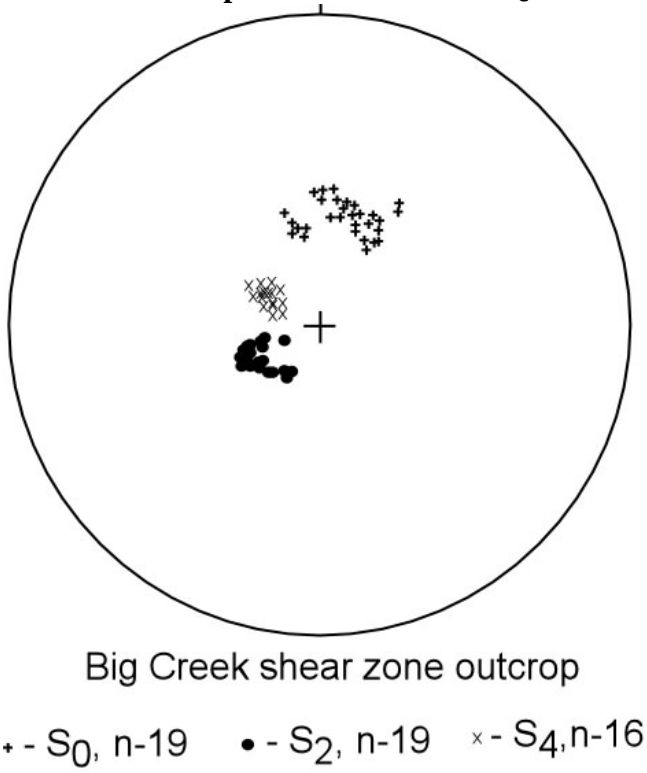

Figure 2.24 - Equal area net of poles to S_0, S_2 and S_4 S/C fabric in the shear zone north of Big Creek (area 2).

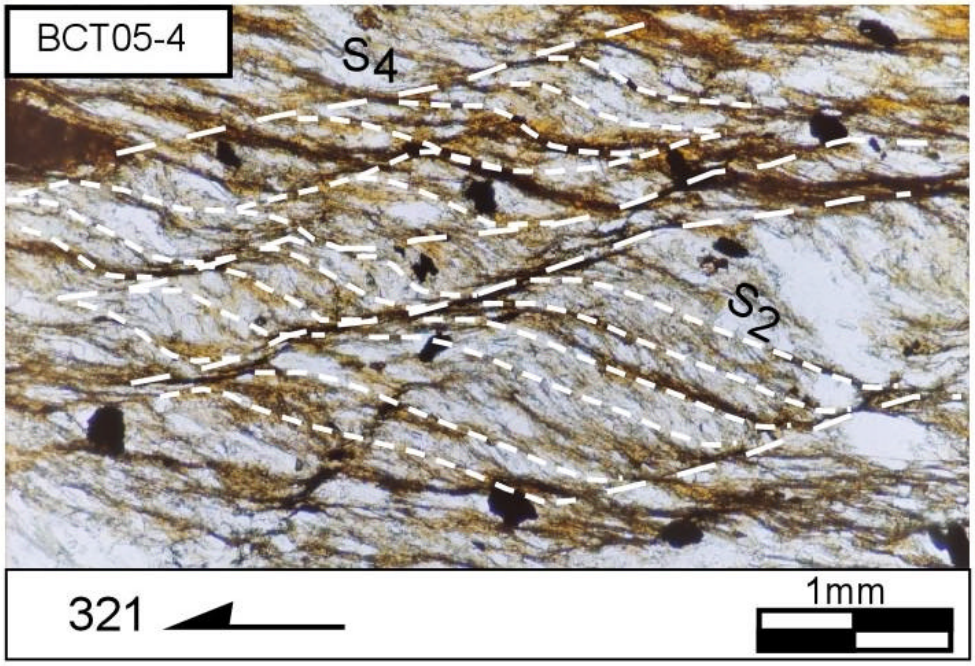

Figure 2.25 - Sheared pCrb at Big Creek displaying S/C fabric. Mica preferred orientation (S_2) is transected by sub parallel shear zones. S_2 is deflected into parallelism with S_4. Shear sense is sinistral; top to the NW. Orientation indicated at the bottom is the strike of the vertical thin-section. Plane light.

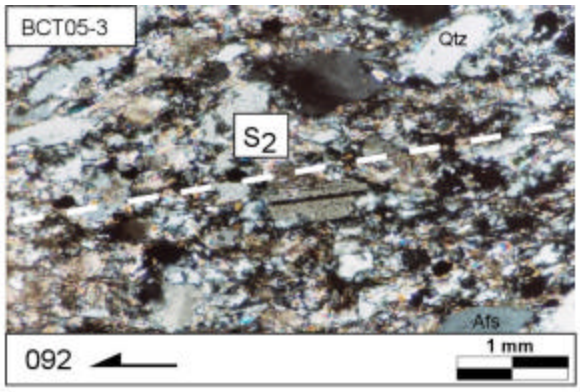

A

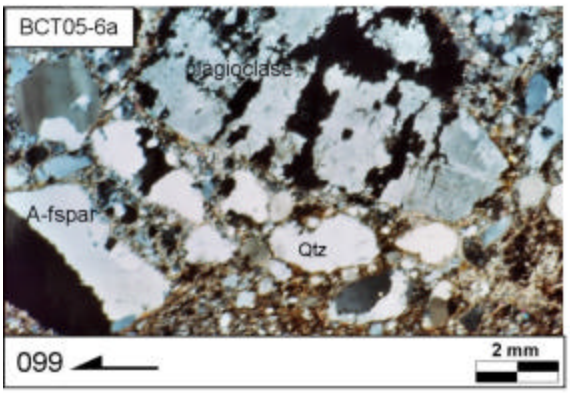

B

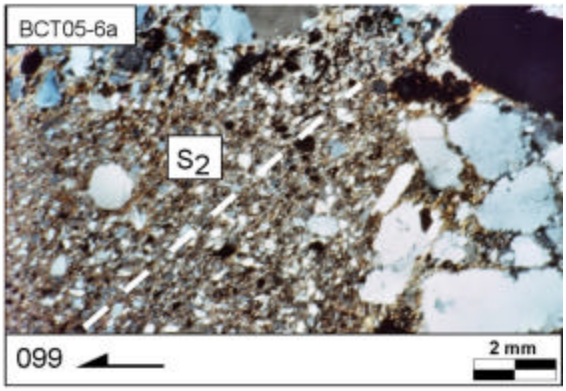

C

Figure 2.26 – Petrographic features of Thunderhead Sandstone at Big Creek include a weak foliation (disjunctive cleavage; S_2) defined by parallelism of biotite, muscovite and chlorite. Orientation indicated at the bottom is the strike of the vertical thin-section. Crossed polars.

microstructures is normal and top-to-northwest (Figure 2.25). Quartz and feldspar grains display a weak lineation. Angular rip-up clasts of dark gray argillite clasts in Thunderhead sandstone (GSG) display a crenulation cleavage (Figure 2.27) most likely imparted post-depositionally. It is noteworthy to mention the meta-feldspathic sands containing these clasts show little if any deformational fabrics. As in the type locality, the fabric appears as a weakly developed disjunctive cleavage in the coarse grained hanging wall units (Figure 2.26).

Fabric Relationships at Mount Sterling

A detailed field map (Area 3, Figure 2.28) of the area shows a dominant foliation that maintains a NE strike while the contact trace and S_0 turn to the south with S_0 being tightly folded (Figure 2.29 and 2.30). Exposures of macroscopic and mesoscopic features at or near the contact become less prevalent in the study area near Mount Sterling (Grt grade). Bedding (S_0) in the SG is characterized by alternating quartzo-fedspathic and argillaceous layers. S_0 in the argillaceous SG units is defined by laminated planar beds that alternate in color from dark to light. S_0 and its orientations are visible on the macroscopic and mesoscopic scale. S_0 in the GSG is characterized by medium- to coarse-grained feldspathic metasandstone, angular rip-up clasts of dark gray argillite, and quartz pebble conglomerate lenses. Orientation of GSG bedding is not well developed or not apparent in macroscopic or mesoscopic scale. Folds at the map scale, inferred from S_0 orientations of the Rich Butt sandstone, indicate tight to isoclinal folding (Figures – 2.29 and 2.30).

Microscopic fabric characteristics at this locality differ from those at lower metamorphic grades (Greenbrier Cove and Big Creek). Primary S_2 is strong, characterized by parallel alignment of muscovite and elongate quartz overgrown by M_1 garnet and biotite porphyroblasts. Garnet porphyroblasts contain inclusions of quartz displaying a preferred orientation paralleling that in the matrix (S_2) (Figure 2.31). Muscovite and chlorite define the continuous cleavage (S_2) and are parallel to S_0 in the pCrb (Figure – 2.31). S_2 is more strongly developed in the fine-grained to argillaceous SG footwall units and weakly developed in the coarse-grained to conglomeratic

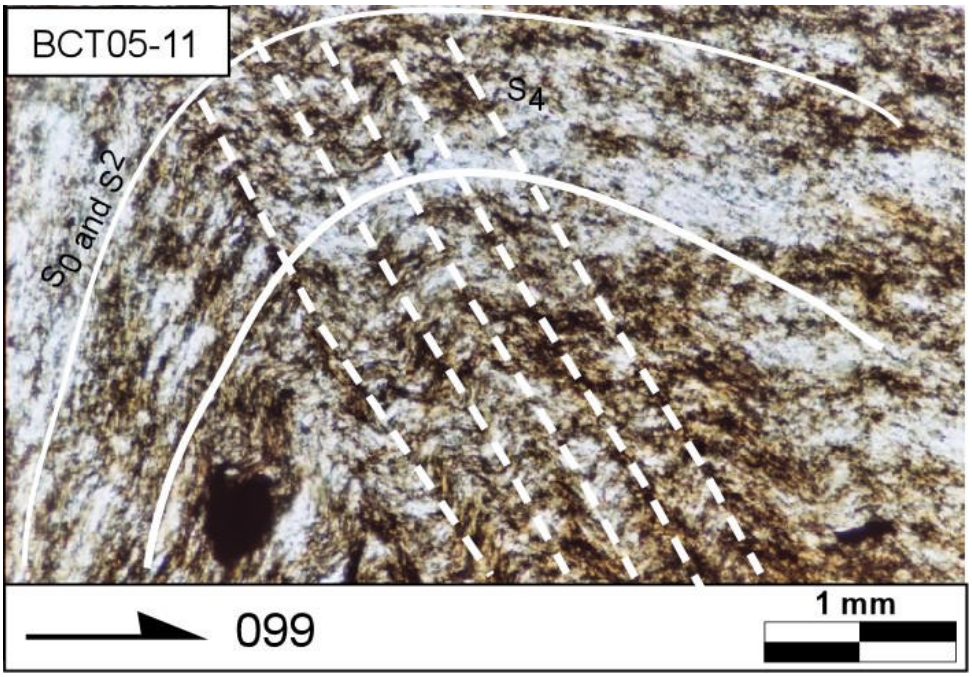

Figure 2.27 – Folded, crenulated argillite clast in Thunderhead sandstone north of Big Creek. A tight fold in the clast displaying the parallel orientation of S_0, S_2, and S_3 in the limbs; and S_3 oblique to S_0/S_2 in the hinges. Orientation indicated at the bottom is the strike of the vertical thin-section. Plane light.

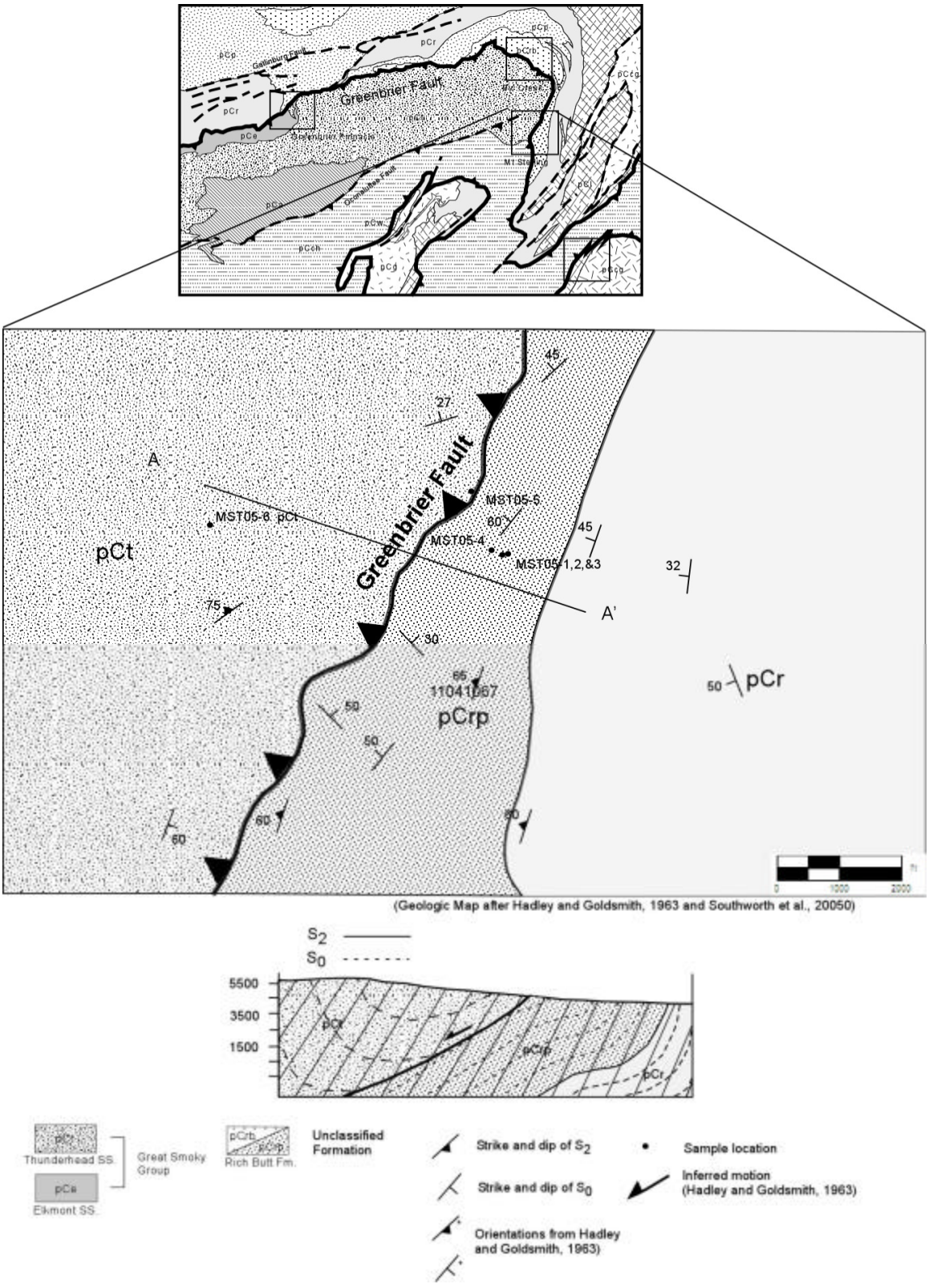

Figure 2.28 – Mount Sterling area geologic map. Thrust motion is inferred from the traditional interpretation of the GBF by Hadley and Goldsmith (1963).

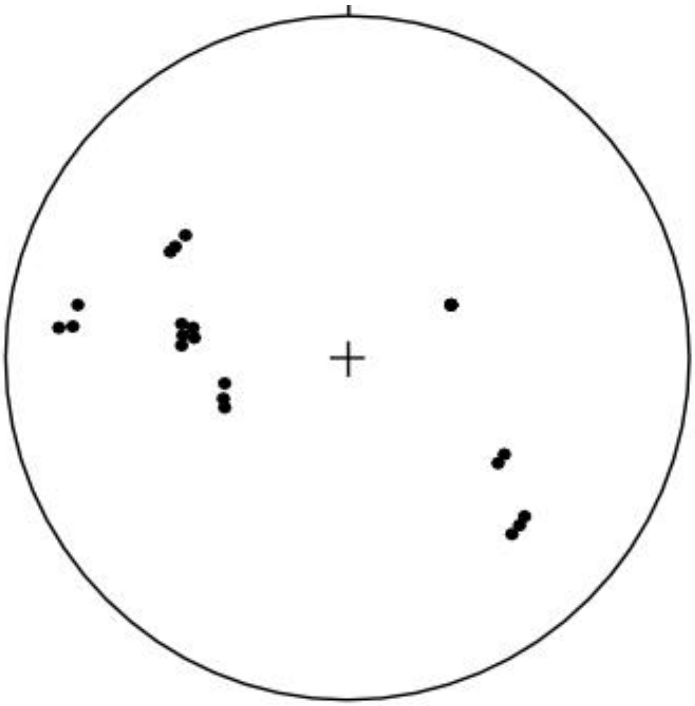

Figure 2.29 - Equal area net of poles to bedding (S_0) throughout the Mount Sterling study area.

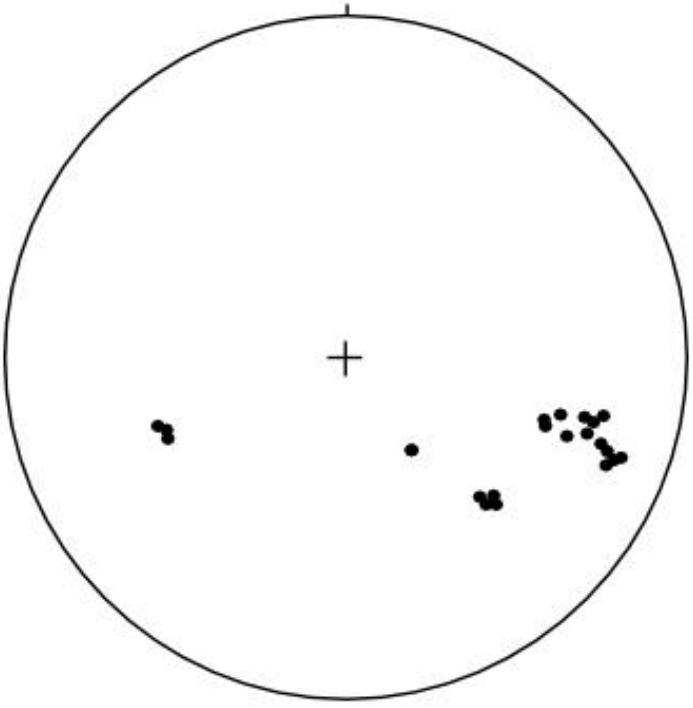

Figure 2.30 - Equal area net of poles to S_2 foliation throughout the Mount Sterling study area.

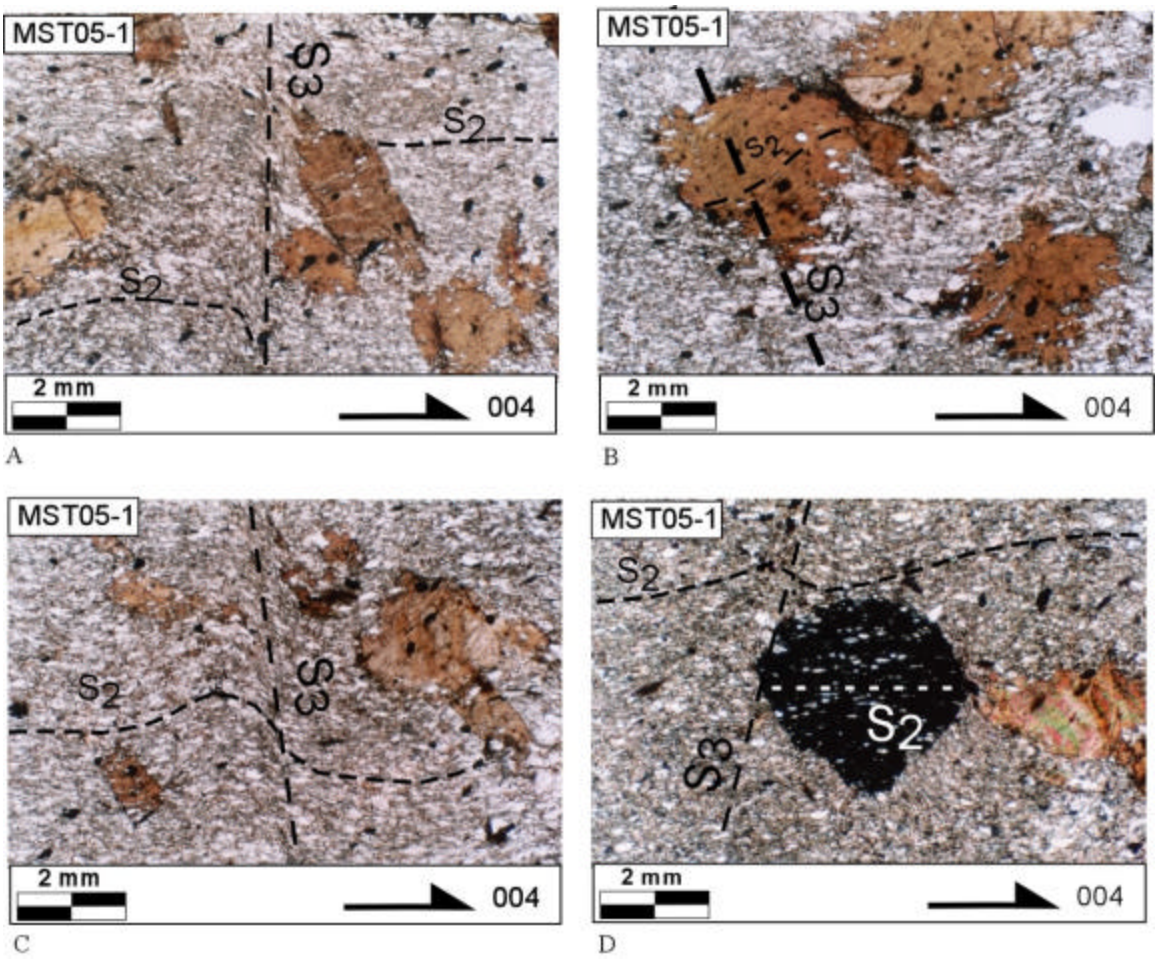

Figure 2.31 – Fabric and metamorphic mineral relationships in the Rich Butt Fm. at Mount Sterling. (A) Steep S_3 crenulating S_2 (muscovite); (B) S_2 preserved in biotite, both kinked by S_3; (C) S_3 crenulating S_2; (D) S_2 preserved in garnet porphyroblast. Inclusions are continuous with matrix foliation.

GSG hanging wall units. S_2 is characterized by dynamic recrystallization of quartz, formation of retrograde (M_2) chlorite, and mica fish. S_2 is manifested as a continuous cleavage in the (SG) and a disjunctive cleavage in the massive quartzo-feldspathic (GSG). S_3 is steep and defined by kinking of biotite and the transposition and crenulation of S_2 (Figure – 2.31). A slab of Rich Butt float near the summit of Mount Sterling preserves a premetamorphic, decimeter-scale fault defined by offset of bedding (S_0). The fault is overgrown by prograde biotite. Bedding orientation is unknown and there was no strong preferred orientation (S_1 or S_2) developed (Figure 2.32).

Fabric Relationships at Cove Creek

Near Cove Creek, NC, (Area 4, Figure 2.33) the contact displays spectacular isoclinal folding (Figure 1.34) and attenuation of GSG and SG (Figure 2.34 and 2.36). Kyanite grade units along the contact near Cove Creek are characterized by tight to isoclinally folded Great Smoky group with foliation (S_2) trending ~NE. The contact displays a foliation defined macroscopically as a steep schistosity in the Great Smoky group units. The GSG at this locality contains kyanite, garnet, muscovite, and biotite. The Snowbird group (Longarm Quartzite) on the southeast side of the contact at this locality is devoid of metamorphic assemblages useful in marking isograds.

S_2, the only foliation apparent here, is characterized by schistosity in the GSG. Folds in the SG Longarm quartzite are visible in tightly folded quartz veins (Figure 2.35). The premetamorphic relationship of the two units in this area is impossible to ascertain. SG and GSG are mylonitic and display spectacular ductile microstructures which strongly overprint the regional metamorphic assemblages and foliations. These microstructures define a planar fabric which is penetrative and appears to be the manifestation of S_3 in the high-grade units because both fabrics produce microstructures and fabric asymmetries suggestive of shearing. These microstructures include: dynamic recrystallization of quartz (Figure 2.37), feldspar, biotite, and sphene; feldspar sigma-clasts; mica and kyanite fish (Figures 2.38, 2.39, and 2.40); and S/C fabrics. Flattening of foliation around garnet porphyroclasts (Figure 2.41) and

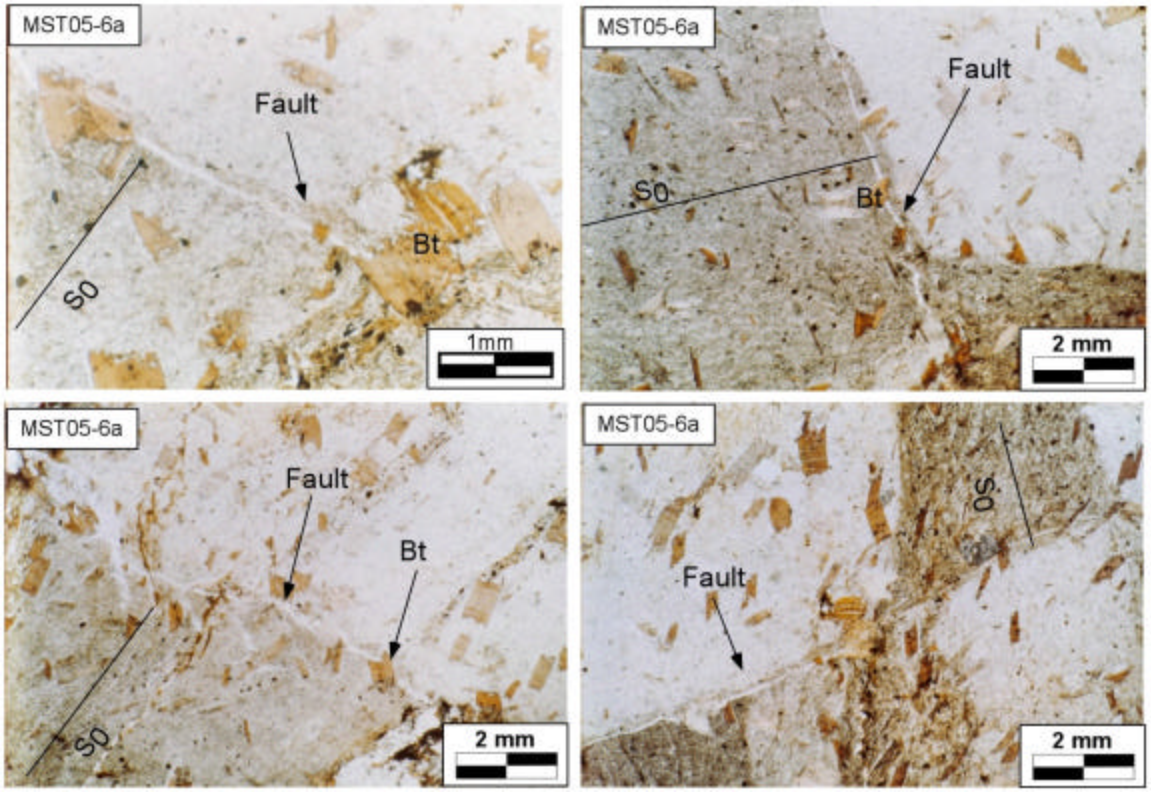

Figure 2.32 – Premetamorphic brittle fracture preserved in Thunderhead sandstone. Biotite porphyroblasts overgrow the fault surface. Orientation indicated at the bottom is the strike of the vertical thin-section. Plane light.

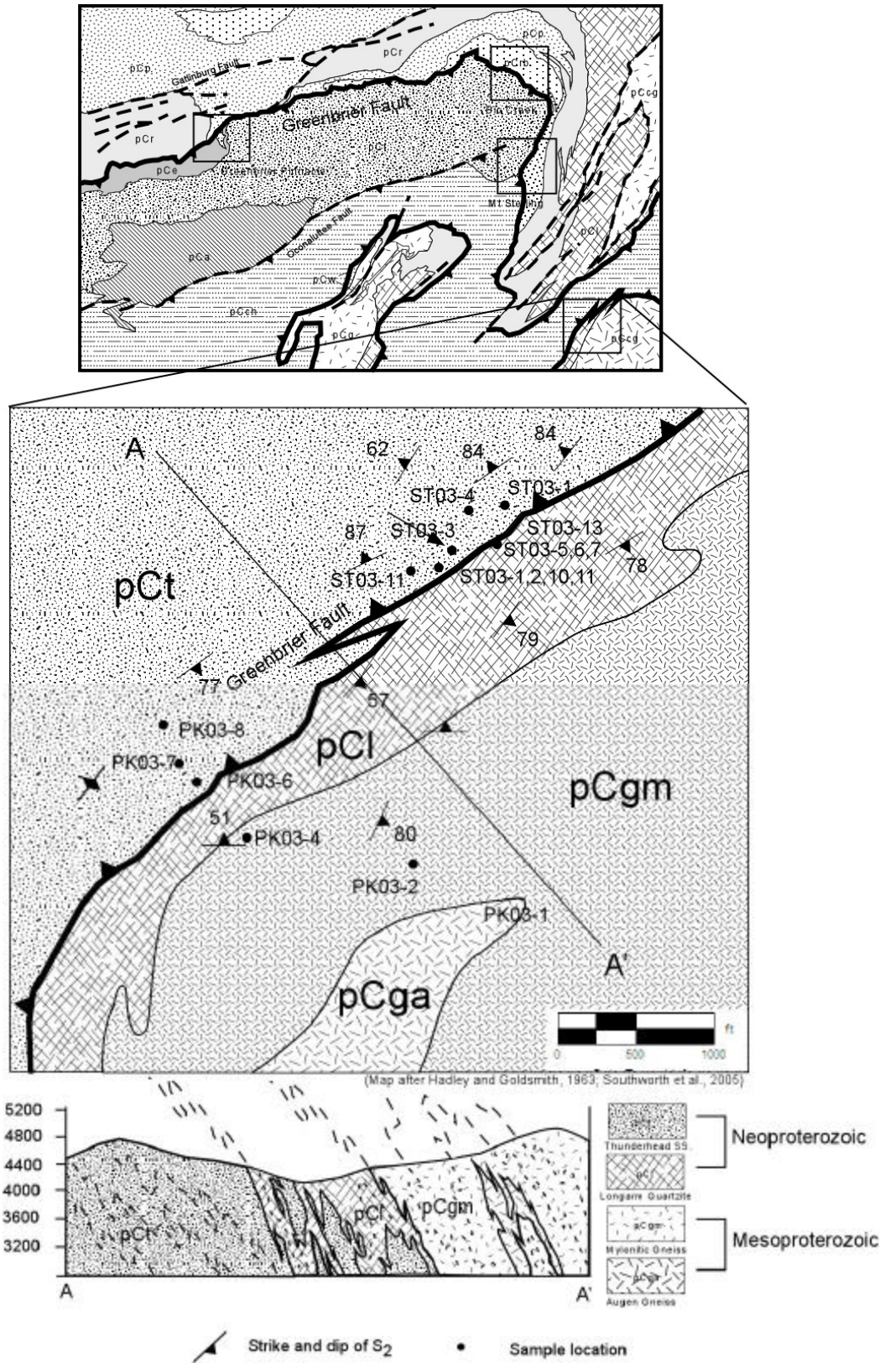

Figure 2.33 – Cove Creek area geologic and sample location map.

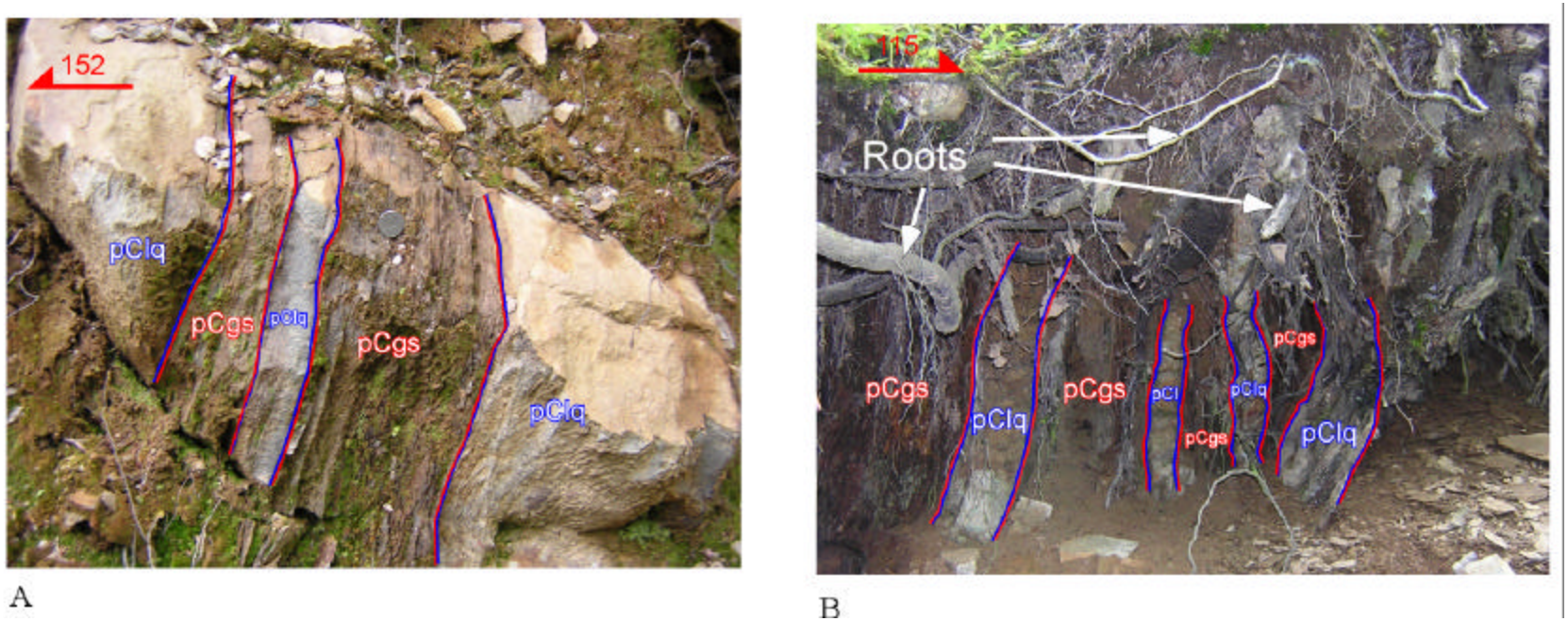

Figure 2.34 – (A) Interfolded GSG (Thunderhead Fm.; pCgs) and SG (Longarm quartzite; pClg); (B) Attenuated isoclinally folded Longarm quartzite and Thunderhead sandstone (mica schist).

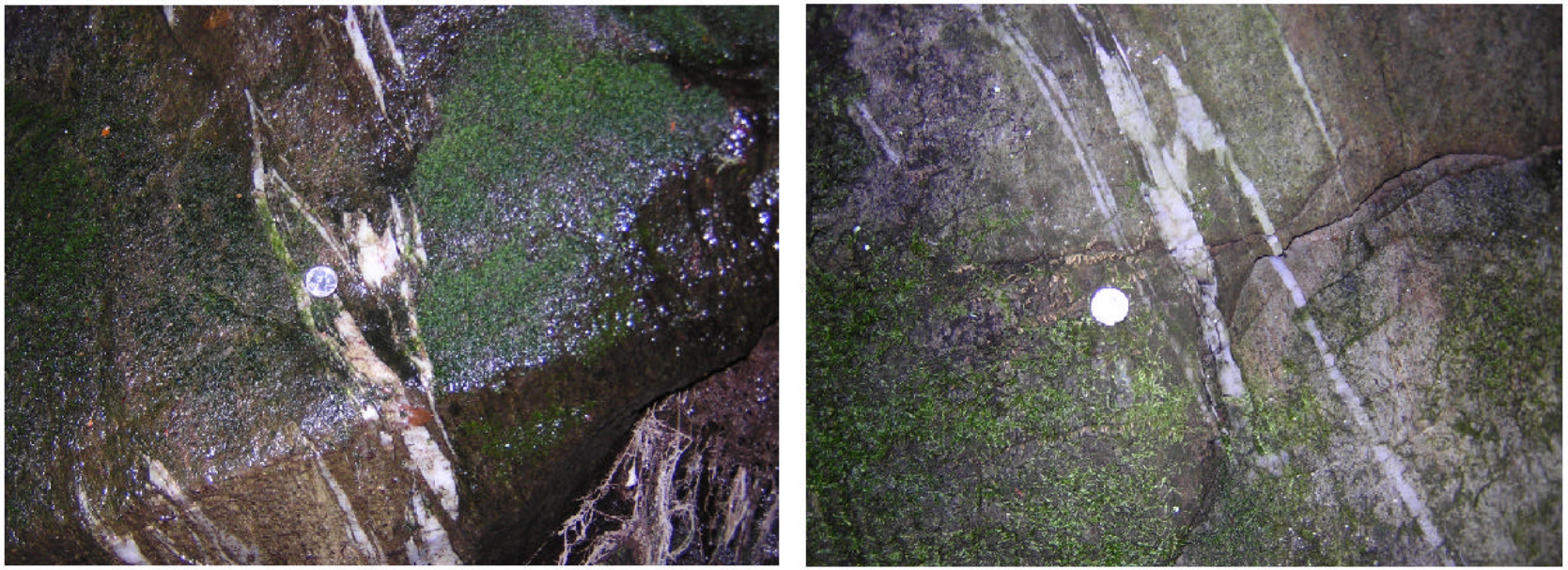

A B

Figure 2.35 – A and B: isoclinally folded quartz veins in SG Longarm quartzite

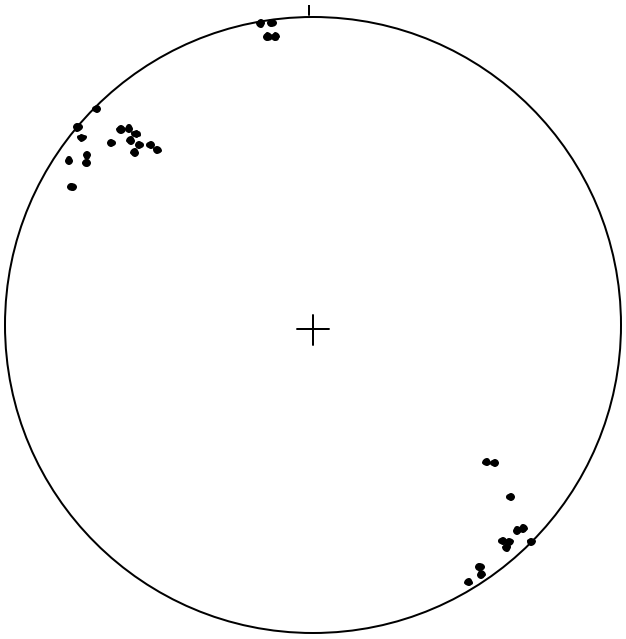

Figure 2.36 - Equal area net of poles to S_0/S_2 foliation throughout the Cove Creek study area (area 4). S_0 (contact orientation) and S_2 (schistosity) are parallel at this locality.

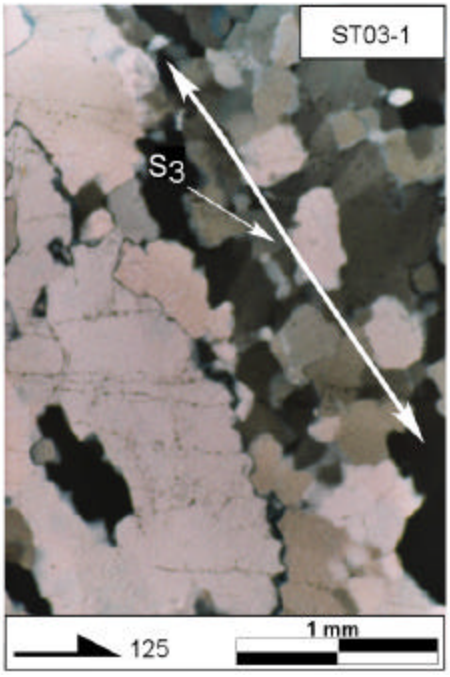

Figure 2.37– Longarm quartzite (SG) showing dynamic recrystallization of quartz. Orientation indicated at the bottom is the strike of the vertical thin-section. Crossed polars.

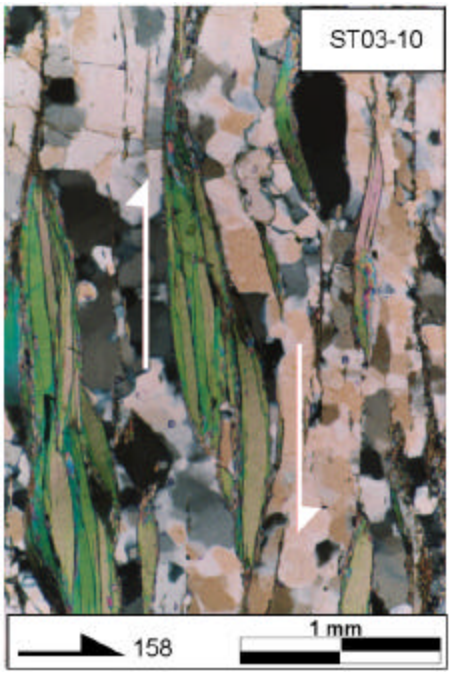

Figure 2.38- Mica fish in the Longarm quartzite, a manifestation of S_3 as a disjunctive foliation. Orientation indicated at the bottom is the strike of the vertical thin-section. Crossed polars.

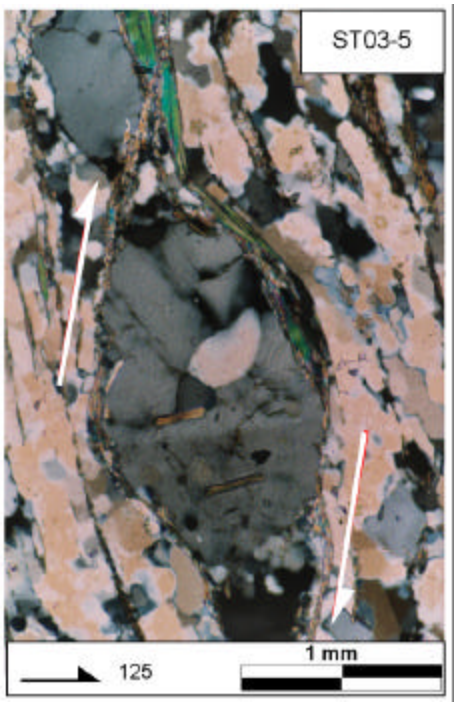

Figure 2.39– Feldspar sigma porphyroclast in Longarm quartzite (SG). Sub-vertical dextral shear sense. Orientation indicated at the bottom is the strike of the vertical thin-section. Crossed polars.

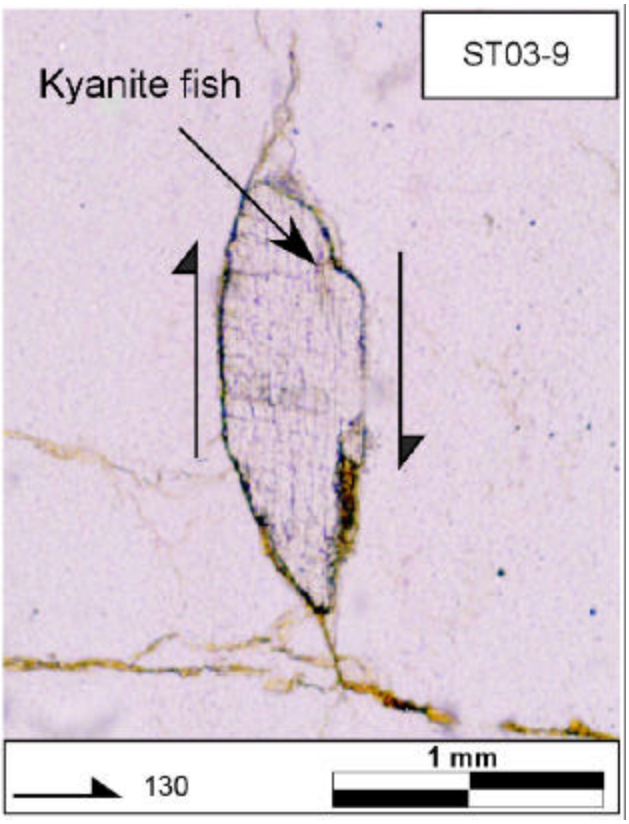

Figure 2.40 - Kyanite fish in Longarm quartzite (SG). Vertical dextral shear sense. Orientation indicated at the bottom is the strike of the vertical thin-section. Plane light.

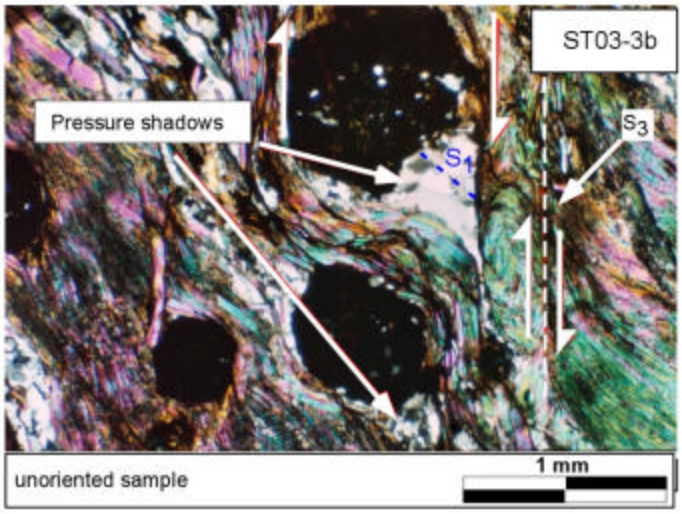

Figure 2.41– Flattening of foliation around garnet porphyroclasts in the Thunderhead sandstone. An earlier foliation (S_1?, S_2?) is preserved in the pressure shadow. Unoriented thin section. Cross polars.

boudinaged kyanite porphyroclasts (Figure 2.42) occur in the Thunderhead formation (GSG). The sense of shear in this locality based on asymmetry of microstructures along a vertical shear plane is southeast side down motion. Retrograde breakdown of garnet is limited to the formation of biotite during shear. No premetamorphic microstructures can be determined in the GSG or SG in the Cove Creek, NC area, and based on the lack of premetamorphic evidence, the contact appears lithologic. These microstructures are a manifestation of F_3/D_3 folding to produce S_3. A similar post-metamorphic phase of foliation in kyanite grade rocks southeast of Cove Creek, similar to the foliation seen at Cove Creek, indicates this is a late regional deformation event (Massey and Moecher, 2005; Moecher et al., 2005). Assuming the kyanite grade metamorphism is Taconian, the fabrics imply a period of deformation along the contact during Acadian and/or Alleghanian orogenesis. Evidence for premetamorphic faulting was not seen at or near the GSG-SG contact at any metamorphic grade.

2.7 Summary of fabrics

All foliations in the study area are not related to folding and all folding events are not foliation-generating events. Due to composition and competency, foliations tend to be more strongly developed in the SG than in the GSG.

S_0 Bedding

Bedding (S_0) throughout the study area is consistently characterized by alternating laminated planar beds of quartzo-fedspathic and argillaceous layers in the SG that alternate in color from dark to light beds. S_0 in the GSG is characterized by thin bedded to massive, medium- to coarse-grained feldspathic metasandstone with interbedded

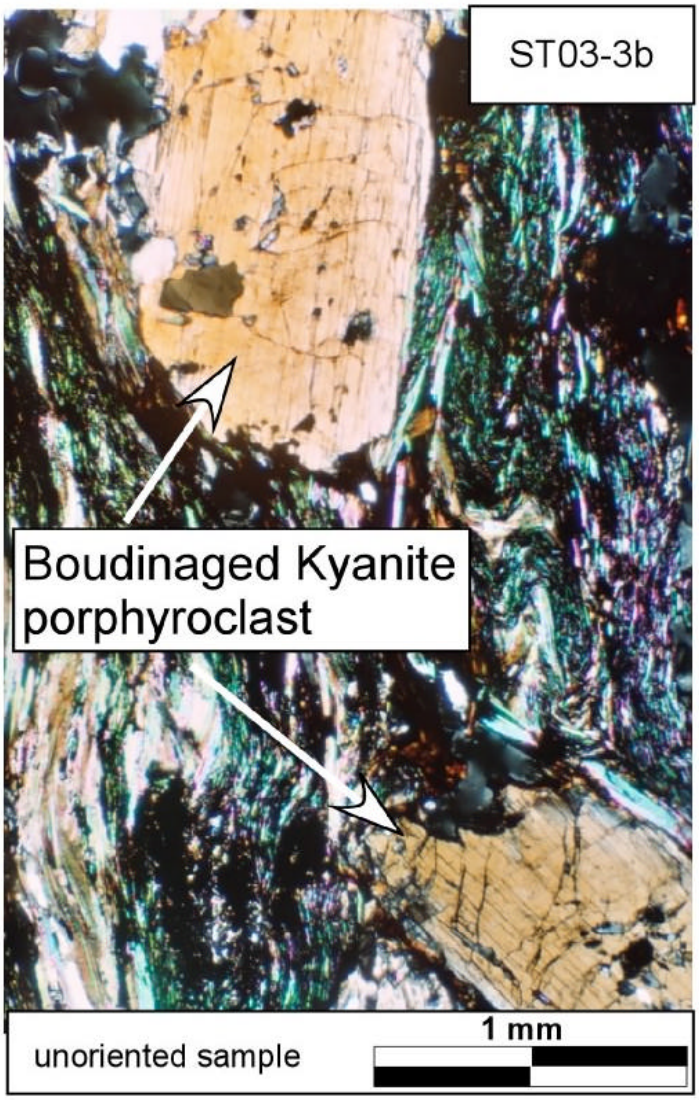

Figure 2.42– Boudinaged kyanite in Thunderhead sandstone (GSG). Unoriented thin section. Cross polars.

metaconglomerate (Figure 2.6). Orientation of GSG bedding is weak or not apparent in macroscopic or mesoscopic scale. Bedding (S_0) can be seen in a variety of orientations throughout the study area, ranging from horizontal to vertical. Although no fold hinges were observed, the orientation of S_0, depicted in Figures 2.7 and 2.21 suggest either isoclinal folding or homoclinal beds. The lack of a strong penetrative fabric throughout the Pigeon suggests the latter.

S_1 Foliation

S_1 is non-penetrative and defined by the weak preferred orientation of relict M_1 biotite in the low grade areas (Greenbrier Cove and Big Creek). In the medium to high grade areas, S_1 is defined by parallelism of muscovite and biotite.

S_2 Foliation

The previous discussion regarding (1) S_0 - F_1, (2) S_1, and (3) F_2/ S_2 indicate no strong consistent relationship among the three fabrics. Thus, in regard to the seemingly dominate nature of S_2 locally and regionally, the prevailing foliation is referred to as S_2 except in certain places where S_1 and S_2 can be separated. Almost all lithologies in the GSG and SG display the dominant (S_2) foliation, but many showing evidence for late (post-S_2) deformational overprint(s). S_2 is manifested as a disjunctive cleavage (secondary spaced foliation without fold hinges in the microlithons) or continuous cleavage in all areas up to garnet and kyanite grade where it is manifested as schistosity.

S_3 Shear Band Cleavage

Thin-section analysis of tight to isoclinally folded SG units (Pigeon siltstone and Roaring Fork sandstone) shows transposition of S_2 into a steep planar shear band cleavage position, S_3. The new foliation (S_3) is defined by reorientation and neocrystallization of micas. The S_3 foliation appears as a spaced (0.05-1.5 mm) shear band fabric characterized by offset (0.02-0.05mm) of S_0 and S_2 foliation. Quartz appears to be markedly strained by S_3 foliation development as indicated by the undulose extinction, lobate grain boundaries, and subgrain development. In Rich Butt sandstone in the garnet isograd (Mount Sterling), S_3 is characterized by kinking of biotite

porphyroblasts and steep crenulation of S_2 foliation. In the kyanite grade area at Cove Creek, S_3 manifests itself as a steep pervasive foliation defined by microstructures that strongly overprint the regional metamorphic assemblages and foliations. These microstructures appear in Pigeon siltstone as a shear band cleavage transposing S_2, in Rich Butt sandstone (SG) as kinked biotite and crenulated S_2, in Longarm quartzite (SG) as the dynamic recrystallization of quartz (Figure 2.37), feldspar, biotite, and sphene; development of mica, feldspar, and kyanite fish (Figure 2.38, 2.39, and 2.40); flattening of the foliation around garnet porphyroblasts (Figure 2.41); and extension/boudinage of kyanite porphyroblasts (Figure 2.39) and dynamic recrystallization of quartz in the Thunderhead sandstone (GSG). Sense of shear based on asymmetry of microstructures at this grade is vertical SE side down.

S/C Fabric

Outcrop and thin-section observations of Snowbird footwall units (Pigeon siltstone, Roaring Fork sandstone, and Rich Butt sandstone) show transposition of S_2 and S_3 to phyllonitic S/C or crenulation position, S_4 (Figure 2.29). The new foliation (S_4) is defined by reorientation and crystallization of micas, dynamic recrystallization of quartz, and quartz ribbons exhibiting undulose extinction parallel to the contact between the GSG and SG (Figure – pCr and pCrb thin sections). The S_4 fabric is restricted to the less competent - more argillaceous footwall units.

Area	*Folding*	*Metamorphism*	*Foliations/Fabrics*		*Faulting*
Greenbrier Pinnacle	monocline	M_1 biotite, M_2 chlorite	S_0	well developed	Ductile
			S_2	well developed	
			S_3	well developed	
			S/C	well developed	
Big Creek	open to tight	M_1 biotite, M_2 chlorite	S_0	well developed	Ductile
			S_2	well developed	
			S/C	well developed	
Mount Sterling	tight	M_1 biotite and garnet, M_2 chlorite	S_0	not apparent	premetamorphic and brittle
			S_2	well developed	
			S_3	well developed	
Cove Creek	isoclinal	M_1 biotite, garnet and kyanite, M_2 chlorite, muscovite, and biotite	S_0	visible as contact between SG and GSG	Na
			S_2	well developed	
			S_3	well developed	

Table 2.1 – Deformation style, folding, foliation development, and faulting within the study area.

2.8 Interpretations

Structural Evolution

Bedding (S_0) is preserved in the biotite and garnet grade areas (Greenbrier Pinnacle, Big Creek, and Mt. Sterling) as compositional layering between siltstone, sandstone and argillite; however, increasing deformation and metamorphic differentiation to the southeast are complex and bedding/fabric relationships in the southeast part of the study area (Cove Creek) completely obliterate S_0. S_1 is weak to absent (see Figure 2.25) and it is unclear what relationship, if any, it has with the dominant regional cleavage (S_2).

The S_2 fabric is parallel to regional fold axes (F_2), and two younger foliations (S_3 and an S/C fabric) overprint S_0, S_1, and S_2 at roughly the same orientation as S_0 strike. The S_0/S_2 relationship requires (1) F_1 tight folding of S_0 and (2) open regional folding (F_2) where S_2 develops sub-parallel to S_0 in fold limbs. S_3 shear band cleavage is late, overprints S_0, S_1, and S_2, is spaced, active and not parallel to tectonic strain axes. The S/C overprints all assemblages and fabrics near the contact and likely was imparted during a late reactivation and northwest-directed movement (based on asymmetries in microstructures) along the GSG-SG contact.

Discussion

With the exception of the Thunderhead sandstone float (Figure 2.32), no petrographic evidence for premetamorphic faulting was seen at or near the SG-GSG contact at any metamorphic grade. Based on the truncation of S_0 by the contact in the low-grade areas, it is reasonable to infer that the contact is a fault. However, if the fault is a major discontinuity and involves $\geq$ 23 km of displacement (Hadley and Goldsmith, 1963), it would be reasonable to expect bedding to be interrupted or obliterated. Is lack of this significant? It is also reasonable to expect some cataclastic textures to be preserved in the biotite-grade type locality. No brittle fabrics or structures were found at or near the lowest -grade exposures of the contact. If brittle fabrics were to survive peak metamorphic conditions, what would they be expected to look like? Offset along thin bedding planes and laminations should be overgrown by M_1 biotite and M_2 chlorite and muscovite. No such relationships were seen at any metamorphic grade. Also, it is clear that $D_1/ M_1/ S_1$ was weak. Metamorphism, as defined by growth of biotite and garnet

porphyroblasts at Mount Sterling, appears to be static in agreement with the conclusion of Hadley and Goldsmith (1963). Premetamorphic fault structures (e.g. mylonites, cataclasites, and breccia) should be present, but none are observed.

Evidence of a fault relationship is obscured and complicated in areas where the Rich Butt sandstone (pCrb) separates the GSG/SG because the pCrb contains characteristics of both the SG/GSG. It is unclear how the Rich Butt fits into the traditional interpretation of the Greenbrier fault if this unit is conformable with the GSG and SG and it is found between the two in several locations where the Greenbrier fault has been mapped. Samples from the high-grade areas (upper amphibolite facies) are too intensely metamorphosed and recrystallized to test models regarding the evolution of the Greenbrier Fault.

The S/C fabric is restricted to localized zones in the more argillaceous footwall units which appear to have accommodated strain during a late, post-metamorphic shearing between the GSG/SG contacts. This motion along the contact appears to be a late (Acadian or Alleghanian) reactivation of the Greenbrier fault based on the mineral assemblages deformed by the fabric. The S/C fabric shares many similarities with structures in the Metcalf phyllite (Figure 3.4 and 3.9) and may be correlative. The S/C fabric may represent a thinner zone of displacement related to motion contemporaneous with emplacement of the Great Smoky fault.

Structural interpretations are largely consistent with previous investigations, in regard to fold history and fabric development. However, observations and interpretations of this study have produced new conclusions with implications bearing on the significance of the boundary between the GSG and SG and their present configuration and implications for the tectonics of the southern Appalachians. Specific to the intent of this study, and the greatest implications in regard to tectonic evolution, are the effects of emplacement of the "premetamorphic", Greenbrier fault (SG-GSG boundary). No observations of any kind on any scale, macro-, meso-, or micro-, for the exposures along the contact, indicate "premetamorphic" faulting, shearing, or emplacement of a thrust sheet along the present contact.

Based on the lack of petrofabric evidence for premetamorphic faulting and lack of fabrics indicative of the large amount of offset proposed by Hadley and Goldsmith

(1963), it appears the Greenbrier fault is a minor tectonic feature in the Western Blue Ridge. The history of the GBF appears to have involved the following sequence of events: crustal extension of Precambrian basement creating a basin for the deposition of sediments comprising the Snowbird and Great Smoky groups followed by post-depositional crustal shortening resulting in the folding of SG and GSG. Continued crustal shortening resulted in thrust faulting and minor offset of SG and GSG producing the geometries and lithologic relationships seen within the study area. The GSG maintains its stratigraphic relationship above the SG. Late shear zone fabrics such as those seen at Greenbrier Pinnacle and Big Creek represent either (A) initial faulting or (B) a late reactivation along this boundary related to subsequent deformational events (Figure 2.43).

Additional Work

Relationships among the features across the SG-GSG contact, relating to southern Appalachian orogenesis, will require further work on the local and regional scale in order to fully assess the significance of the results presented here. A detailed geochronologic investigation of metamorphism and deformation using Rb-Sr analysis of muscovite, focusing on the absolute age of S_3 and the S/C should place limits on these late penetrative ductile features. On a regional scale, the location of the contact between the SG and GSG should be mapped in greater detail. The nature of the boundary in the east and southeast is highly uncertain. Location of ductile shear zones (S/C) along the contacts trace may further elucidate the nature of the boundary. Furthermore, there is an uncertain relationship between the Rich Butt sandstone units in the GSG and SG. Resolving the stratigraphic relationship of this unit is critical for evaluating the relationship between the SG and GSG in the east. Other unresolved issues include: (1) the need for more convincing evidence for the nature of the F_1 deformation event; (2) the relationship of peak metamorphic mineral growth to F_1 folds; and (3) the relationship of S_2 and F_2 folds.

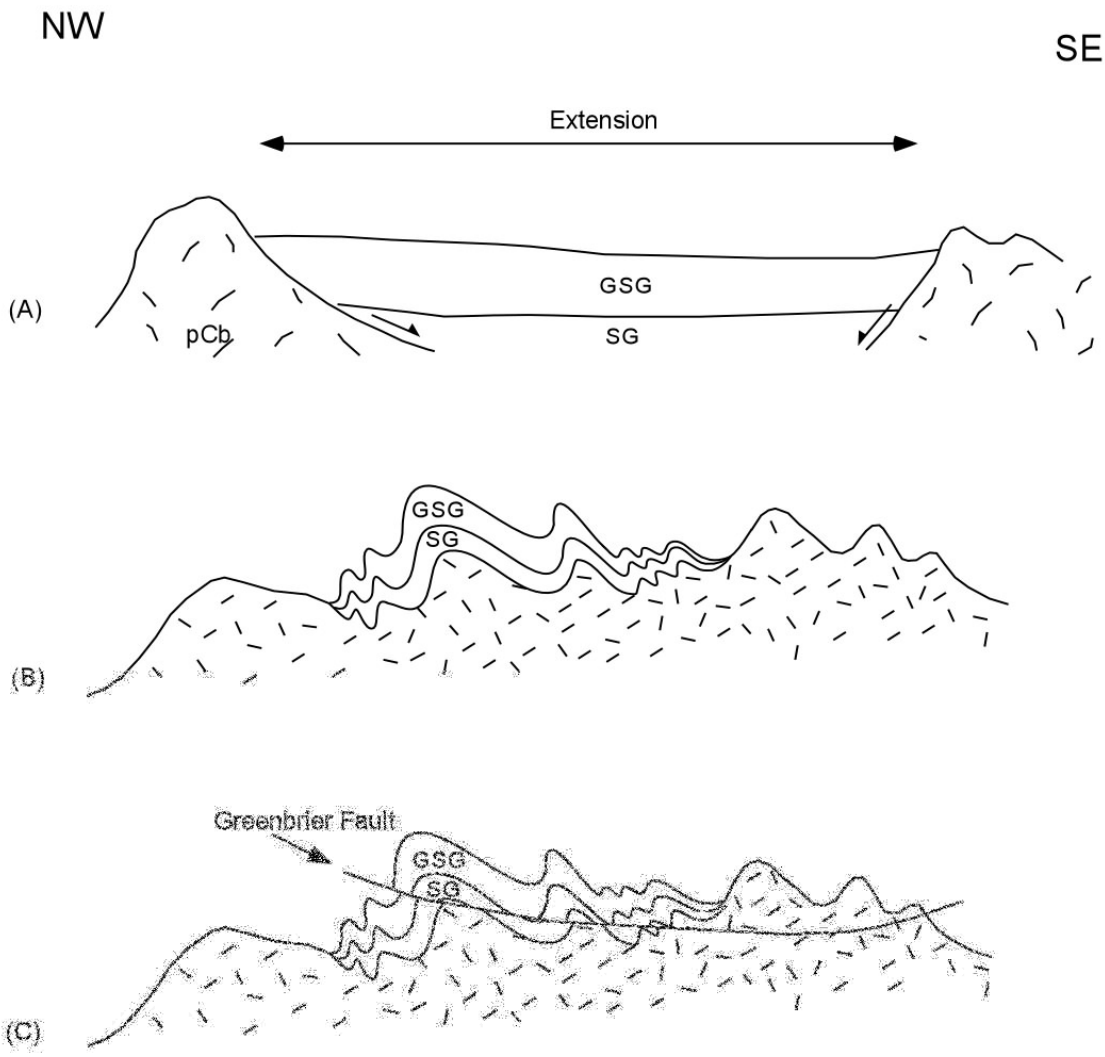

(A) Crustal extension of Mesoproterozoic rocks creating a basin for the depostion of the Snowbird and Great Smoky Grps. (B) Post-depositional crustal shortening resulting in the folding of SG and GSG. (C) Continued crustal shortening resulting in thrust faulting and minor offset of SG and GSG producing geometries and lithologic relationships seen within the study area. The GSG maintains its stratigraphic relationship above the SG. Late shear zone fabrics such as those seen at Greenbrier Pinnacle and Big Creek may represent a late reactivation along this boudary.

Fig. 2.43 Tectonic model for the Greenbrier Fault

2.9 Conclusions

The character of the Greenbrier fault changes along its trace from low to high grade. In the low-grade areas (Bt-Grt) there is evidence for a potential premetamorphic fault relationship between the GSG and SG based on the truncation of folded bedding in the footwall and hanging wall. In the high-grade (Grt-Ky) areas, the contact displays no evidence of S_0, and any premetamorphic fabrics/textures that may have existed are overprinted and annealed; therefore the premetamorphic relationship between the GSG-SG is unclear.

The GSG and SG exhibit a different fold history and fabric development, but are at the same metamorphic grade. Ductile deformation in the form of F_1 tight to isoclinal folding in the footwall (SG) and open folds in the hanging wall (GSG) inferred from bedding orientation characterize fold styles within the study area. Foliation (S_1) generation is not associated with folding of S_0; S_2 is associated with F_2 folds and is the dominant fabric throughout the study area. S_3 is a spaced shear band cleavage that overprints early fabrics through transposition. The overprinting S/C in localized sheared footwall units in close proximity to the contact and is the youngest fabric recognized in the study area. This fabric is the manifestation of late northwest slip of the GSG along the GSG – SG contact.

Mineral assemblages range from biotite to garnet grade along the contact's trace. Biotite at Greenbrier Pinnacle appears to be pre-S_2 , but biotite and garnet at Mount Sterling are the most convincing evidence of peak metamorphism are post-S_2 and static. S_3 is clearly post-peak-metamorphic and can be correlated from biotite to kyanite grade.

Late ductile deformation shearing is observed in the SG near the contact at two localities. No evidence for premetamorphic faulting or shearing along the GSG/SG boundary, or "Greenbrier fault", is recognized. If this boundary is a fault, fault fabrics must have been completely reconstituted during Taconian deformation and metamorphism. However, this is unlikely, due to the pristine appearance of bedding (S_0) at the type locality in close proximity to the contact.

Detailed field mapping, structural analysis, and petrography, focusing on petrofabrics and formation of mineral assemblages, indicate the GSG-SG boundary is the

complicated amalgamation of a folded-faulted contact and conformably folded lithologic contact between metasedimentary assemblages in the GSG and SG.

Chapter 3

Is the Metcalf Phyllite the tectonized equivalent of the Pigeon Siltstone? Geochemical Correlation of Ocoee Supergroup Units

3.1 Introduction

The southern Appalachian Mountains are a composite orogen produced by series of Paleozoic collisional events (Hatcher 1987, 1989). Metamorphic and deformational processes affecting the Laurentian basement and metasedimentary cover strata assemblages began with the late Cambrian Penebscot collisional event and continued through the middle Ordovician Taconian Orogeny, late Devonian/early Missippian Acadian orogeny, and the Pennsylvanian-Permian Alleghanian orogeny (Adams et al., 1995; Drake et al., 1989; Goldberg et al., 1989; Hatcher 1981, 1987, 1989; Rast and Kohles, 1986).

The Great Smoky Mountains region of the southern Appalachians is a subdivision of the Blue Ridge province (Figure 3.1) and is underlain by lithologies constituting the Ocoee Supergroup: Chilhowee, Walden Creek, Great Smoky, and Snowbird Groups. (Figure 3.2) (Hadley and Golsdmith, 1963; King, 1964). Although stratigraphic relationships within each group are reasonably well constrained, the relationship of the Metcalf phyllite to the rest of the Snowbird group has complicated interpretation of Snowbird stratigraphy.

The relationship between the Metcalf phyllite and Pigeon siltstone is particularly problematic. The Metcalf has been proposed to be the tectonized equivalent of the Pigeon siltstone (King, 1964). Hadley and Goldsmith (1963) and King (1964) recognized that the Metcalf phyllite (pCm) shared lithologic characteristics with the Pigeon Siltstone (pCp). King (1964) suggested that the rocks were most likely equivalent, despite the fact that the Metcalf is foliated, folded, and penetratively sheared over most of its extent. Primary sedimentary structures have been obliterated over most of the exposed area of the Metcalf phyllite. King's preliminary chemical analyses of the Metcalf Phyllite and Pigeon Siltstone are geochemically similar , and the two units were differentiated based primarily on the greater degree of deformation of the Metcalf phyllite (King, 1964) (Appendix II, Table 1 King geochemistry). The spatial distribution, correlation, and

mapability along strike suggest an equivalency as well. In areas where the Pigeon siltstone is near faults, it is strongly and pervasively sheared and converted from finely-laminated dull green slaty-cleaved Pigeon metasiltstone into gray-green, muscovite and chlorite-rich phyllite containing several cleavages that characterize the Metcalf Phyllite (Southworth, et al. 2005).

Shearing is the proposed mechanism for deformation and recrystallization of mineral assemblages within the Pigeon siltstone to form the Metcalf phyllite (King, 1964). The focus of this study is a comparison of the two units. The purpose is to test the hypothesis that the Metcalf phyllite is the deformed equivalent of the Pigeon siltstone. The study will employ geochemical, petrologic, petrofabric and field relationships to

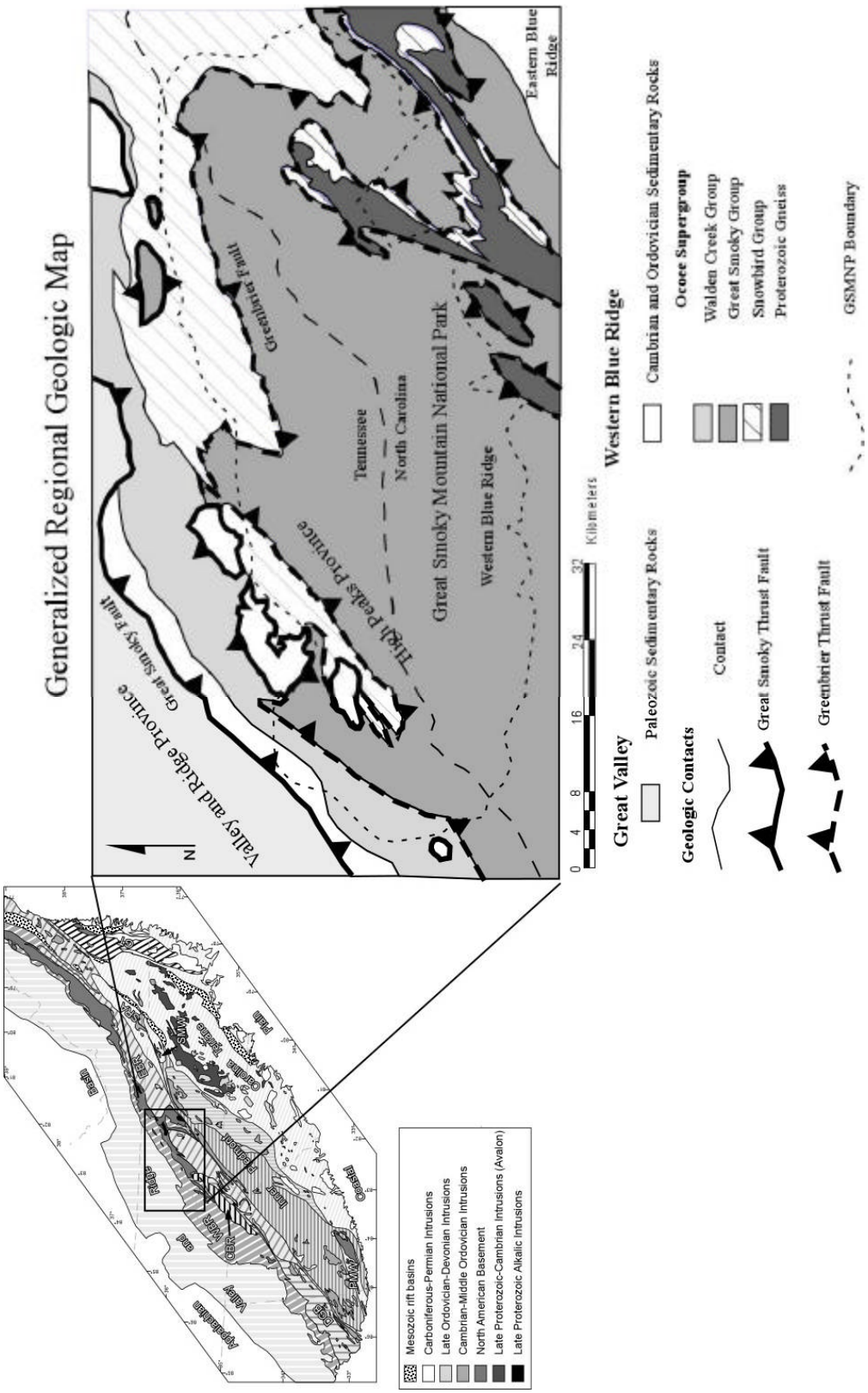

Figure 3.1 – Regional geologic maps showing location of study area.

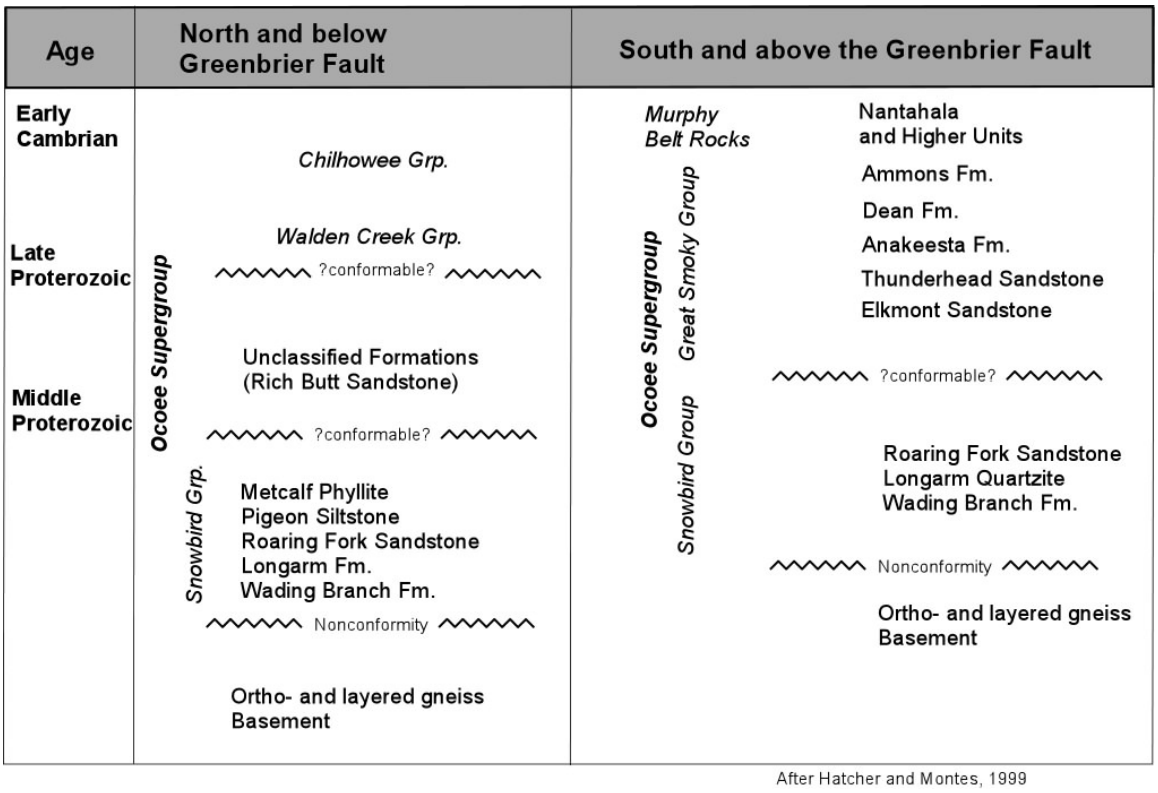

Figure 3.2 - Ocoee Supergroup stratigraphy.

demonstrate that the two units can be correlated and are the same original sedimentary deposit.

3.2 Geologic Setting

Foothills Belt strata of the Great Smoky Mountains are predominantly fine- to coarse-grained clastic rocks of the Neoproterozoic Walden Creek Group, medium- to fine grained sedimentary rocks of the Neoproterozoic Snowbird Group, Lower Cambrian sandstone of the Chilhowee Group, Middle Ordovician Jonesboro Limestone, and metasandstone and metaconglomerate of the Neoproterozoic Great Smoky Group (Southworth et al. 2005). In contrast to the higher-grade metamorphic rocks of the Great Smoky highlands, the rocks in the foothills belt are low-grade greenschist facies or sub-greenschist facies lithologies. Coarse-grained and quartz-rich rocks form the high knobs, such as Webb Mountain, Shields Mountain, Green Mountain, and Chilhowee Mountain, whereas carbonate rocks and siltstones underlie the valleys and coves. The Foothills are bounded on the north by the Great Smoky fault and are bounded to the south by the Gatlinburg fault system (Southworth et al. 2005). The Metcalf phyllite occurs from Gatlinburg, TN to the Cades Cove area in a northeast-southwest trending band (Figure 3.3). It is fault bounded above and below, with Ordovician strata beneath it along the Great Smoky fault, Walden Creek group, beneath it, along the Dunn Creek fault, and it is and overlain by Great Smoky group along the Greenbrier fault. The Pigeon siltstone occurs from Gatlinburg to I-40 in the northeast with the same trend as the Metcalf phyllite (NE-SW) (Figure 3.3). The base of the Pigeon is in fault contact with the Walden Creek group, and it is both conformably overlain by the Rich Butt Sandstone (Snowbird group?) and fault bounded by Great Smoky group strata. The apparent relationship is either a) the Pigeon is faulted over the Metcalf or b) the Metcalf is a structurally lower, tectonized portion of the Pigeon siltstone (Figure 3.3 and 3.4).

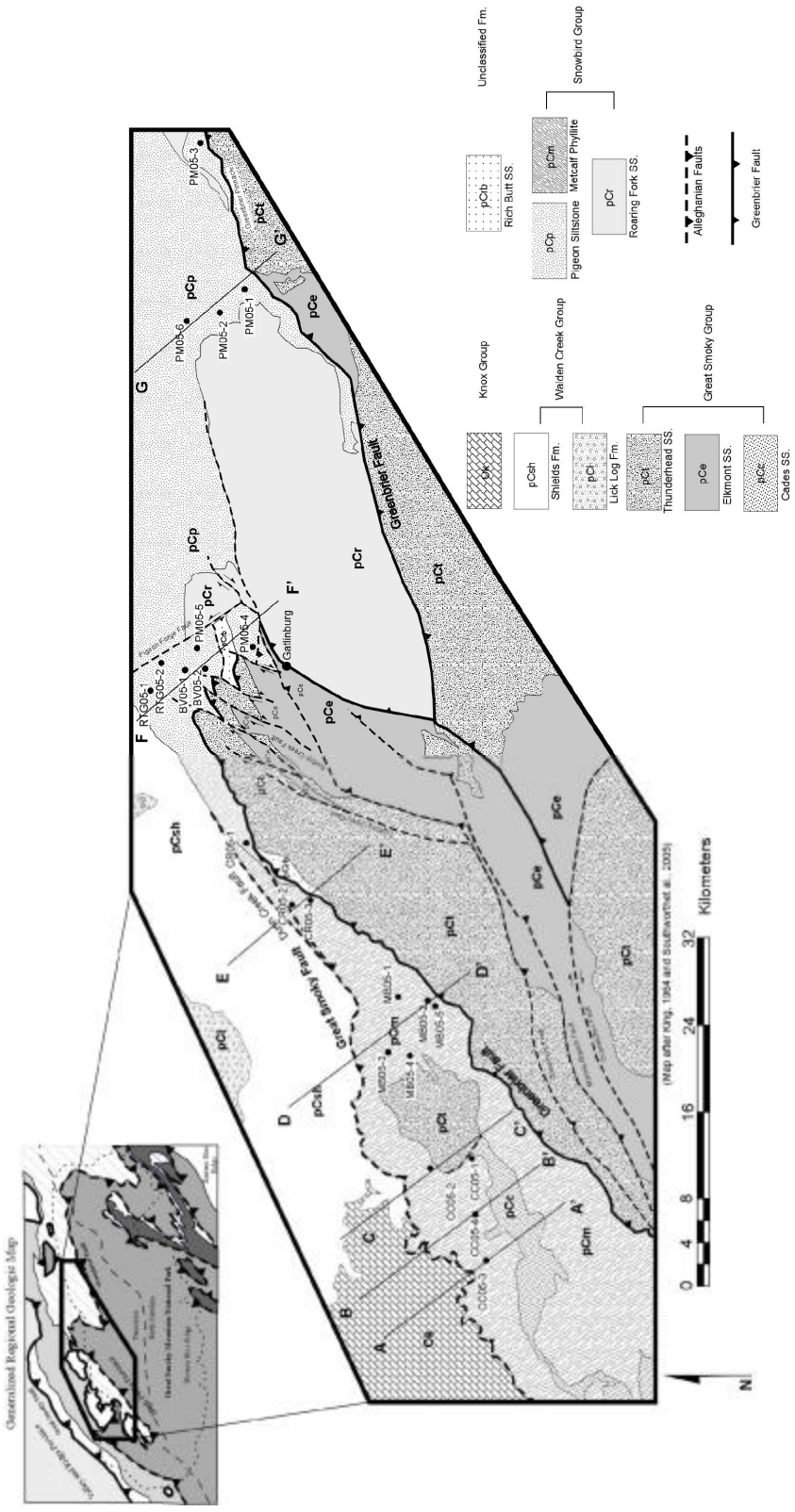

Figure 3.3 - Location of study area, indicated by outline, in relation to (a) regional tectonics (after King, 1964 and (b) local geology (after King, 1964; Southworth et al, 2005).

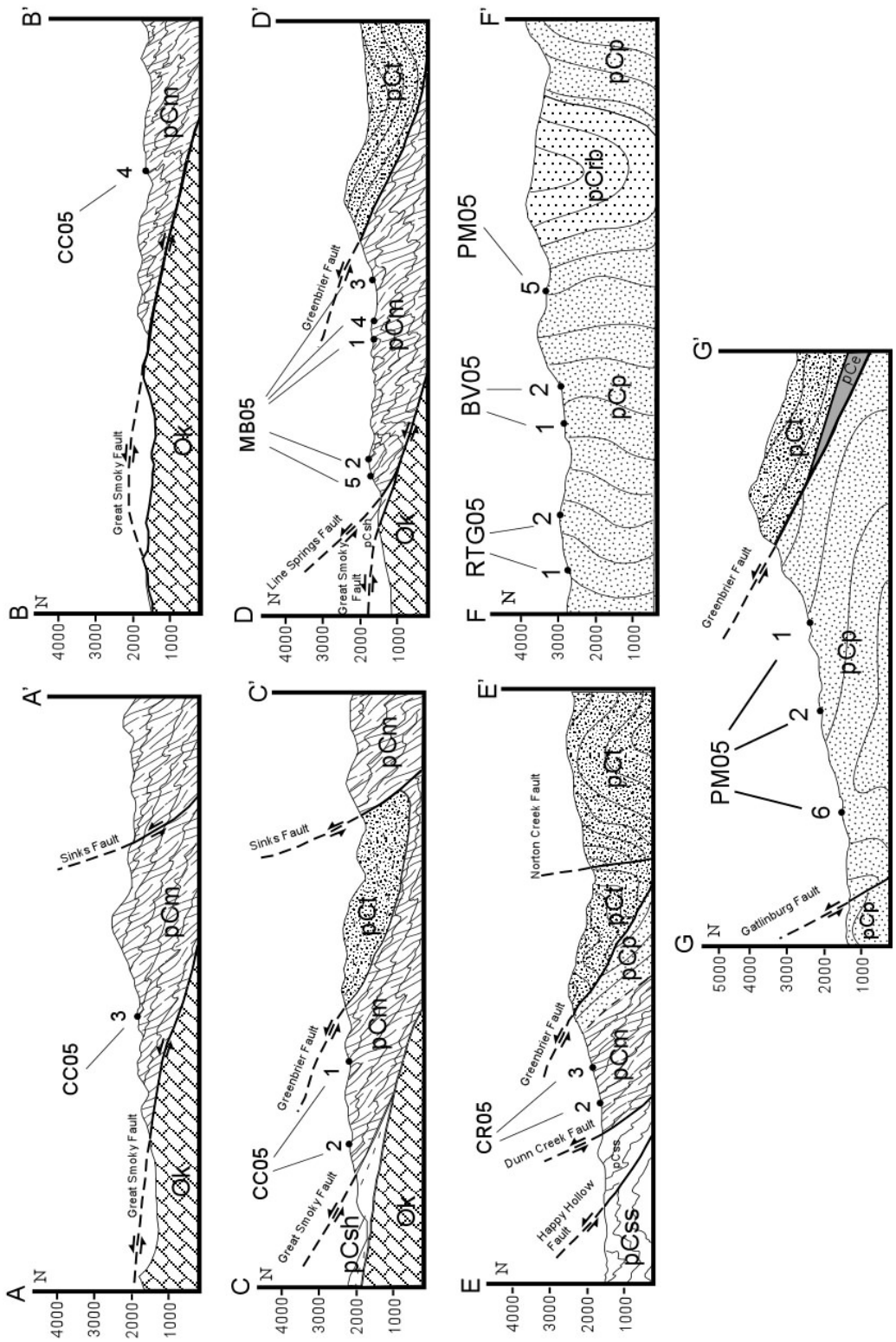

Figure 3.4 - Cross sections (modified from King, 1964, and Hadley and Goldsmith, 1963) perpendicular to strike showing sample locations.

3.3 Lithologic Descriptions

Pigeon Siltstone

The Pigeon siltstone (pCp) is a lithologically homogeneous metasiltstone. It ranges in thickness from 10,000 to 15,000 ft (3050 to 4575 m) (Southworth et al. 2005). It consists of uniform, massive to laminated, greenish-gray metasiltstone characterized by dark and light-colored laminae. The laminated planar beds (S_0) alternate in color from dark green to light green. The lighter more feldspathic and quartzose layers are typically thicker (0.1-0.5 cm) and coarser-grained than the darker layers (0.05-0.3 cm) which were presumably more argillaceous and are now chlorite- and muscovite-rich (Appendix I, Table 1a and b - Petrography). Primary sedimentary structures include planar laminations, small scale cross-laminations and small scale ripple marks (King, 1964; Hadley and Goldsmith, 1963). Beds are not graded (Hamilton, 1961). Metasiltstone consists of silt to very fine-grained quartz and plagioclase (dominant) and potassium feldspar (subordinate) that increase in abundance to the east-southeastward area of outcrop (Hamilton, 1961). Folds in bedding vary from open to tight and isoclinal. The dominant (S_2) foliation is a continuous cleavage oriented northeast-southwest and is defined by the preferred orientation of chlorite and occurs at varying angles to bedding (Figure 3.5). The secondary foliation (S_3) (refer to fabrics in chapter 1) is a shear band cleavage defined by spaced micas rotated into parallelism (Figure 3.6). The Pigeon siltstone thins and coarsens eastward, and it intertongues with the Roaring Fork Sandstone. The upper-most rocks of the Pigeon Siltstone are overlain conformably by the Rich Butt Sandstone in the east. The uppermost units of the Pigeon contain iron-bearing ankerite and calcite (Southworth et al., 2005).

Samples of Pigeon siltstone taken from localities along strike and used for XRF analysis (Appendix II, Table 3 and 4a/b) consist of primary detrital quartz, plagioclase, and alkali-feldspar. Quartz and feldspar grains are rounded to subangular and 0.03 to 0.10 mm in diameter. Trace accessory detrital grains include magnetite, pyrite, sphene, tourmaline and zircon. Metamorphic minerals are dominated by chlorite with lesser amounts of muscovite. Both are very fine-grained (< 0.03 mm) and granoblastic. Bedding is defined by differing grain size and modal proportion of quartz, alkali-feldspar, and plagioclase in alternating light and dark colored layers (Figure 3.7).

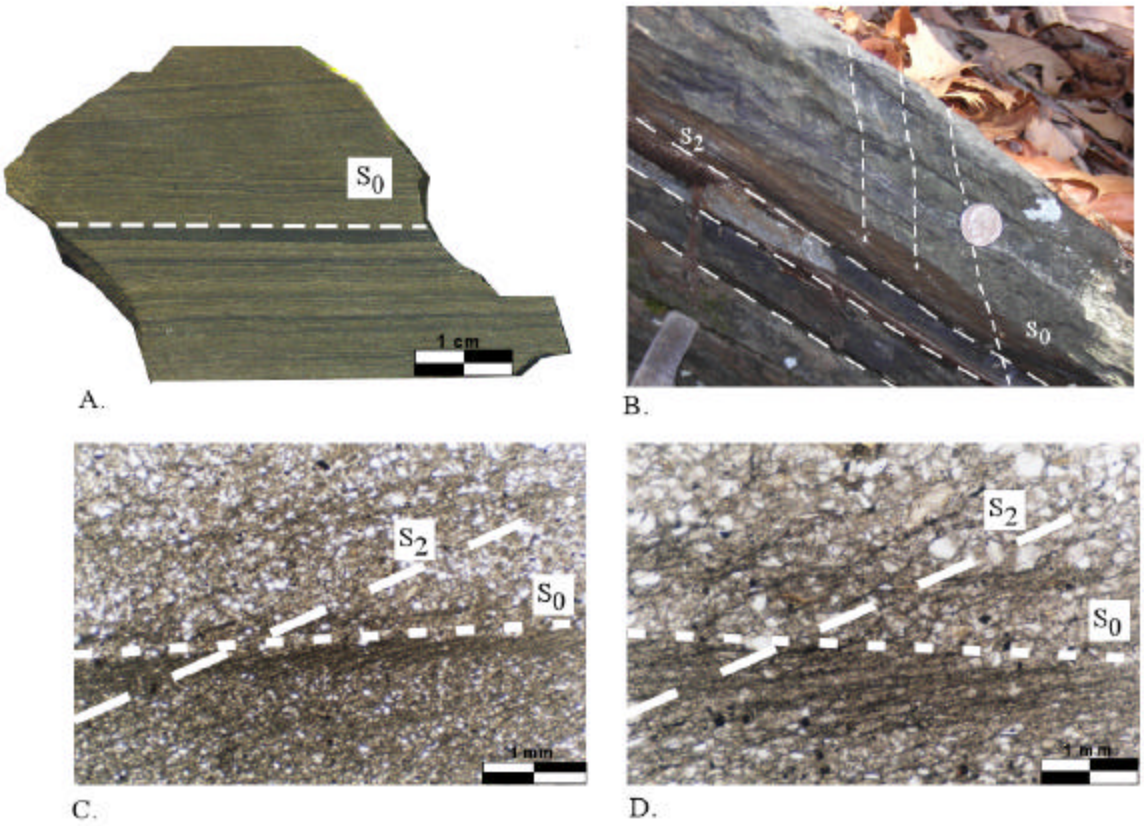

Figure 3.5 - Pigeon siltstone: (A) Hand sample displaying S_0; (B) Mesoscopic S_0 overprinted by S_2, fold style inferred from S_0 orientation and map. C and D: Photomicrographs displaying the relationship between S_0 and S_2. S_2 pressure solution cleavage (thin sections in plane light).

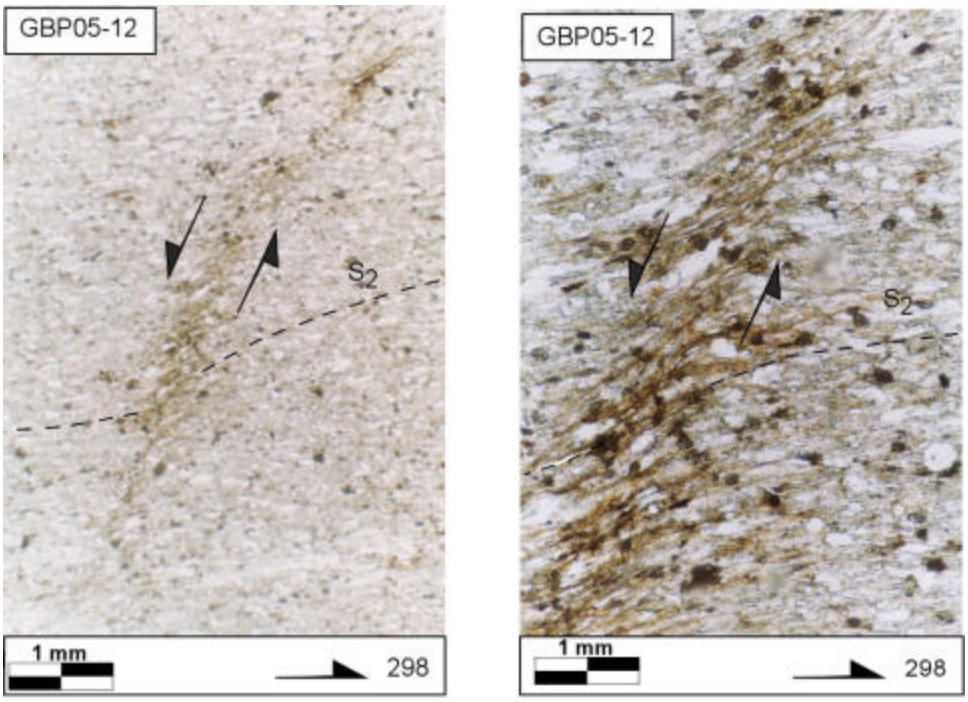

Figure 3.6 – Pigeon siltstone PM05-5. Photomicrographs A and B displaying the relationship between S_0 (fine dash), S_2, and S_3 (shear band cleavage). S_2 has rotated S_0 and S_2 into parallelism with the axial planes of regional folds.

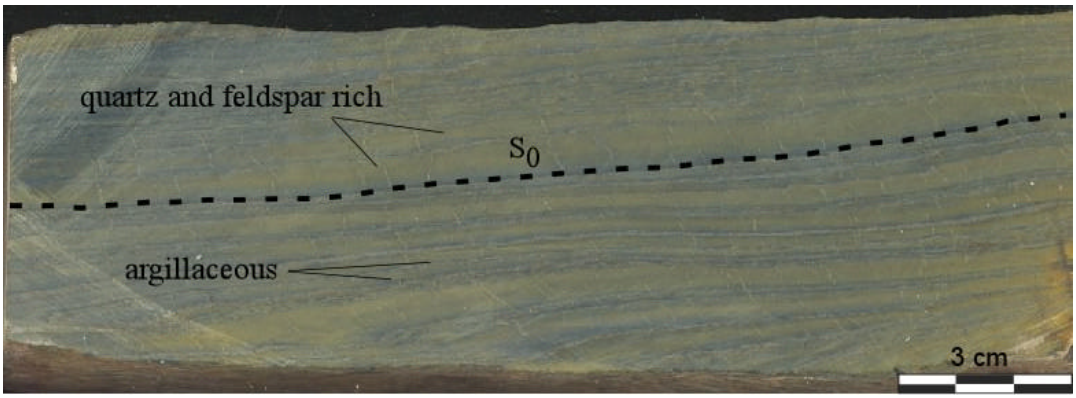

Figure 3.7 - Hand sample from Pigeon siltstone displaying bedding (S_0) defined by differing grain size and modal proportion of quartz, alkali-feldspar, and plagioclase in alternating light and dark colored layers. The lighter layers are feldspathic and quartzose rich and are typically thicker (0.1-0.5 cm) and coarser-grained than the darker layers (0.05-0.3 cm) which were more argillaceous and are now chlorite and muscovite rich.

Metcalf Phyllite

The Metcalf is a greenish-gray, strongly foliated phyllite that displays a well-developed shear-band cleavage exhibiting top-to-the northwest motion with offsets ranging from 0.5 mm – 10 mm (Figure 3.8). Primary laminae (S_0) are defined by differentiation of grain size in argillaceous and silty layers, are tight to isoclinally folded, and are perpendicular to northeast striking faults (e.g. Great Smoky fault, Dunn Creek fault, Line Springs fault). Primary foliation (S_1) is parallel to bedding and is defined by the preferred orientation of muscovite and chlorite. A secondary foliation (S_2) is a disjunctive cleavage that is defined by spaced micas rotated into parallelism with the axial plane of regional scale folds. As in the Pigeon, S_2 has folded and crenulated S_0 and S_2. Iron-oxide along S_2 planes suggests that it may have formed by pressure solution. S_4 is a shear fabric defined by a pervasive deflection of micas, crenulations and S/C structures which parallel the Great Smoky and associated faults. Over most of the extent of the Metcalf, S_4 overprints or completely obliterates S_2 and S_3 (Figure 3.9). In other areas, away from faults where the Metcalf is less deformed, it resembles the Pigeon Siltstone (Figure 2.10).

Samples of Metcalf phyllite from localities along strike and used for XRF analysis (Appendix II, Table 3 and 4a/b), consist of fine grained muscovite and chlorite with subordinate quartz, alkali feldspar, and plagioclase (<0.01 – 0.08 mm). Relict bedding is discernable where the quartz, feldspar, and metamorphic minerals alternate in thin laminae (~ .5 to 1.5 mm thick) (Figure 3.11). All samples display a late shear band cleavage characterized by S_0, S_2 deflected into parallelism with Alleghanian faults (Figure 3.12). Sections from the Caney Creek area (Figure 3.13) have a greater proportion of subangular to subrounded and partly to completely recrystallized quartz and feldspar. These samples have a weak foliation defined by the parallelism of less prevalent chlorite, muscovite, and sericite that cross- cuts bedding. Trace accessory minerals include apatite, pyrite, sphene, tourmaline, and zircon.

^{40}Ar-^{39}Ar analysis of fine-grained white-mica in the Metcalf yields ages of approximately 350 Ma. Southworth et al., (2005) interpret this age to represent muscovite growth during the formation of the shear-band cleavage.

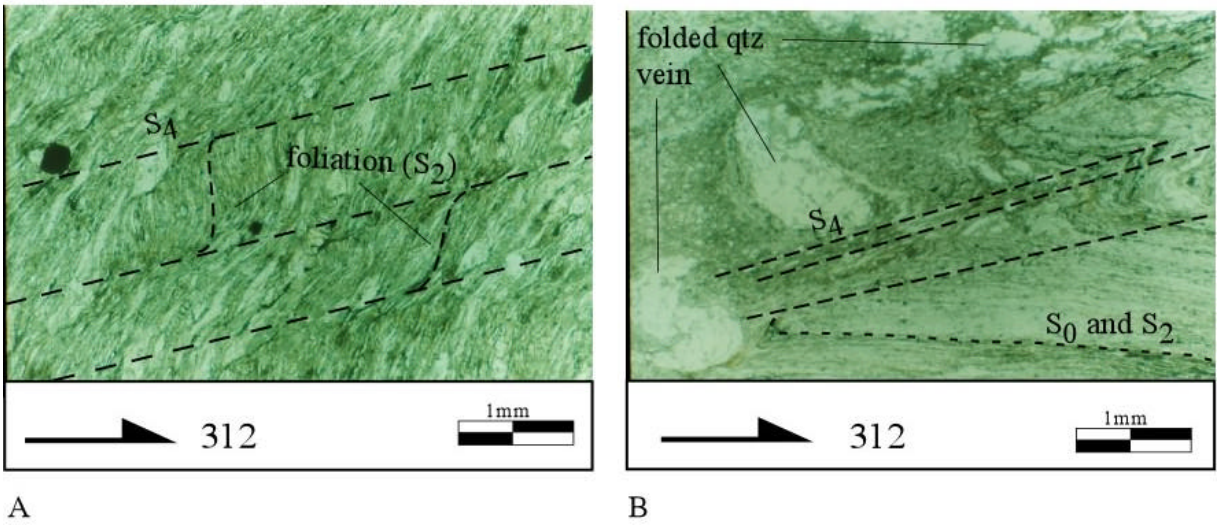

Figure 3.8 (A) Metcalf phyllite displaying shear band cleavage (S_4) exhibiting top-to-the northwest motion with offsets ranging from 0.5 mm – 10 mm. B) CC05-4, S_0 and S_2 sheared and crenulated by S_4.

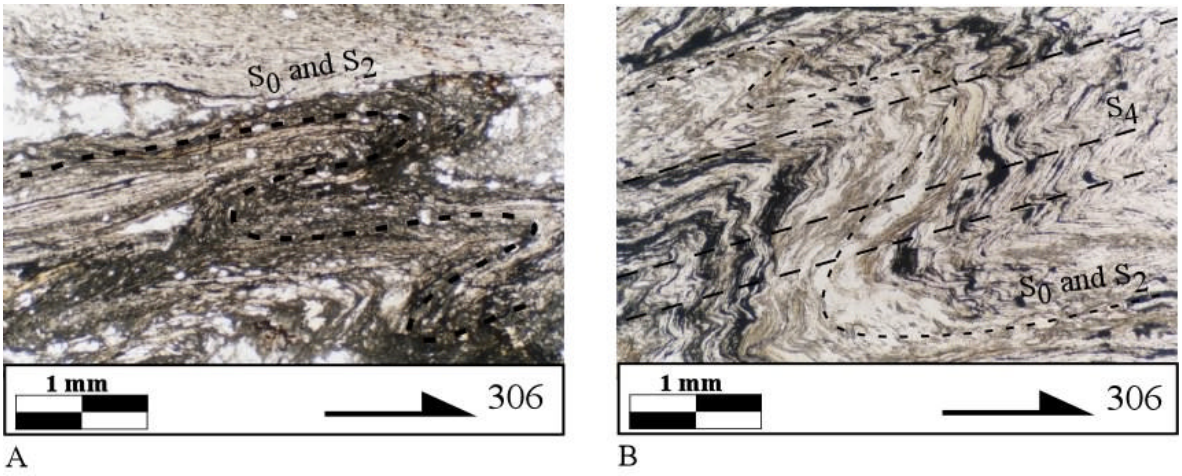

Figure 3.9 – CC05-4, Metcalf displaying folded S_0 and S_2 folded and overprinted by S_4 (S_2 obliterated). (A) Tight fold and (B) tight fold with parallel orientation of S_0, S_2, and S_4 in the limbs and S_4 oblique to S_0/S_2 in the hinges.

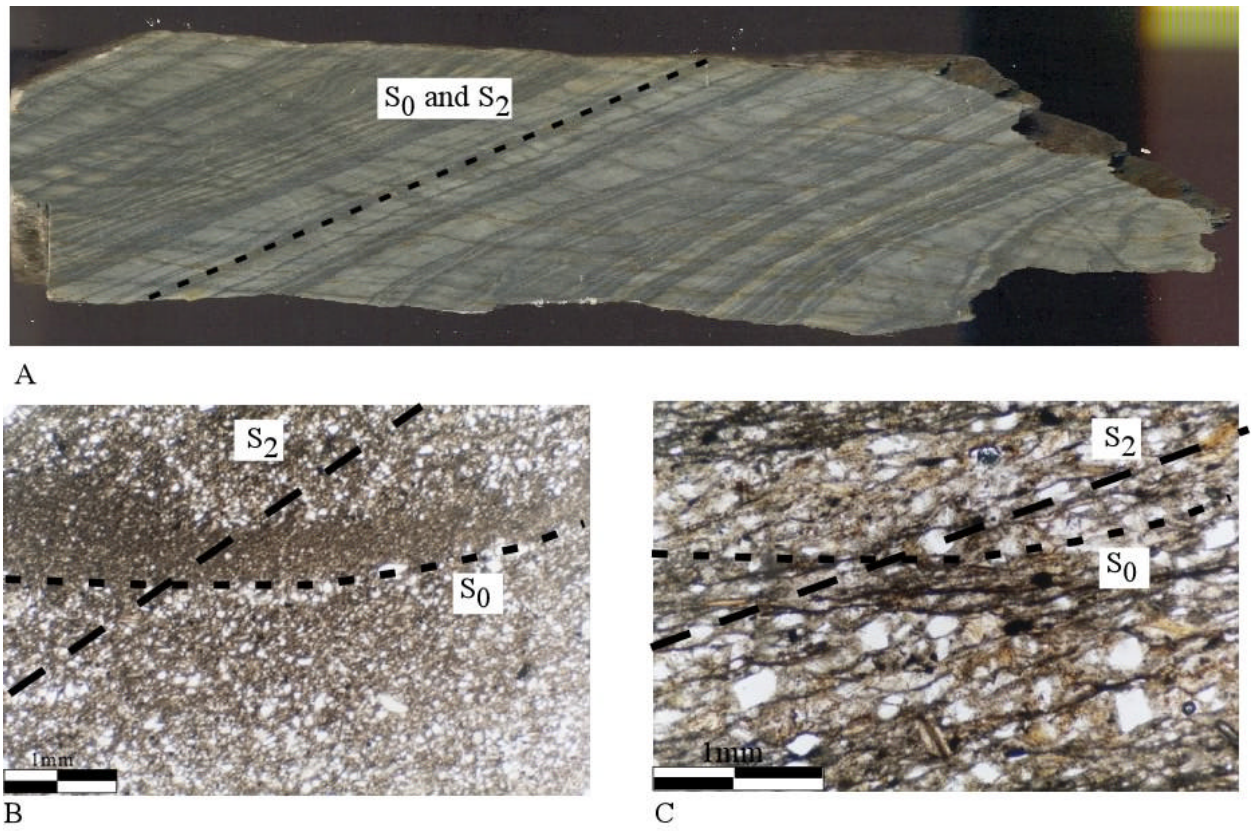

Figure 3.10 (A) MB05-3 slab displaying bedding strongly resembling pCp, B and C: CR05-3, weakly deformed Metcalf phyllite strongly resembling Pigeon siltstone. Iron-oxide in the cleavage suggests that it may have formed by pressure solution.

3.4 X-ray Fluorescence Geochemistry

Methods

XRF analysis of major and selected minor and trace elements permits chemical comparison of the Pigeon siltstone and Metcalf phyllite in order to ascertain if the two lithologies are equivalent and to determine if the Pigeon siltstone is the protolith of the Metcalf phyllite.

X-ray fluorescence was performed at the Kentucky Geological Survey. 22 samples were collected from 11 localities for each formation (Figure 3.3). Samples for geochemical analysis consisted of 10 kg of blocks and chips, collected from the fresh interiors of outcrops. Rock samples were further reduced to 4 cm fragments for crushing. After homogenization, splits of approximately 200 grams of chips were pulverized to a powder in a centrifugal crusher.

Lithium tetraborate-fused disks were used for determination of major and minor element oxides. Samples consisted of a precise 1:9 ratio of 1.125000 ± 0.0003 g of powder to 10.000 ± 0.0003 g of flux. Each mixture was subsequently shaken for 10 minutes to produce a homogeneous mixture and melted in a 1050° C Claisse Disk Fuser furnace to prepare glass disks. Lithium tetraborate pressed pellets were made for analyzing selected trace elements (Ba, Co, Cr, Cu, Mo, Nb, Rb, Sr, Vn, Y, Zn and Zr). Pressed sample preparation involved combining 3 grams of sample with 6 grams of flux. This mixture was pressed into pellets using a Carver Laboratory Press. Calibration used USGS standards GSP-2, MRG-1, and MGR-1; and CCRMP (Canadian Certified Reference Materials Project) standard WCB-1. The results of the XRF whole-rock analyses are reported in Appendix I, Tables 3 and 4a and b. These data are presented as chemical discrimination plots in Figures 3.13 and 3.14. Rock densities were measured on a Mettler H54AR balance with chips used for thin section preparation. These data are presented in Appendix II, Table 5.

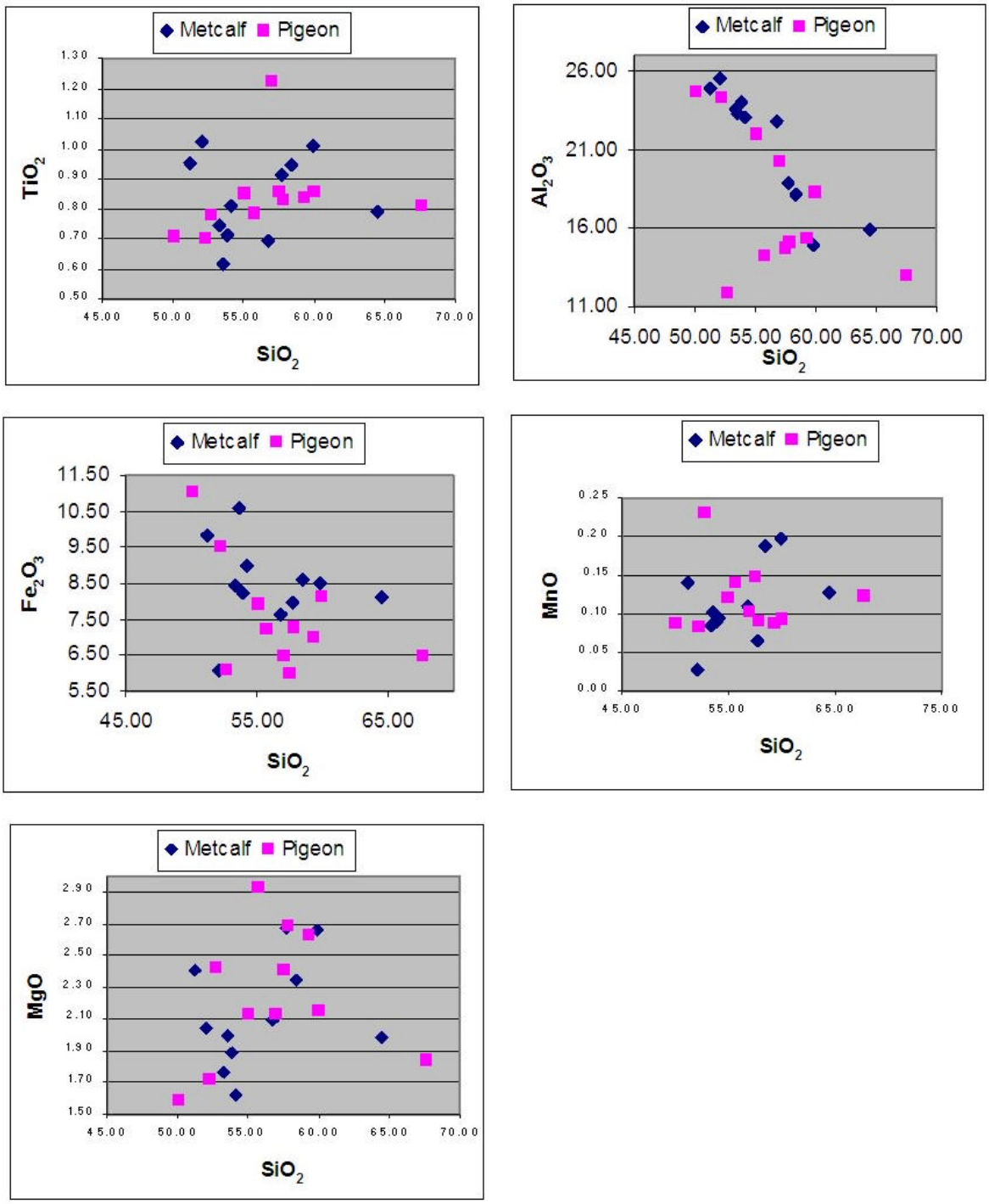

Figure 3.11 - Chemical discrimination plots for selected major and minor elements.

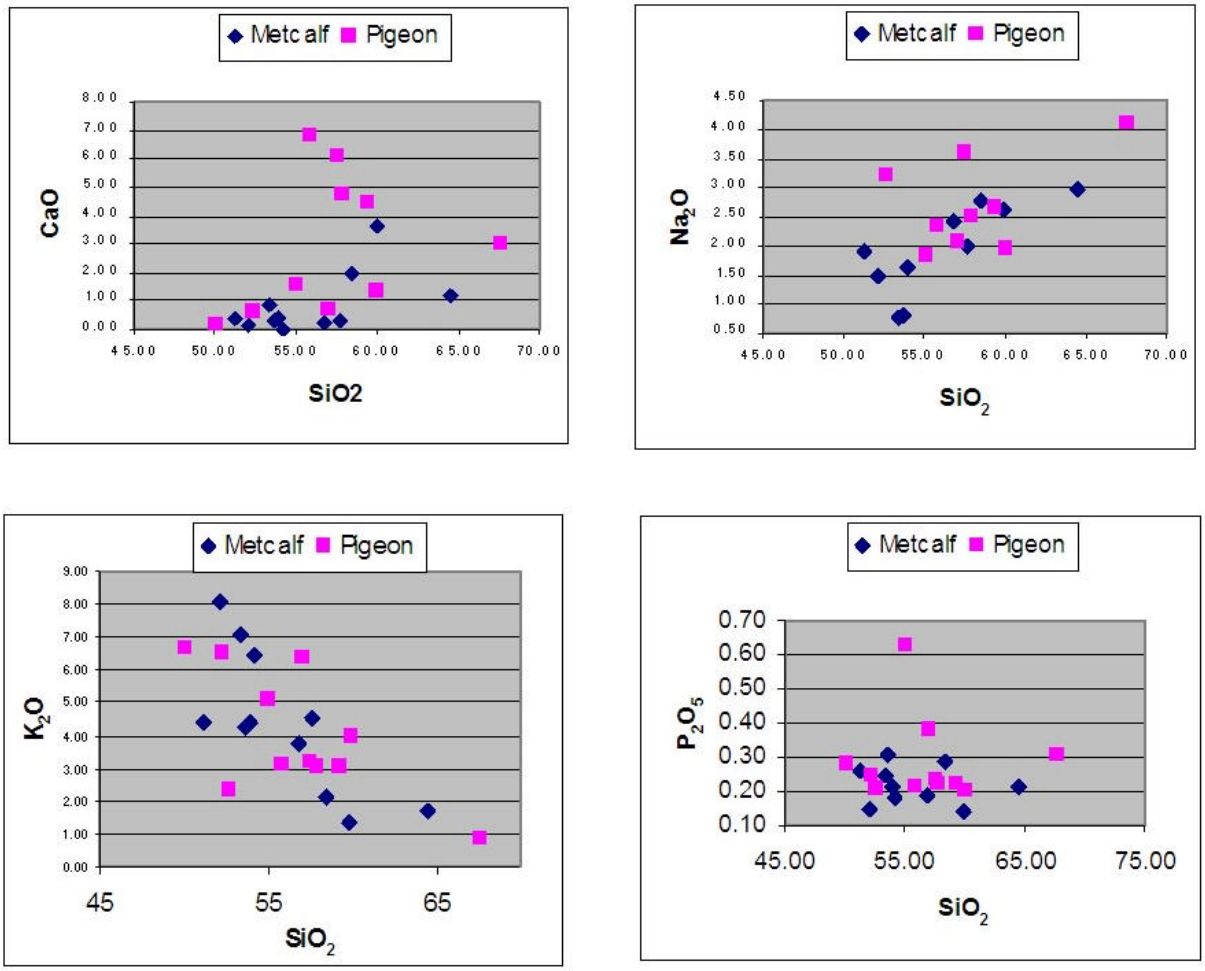

Figure 3.12 - Chemical discrimination plots for selected major and minor elements.

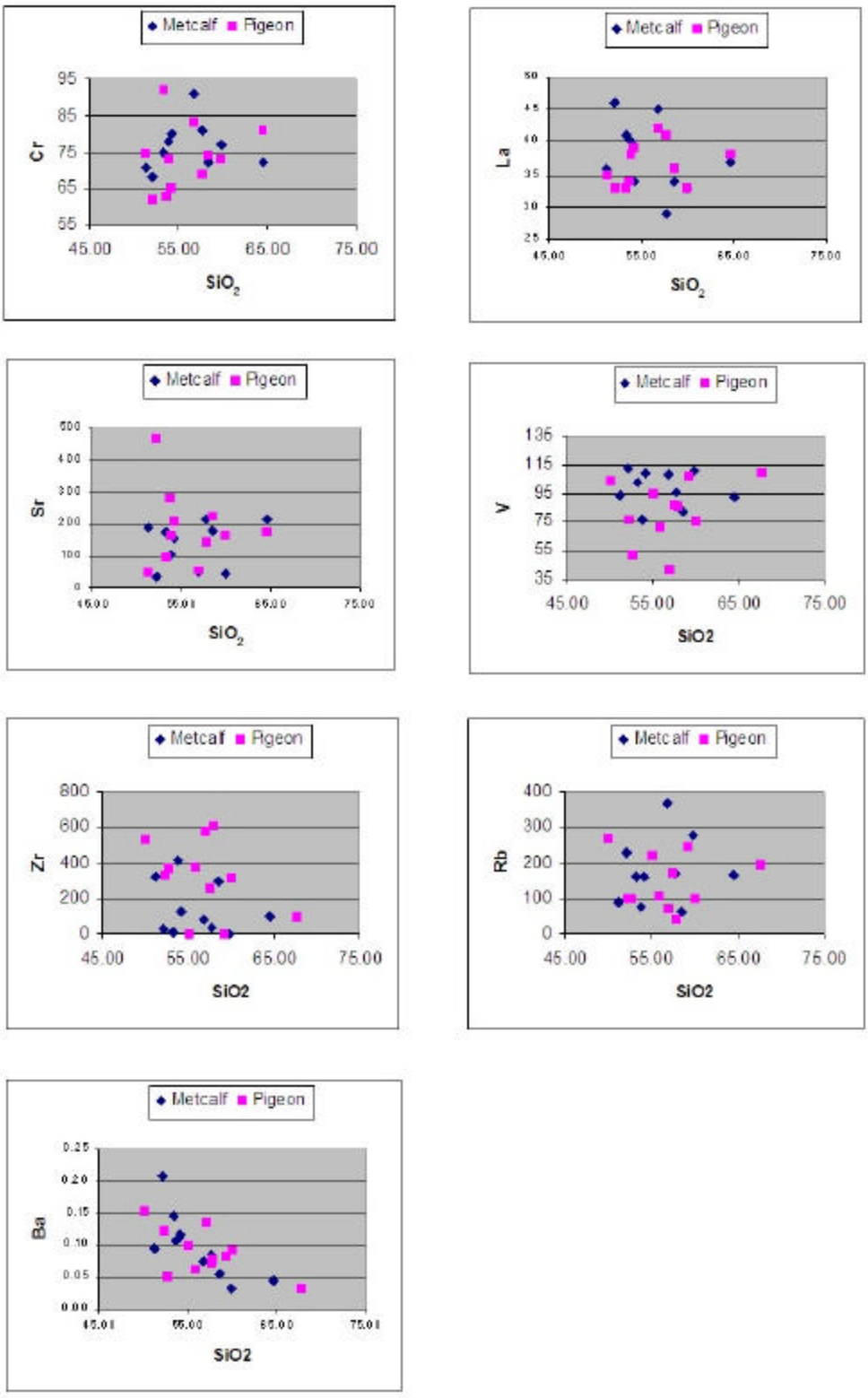

Figure 3.13 - Chemical discrimination plots for trace elements.

3.5 Results

Whole Rock Geochemistry

With the exception of CaO, mean values for the major oxides examined in this study, are broadly similar (within the statistical error calculated in Appendix I Tables 6a, b, c, and d) in the Pigeon siltstone and the Metcalf phyllite. There tends to be slightly lower elemental variability in the Metcalf, as indicated by the lower standard deviations of averages and scatter on the discrimination plots.

Discrimination plots for TiO_2, MnO, MgO, and K_2O versus SiO_2 (Figure 3.13) reveal a wide range of scatter in the data for individual samples for both lithologies, however there is significant overlap of values between lithologies. The discrimination plots of Al_2O_3 vs. SiO_2 exhibits linearity for the Metcalf but significant variation within the Pigeon. Figure 11 shows CaO vs. SiO_2 and possible linear relationship in the Metcalf, whereas the Pigeon displays scatter and is enriched in CaO. Patterns for Na_2O versus SiO_2 show a similar trend, however, the error within the measurement of Na_2O is significant enough to make an interpretation problematic. Discrimination plots for trace elements display a similar amount of scatter, but as with the major elements, there is significant overlap between the two lithologies. The scatter about this line may be due to a combination of analytical uncertainty, Pigeon siltstone (protolith) heterogeneities, and selective mobility of some elements.

Isochon analysis (O'Hara and Blackburn, 1988; O'Hara, 1990) indicated depletion of CaO and Zr in the Metcalf relative to the Pigeon. With the exception of these two elements, there was no significant enrichment or depletion of major or trace elements in either unit (Figure 2.14). The sheared Metcalf phyllite is not depleted in elements such as TiO_2, P_2O_5, Y, V, La, and Ce or in SiO_2 in comparison to the Pigeon siltstone. The apparent immobile element of Zr can be accounted for by point counting the amount of detrital zircon in each lithology.

Zircon abundance was calculated by counting four random areas on each thin section of the Pigeon siltstone and the Metcalf phyllite and examining these areas at 10x magnification on a petrographic microscope. This method of zircon grain counting revealed the Pigeon siltstone contained significantly higher amounts of zircon grains than the Metcalf phyllite (Appendix I, Table 7). Also, detrital grain size in the Metcalf is typically much finer than in the Pigeon. To

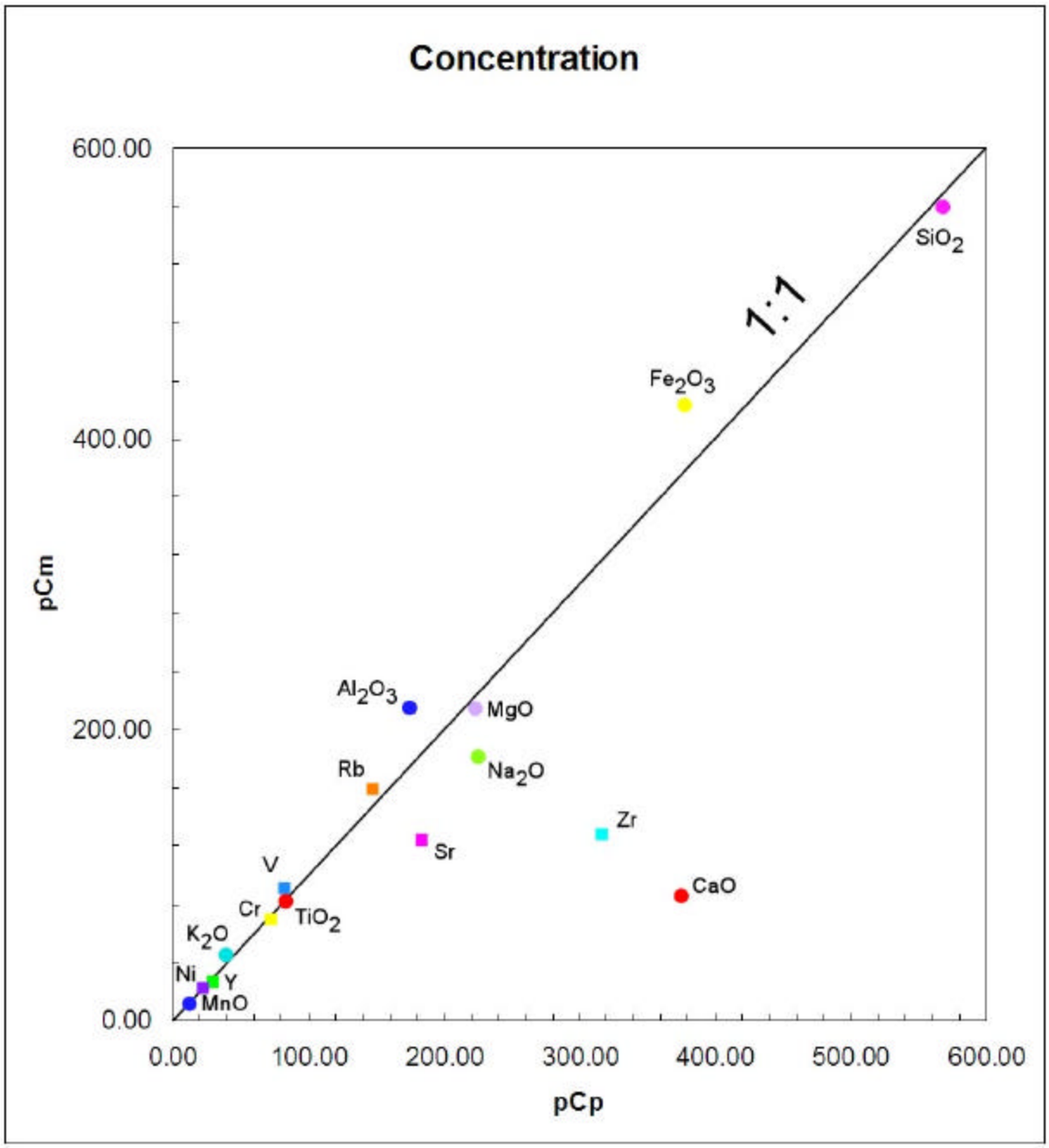

Figure 3.14 – Isochon plot of average concentration of "immobile trace elements (Ti, Zr, Y, Mn, and V) and selected major elements averages in the Pigeon siltstone vs. average concentration in the Metcalf phyllite. The 1:1 line represents the slope of the line if there was no change in mass. Based on data from Tables 3, 4a, and 4b, arbitrarily scaled to fit on the diagram.

test this method of grain counting, it is recommended that further counting be performed using a back scatter electron imaging or Zr x-ray mapping on the electron microprobe.

Rock density measurements revealed a mean density (?) of 2.77 for the Pigeon siltstone (standard deviation 0.034) and a mean density (?) of 2.78 for the Metcalf phyllite (standard deviation 0.034) (Appendix 2, Table 5).

The relationship between trace element enrichment and finite strain in the context of fluid-rock interaction may be assessed through isochon analysis. By mass balance, the change in the concentration of an element in a fluid-rock system is given by: (1) $C_iM_i = C_w(M_i - M_r) + C_fM_f$, where C_i and C_f refer to initial and final concentrations, and M_i and M_f refer to initial and final masses in the rock, respectively. C_w refers to the concentration in the fluid. If, however, the element in question is assumed to be immobile, then C_w will be close to zero. Because there is no density change between the lithlogies (Appendix 2, Table 7), equation (1) reduces to: (2) $C_iV_i=C_fV_f$ where V refers to volume. In terms of the more familiar dilation which is defined as: $? = (V_f - V_i)/V_i$, equation (2) can be rewritten as: (3) $C_f/C_i = 1/(1 + A)$ or (4) $C_f/C_i = 1/[(1 + e_x)(1 + e_y)(1 + e_z)]$, where e_x, e_y and e_z are the maximum, intermediate and minimum principal finite elongations, respectively. C_f/C_i is an enrichment factor and graphically it represents the slope of the best-fit line to immobile trace element data on a plot of the concentration in the protolith versus the concentration in the deformed rock (O'Hara, 1990).

Petrographic examination revealed a much higher modal percentage of quartz in the Pigeon than in the Metcalf (Table 1a and 1b). Alkali-feldspar and plagioclase were slightly less abundant in the Metcalf. Modal percentage of muscovite was more than two times greater in the Metcalf than in the Pigeon. Chlorite was three times greater in the Pigeon compared to the Metcalf.

Discussion

Geochemically, the Pigeon and Metcalf formations are nearly identical, with the exception of CaO and Zr being lower in the Metcalf relative to the Pigeon. This is strong supporting evidence for the hypothesis that the Pigeon is the protolith of the Metcalf. The minor differences in whole-rock chemistry can be attributed to the solubility of Ca and Zr in

intergranular fluids during faulting/shearing of the Pigeon siltstone. With the exception of these two elements, rock density and isochon analysis indicate geochemical changes and metamorphic reactions during shearing were nearly isovolumetric. If volume changes were occurring during deformation, then mobile elements such as Na, Ca, and K, and to a much lesser extent Si should be depleted in the tectonized Metcalf, while trace immobile elements should be equal when compared with samples in both populations. The former condition is clearly not the case, but the latter is consistent with generally isochemical deformation.

Dynamic metamorphic reactions related to shearing in the Pigeon siltstone in the hanging wall of the Great Smoky and associated faults created the Metcalf phyllite and its S-tectonite character. Deformation-induced breakdown of potassium-feldspar and plagioclase in the Pigeon siltstone resulted in formation of white mica in the Metcalf phyllite and can be explained qualitatively by reactions such as:

- (Sodic Plagioclase + H_2O ? Paragonite + SiO_2 + Ca^{++})
- (K-feldspar + H_2O^+ ? Musc + SiO_2)
- ($KAlSi_3O_8$ + $NaAl_2Si_3Al(OH)_{10}(OH)_2$? $NaAlSi_3O_8$ + $KAl_2Si_3AlO_{10}(OH)$)

Ca and Na originate in plagioclase (An/Ab solid solution), but only Na is accommodated in the muscovite in solid solution as paragonite component. This may account for the lack of Na_2O depletion in the Metcalf. Microprobe analysis of muscovite would permit testing of this hypothesis.

Zircon is the only Zr-rich phase in these two units and while Zr is commonly cited as being an immobile element, on average it varies between the Metcalf and the Pigeon (Fig. 2.13, 3.14). Normally, zircon is highly insoluble in most hydrous metamorphic fluids, but high strain combined with fluid flow may have caused it to be dissolved in the Pigeon and removed from the system. Zircon grain counts made using the method outlined above support the geochemical evidence revealed by the XRF analysis that Zr was removed from the Metcalf during deformational shearing. This hypothesis is plausible based on experimental data by Ayers and Watson (1991) and Liermann et al. (2002). In a high pressure environment, zircon is soluble in aqueous fluids and rising temperature. Pressure has also been shown to have a marked effect on

zircon solubility by Manning (1998) and Philippot and Selverstone (1991) as evidenced by Zr mobility and the formation of Zr phases as daughter minerals in fluid inclusions from eclogites.

The major, minor and trace element geochemistry of metasedimentary rocks are influenced by provenance, weathering, transport, sedimentation and metamorphism. Easily soluble elements (Ca, Na, and Sr) are mobile in the presence of fluids and/or during deformation. Their removal from a system during metamorphism may result in the formation of new mineral assemblages. Concentrations of these elements can also be used to measure volume loss by calculating the relative enrichment in relatively insoluble elements and the depletion of soluble elements. Other parameters, e.g., Al_2O_3/SiO_2 reflect the composition of the former sediments. Because of their relative low mobility during sedimentary processes and relatively stable behavior during metamorphism, major and trace elements such as Al, Ti, Zr, Sc, and Cr can be used to constrain the tectonic setting of sediment deposition. These processes lead to typical chemical signatures in metasediments. This signature has been used to confidently correlate the Pigeon siltstone with the metamorphosed Metcalf phyllite.

3.6 Conclusions

Major and trace elements are virtually identical between the lithologies with the exception of CaO and Zr. The system appears to have been open with respect to Ca, Zr, and possibly Na during shearing and these elements were likely removed by intergranular fluids during deformation (Figure 3.4). Quartz in the Metcalf displays evidence for dynamic recrystallization and together with the secondary mineral assemblages suggest that deformation occurred at temperatures of 300° C to 500° C in the presence of a fluid. Evidence supporting the hypothesis that the Metcalf phyllite is the tectonized equivalent of the Pigeon Siltstone include: (a) where the Metcalf is higher within the footwall (farther from the Great Smoky fault) it is much less deformed and resembles the Pigeon and samples of Metcalf farther away from the Great Smoky and other bounding faults that are almost indistinguishable petrographically from the Pigeon siltstone, and (b) rock densities for both units are identical.

Appendix 1 – Geochemical and petrographic analyses.

Table 1a. - Estimated modal composition of the Pigeon siltstone.

Table 1a – Estimated Modal Composition of the Pigeon Siltstone											
	PM05-1	PM05-2	PM05-3	PM05-4	PM05-5	PM05-6	RTG05-1	RTG05-2	BV05-1	BV05-2	CR05-1
Detrital minerals											
Quartz	39	42	37	38	41	40	33	37	45	37	39
Feldspar	10	15	7	15	8	12	10	10	7	10	12
Sphene	trace	trace	Trace	trace	trace	trace	trace	trace	trace	trace	trace
Apatite	trace	-	Trace	-	-	trace	-	trace	trace	-	-
Zircon	-	-	Trace	trace	trace	-	-	trace	-	trace	trace
Tourmaline	trace	1	1	1	trace	1	1	trace	1	trace	-
Opaque phase	3	1	5	2	4	2	2	3	1	2	3
Metamorphic minerals											
Muscovite	14	9	18	15	15	13	15	24	18	17	10
Chlorite	30	32	32	30	30	28	36	25	25	33	35

Table 1b - Estimated modal composition of the Metcalf phyllite.

Table 1b – Estimated Modal Composition of the Metcalf Phyllite											
	CC05-1	CC05-2	CC05-3	CC05-4	CR05-1	CR05-2	MB05-1	MB05-2	MB05-3	MB05-4	MB05-5
Detrital minerals											
Quartz	15	18	21	16	12	24	20	15	18	18	15
Feldspar	8	10	10	7	8	12	10	10	7	10	12
Sphene	trace	trace	trace	trace	trace	trace	trace	trace	trace	trace	trace
Apatite	-	-	trace	-	-	-	-	-	-	-	-
Zircon	-	-	trace	-	trace	-	-	trace	-	-	trace
Tourmaline	trace	-	-	trace	trace	-	-	trace	-	trace	-
Opaque phase	5	1	2	2	2	2	2	5	1	2	3
Metamorphic minerals											
Muscovite	55	55	55	56	69	48	60	58	65	58	62
Chlorite	8	10	9	16	8	10	6	7	8	10	8
Biotite	-	-	-	-	-	-	-	-	-	trace	-
Calcite	3	3	1	-	-	-	-	4	-	-	-

Appendix 2. Geochemical Analyses.

Table 2- King Chemical analysis of Metcalf phyllite and Pigeon siltstone (King, 1964).

Sample	*SiO_2*	*TiO_2*	*Al_2O_3*	*Fe_2O_3*	*MnO*	*MgO*	*CaO*	*Na_2O*	*K_2O*	*P_2O_5*	*FeO*	*CO_2*	*ZrO_2*	*S*	*C*
pCm	55.52	1.06	21.43	0.65	0.12	2.62	1.31	1.62	3.60	0.22	6.76	0.38	0.00	0.00	0.00
pCp	56.28	0.81	21.36	0.94	0.11	2.21	1.16	1.52	4.92	0.24	6.04	0.03	0.00	0.00	0.00

Table 3 – Major and minor element analysis, in percent, of Metcalf phyllite and Pigeon siltstone.

Sample	CC05-1	CC05-2	CC05-3	CC05-4	CR05-2	CR05-3	MB05-1	MB05-2	MB05-3	MB05-4	MB05-5
	pCm	pCm	pCm	pCm	pCm	pCm	pCm	pCm	pCm	pCm	pCm
Location	N 35.6390º W 83.7235º	N 35.6403º W 83.7192º	N 356614º W 83.7059º	N 35.6738º W 83.6942º	N 35.7474º W 83.5624º	N 35.7420º W 83.5658º	N 35.6717º W 83.6390º	N 35.6717º W 83.6390º	N 38.6724º W 83.6570º	N 38.6772º W 83.6549º	N 35.6710º W 83.6394º
SiO2 (%)	59.90	51.24	52.10	64.52	57.70	53.34	58.46	54.18	56.78	53.89	53.63
TiO2 (%)	1.01	0.95	1.02	0.79	0.91	0.75	0.94	0.81	0.69	0.71	0.62
Al2O3 (%)	14.97	24.92	25.49	15.88	18.92	23.60	18.17	23.11	22.83	24.10	23.31
Fe2O3 (%)	8.47	9.86	6.07	8.15	7.98	8.45	8.63	8.97	7.64	8.24	10.56
MnO (%)	0.20	0.14	0.03	0.13	0.06	0.08	0.19	0.09	0.11	0.09	0.10
MgO (%)	2.66	2.41	2.05	1.98	2.68	1.77	2.34	1.63	2.10	1.89	2.00
CaO (%)	3.61	0.38	0.16	1.16	0.29	0.85	1.95	0.00	0.24	0.37	0.30
Na2O (%)	2.61	1.90	1.49	2.98	1.97	0.79	2.79	0.43	2.41	1.64	0.82
K2O (%)	1.37	4.36	8.11	1.73	4.56	7.09	2.14	6.43	3.75	4.43	4.23
P2O5 (%)	0.14	0.26	0.15	0.22	0.24	0.25	0.29	0.18	0.18	0.21	0.31
Sr (%)	0.02	0.02	0.00	0.01	0.00	0.00	0.02	0.00	0.02	0.02	0.02
Ba (%)	0.03	0.09	0.21	0.05	0.09	0.15	0.06	0.12	0.08	0.11	0.11
*LOI**	5.27	4.26	4.69	3.34	4.14	4.02	4.30	5.28	3.93	4.39	4.64
Total	100.25	100.79	101.56	100.93	99.53	101.13	100.27	101.24	100.77	100.09	100.63
Sample	PM05-1	PM05-2	PM05-3	PM05-4	PM05-5	PM05-6	RTG05-1	RTG05-2	BV05-1	BV05-2	CR05-1
	pCp	pCp	pCp	pCp	pCp	pCp	pCp	pCp	pCp	pCp	pCp
Location	N 35.7687º W 83.4026º	N 35.7775º W 83.4054º	N 35.7819º W 83.2180º	N 35.7179º W 83.5013º	N 35.7549º W 83.5245º	N 35.7870º W 83.4076º	N 35.7180º W 83.5596º	N 35.6730º W 83.5734º	N 35.7521º W 83.5311º	N 35.7494º W 83.5314º	N 35.7671º W 83.5297º
SiO2 (%)	60.04	55.09	57.05	57.54	67.65	50.15	55.81	57.87	59.34	52.31	52.73
TiO2 (%)	0.86	0.85	1.22	0.85	0.81	0.71	0.79	0.83	0.83	0.70	0.78
Al2O3 (%)	18.31	21.96	20.18	14.69	12.92	24.61	14.26	15.08	15.36	24.28	11.88
Fe2O3 (%)	8.13	7.90	6.49	5.99	6.44	11.01	7.20	7.26	7.01	9.53	6.07
MnO (%)	0.09	0.12	0.10	0.15	0.12	0.09	0.14	0.09	0.09	0.08	0.23
MgO (%)	2.16	2.13	2.13	2.41	1.84	1.58	2.93	2.69	2.63	1.72	2.42
CaO (%)	1.38	1.62	0.73	6.08	2.98	0.15	6.77	4.72	4.46	0.67	11.63
Na2O (%)	1.94	1.84	2.07	3.61	4.12	0.23	2.36	2.49	2.66	0.13	3.20
K2O (%)	3.98	5.09	6.40	3.17	0.82	6.66	3.09	3.03	3.06	6.54	2.33
P2O5 (%)	0.20	0.62	0.38	0.24	0.31	0.28	0.21	0.22	0.22	0.24	0.21
Sr (%)	0.02	0.01	0.01	0.02	0.02	0.00	0.03	0.02	0.02	0.00	0.06
Ba (%)	0.09	0.10	0.13	0.07	0.03	0.15	0.06	0.08	0.08	0.12	0.05
*LOI**	5.87	4.49	7.81	3.58	3.57	3.01	6.78	3.00	4.88	7.66	6.21
Total	103.06	101.82	104.70	98.38	101.64	98.63	100.43	97.38	100.64	103.98	97.79

Table 4a - Trace element analysis, in ppm, of Metcalf phyllite.

Sample	CC05-1	CC05-2	CC05-3	CC05-4	CR05-2	CR05-3	MB05-1	MB05-2	MB05-3	MB05-4	MB05-5
	pCm	pCm	pCm	pCm	pCm	pCm	pCm	pCm	pCm	pCm	pCm
Ba	324	942	1850	499	550	1091	736	1186	1210	1316	1103
Co	25	29	17	26	26	24	23	24	30	23	27
Cr	72	80	91	78	71	68	72	81	75	77	76
Cu	15	38	7	19	21	31	11	29	49	26	27
La	34	34	45	40	36	46	37	29	41	33	36
Mo	0	0	23	0	0	0	0	5	3	15	0
Nb	14	14	14	17	17	14	14	11	10	15	13
Ni	28	28	23	19	26	29	21	19	16	23	18
Pb	9	37	6	15	16	17	11	43	11	22	35
Rb	62	161	370	77	89	230	165	171	163	277	189
Sr	181	156	51	104	190	37	216	213	177	43	70
Th	10	11	17	10	10	13	12	12	12	14	11
U	6	0	0	2	0	0	0	0	0	0	0
V	82	109	108	77	93	113	92	96	102	110	99
Y	26	30	35	29	28	31	28	29	28	34	154
Zn	152	139	98	191	160	158	121	125	139	96	68
Zr	294	127	85	417	320	29	95	40	6	3	294

Table 4b - Trace element analysis, in ppm, of the Pigeon siltstone.

Sample	PM05-1	PM05-2	PM05-3	PM05-4	PM05-5	PM05-6	RTG05-1	RTG05-2	BV05-1	BV05-2	CR05-1
	pCp	pCp	pCp	pCp	pCp	pCp	pCp	pCp	pCp	pCp	pCp
Ba	939	919	1258	661	247	1532	806	1232	796	535	409
Co	25	22	17	17	20	29	19	25	20	19	15
Cr	81	69	92	74	65	83	73	75	73	63	62
Cu	29	30	3	11	20	55	14	34	22	16	14
La	38	41	33	36	39	42	33	35	38	34	33
Mo	7	0	17	3	0	13	1	6	1	0	0
Nb	15	16	16	14	16	12	14	16	13	11	8
Ni	26	26	27	22	19	30	26	25	24	26	21
Pb	8	30	12	12	8	6	12	24	12	13	12
Rb	171	195	268	109	39	246	100	222	98	98	74
Sr	173	146	94	225	209	54	165	48	167	282	469
Th	12	12	14	11	10	13	11	13	11	10	10
U	0	0	0	3	4	0	2	0	1	0	0
V	87	109	103	71	86	107	76	94	77	52	42
Y	29	33	33	28	28	33	28	35	28	27	24
Zn	143	119	153	116	151	129	116	103	118	127	134
Zr	259	99	531	376	615	3	318	4	333	369	579

Table 5 - Density values - Metcalf phyllite and Pigeon Siltstone.

Sample	*Lithology*	*Location*	mass air	mass H_2O	density
CC05-1	**pCm**	N 35.6390º W 83.7235º	18.01	11.47	2.76
CC05-2	**pCm**	N 35.6403º W 83.7192º	16.39	10.60	2.83
CC05-3	**pCm**	N 356614º W 83.7059º	19.45	12.46	2.78
CC05-4	**pCm**	N 35.6738º W 83.6942º	20.71	13.29	2.79
CR05-2	**pCm**	N 35.7474º W 83.5624º	15.48	9.89	2.77
CR05-3	**pCm**	N 35.7420º W 83.5658º	17.38	11.02	2.73
MB05-4	**pCm**	N 38.6772º W 83.6549º	27.26	17.30	2.74
BV05-1	**pCp**	N 35.7521º W 83.5311º	27.95	17.87	2.77
PM05-3	**pCp**	N 35.7819º W 83.2180º	24.38	15.63	2.78
PM05-4	**pCp**	N 35.7179º W 83.5013º	26.01	16.68	2.79
PM05-5	**pCp**	N 35.7549º W 83.5245º	30.56	19.52	2.77
PM05-6	**pCp**	N 35.7870º W 83.4076º	29.77	19.00	2.77
RTG05-1	**pCp**	N 35.7180º W 83.5596º	28.00	18.00	2.80
RTG05-2	**pCp**	N 35.6730º W 83.5734º	25.35	15.91	2.69

Lithology	mean ?	std. dev.
pCp	2.77	0.03
pCm	2.77	0.03

Table 6a - Mean values and percent difference for major and minor chemical analyses - Metcalf phyllite and Pigeon siltstone.

Major (Mean)	SiO_2 (%)	TiO_2 (%)	Al_2O_3 (%)	Fe_2O_3 (%)	MnO %)	MgO (%)	CaO (%)	Na_2O (%)	K_2O (%)	P_2O_5 (%)	LOI	Total
pCm (mean)	55.97	0.84	21.39	8.46	0.11	2.14	0.85	1.80	4.38	0.22	4.39	100.55
pCp (mean)	56.87	0.84	17.59	7.55	0.12	2.24	3.74	2.24	4.02	0.28	5.17	100.66
Percent diff.	1.57	0.28	21.58	12.03	5.61	4.57	77.41	19.53	9.14	22.75	15.09	0.11

Table 6b - Mean chemical analyses standard deviations for the major and minor elements - Metcalf phyllite and Pigeon siltstone.

Majors Std Deviation	SiO_2 (%)	TiO_2 (%)	Al_2O_3 (%)	Fe_2O_3 (%)	MnO (%)	MgO (%)	CaO (%)	Na_2O (%)	K_2O (%)	P_2O_5 (%)
pCm (stdv)	3.95	0.14	3.72	1.16	0.05	0.34	1.07	0.86	2.17	0.05
pCp (stdv)	4.70	0.14	4.53	1.54	0.04	0.42	3.47	1.24	1.92	0.12

Table 6c- Mean values and percent difference for of trace element chemical analyses - Metcalf phyllite and the Pigeon siltstone.

Trace	Ba (PPM)	Cr (PPM)	Cu (PPM)	La (PPM)	Mo (PPM)	Ni (PPM)	Pb (PPM)	Rb (PPM)	Sr (PPM)	Th (PPM)	U (PPM)	V (PPM)	Y (PPM)	Zn (PPM)	Zr (PPM)
pCm	882	70	22	34	4	21	17	160	124	11	1	89	27	125	129
pCp	849	74	23	37	4	25	14	147	185	12	1	82	30	128	317
percent diff	3.96	5.56	0.81	6.72	4.17	14.71	25.50	8.95	32.68	4.72	20.00	8.63	8.59	2.13	59.38

Table 6d - Mean chemical analyses standard deviations of trace elements - Metcalf phyllite and Pigeon siltstone.

Trace Std Deviation	Ba (PPM)	Cr (PPM)	Cu (PPM)	La (PPM)	Mo (PPM)	Ni (PPM)	Pb (PPM)	Rb (PPM)	Sr (PPM)	Th (PPM)	U (PPM)	V (PPM)	Y (PPM)	Zn (PPM)	Zr (PPM)
pCm	458	7	13	5	8	4	12	95	72	2	2	12	3	29	148
pCp	386	9	14	3	6	3	7	76	118	1	1	22	3	16	214

Table 7 - Zircon abundance estimate.

Pigeon siltstone		Metcalf phyllite	
sample	count	sample	count
PM05-1	62	**CC05-1**	0
PM05-2	18	**CC05-2**	0
PM05-3	17	**CC05-3**	0
PM05-4	7	**CC05-4**	1
PM05-5	11	**CR05-1**	0
PM05-6	4	**CR05-2**	0
RTG05-1	10	**MB05-1**	1
RTG05-2	23	**MB05-2**	0
BV05-1	7	**MB05-3**	0
BV05-2	**4**	**MB05-4**	0
CR05-1	2	**MB05-5**	1

References

Adams, M.G., Stewart, K.G., Trupe, C.H., and Willard, R.A., 1995, Tectonic significance of high-pressure metamorphic rocks and dextral strike-slip faulting along the Taconic suture: *In* Hibbard, J.P., van Staal, C.R., and Cawood, P.A., eds., Current Perspectives in the Appalachian-Caledonian Orogen: Geological Association of Canada, Special Paper 41, p. 21-42.

Ague, J.J., 1991, Evidence for major mass transfer and volume strain during regional metamorphism of pelites: Geology 19, 855-858.

Ayers, J. C. & Watson, E. B., 1991. Solubility of apatite, monazite, zircon, and rutile in supercritical aqueous fluids with implications for subduction zone geochemistry: Philosophical Transactions of the Royal Society of London, Series A 335, 365-375.

Connelly, J.B., and Dallmeyer, R.D., 1993, Polymetamorphic evolution of the western Blue Ridge: Evidence from $^{40}Ar/^{39}Ar$ whole-rock slate/phyllite and muscovite ages: American Journal of Science 293, 323-359.

Connelly, J.B. and Woodward, N.B., 1992, Taconian-style thrust system in the Great Smoky Mountains, Tennessee: Geology 20, 177-180.

Drake, A.A., Jr., Sinha, A.K., Laird, J., and Guy, R.E., 1989, The Taconic orogen, *in* Hatcher, R.D., Jr., Thomas, W.A., and Viele, G.W., eds., The Appalachian-Ouachita orogen in the United States: Boulder, Colorado, The Geological Society of America, The Geology of North America, v. F-2, 101-177.

Fullagar, P.D. and A.L. Odom, 1973, Geochronology of Precambrian gneisses in the Blue Ridge province of northwestern North Carolina and adjacent parts of Virginia and Tennessee: Geological Society of America Bulletin 84, 3065-3080.

Goldberg, S.A., Butler, J.R., Mies, J.W., and Trupe, C.H., 1989, IGC Field Trip T365, The southern Appalachian orogen in northwestern North Carolina and adjacent states: Chapel Hill, University of North Carolina, 55 pp.

Hadley, J.B., Goldsmith, R. 1963. Geology of the Eastern Great Smoky Mountains North Carolina and Tennessee: U.S. Geological Survey Professional Paper 349-B, B74-B95.

Hadley, J.B., and Nelson, A.E., 1971, Geologic map of the Knoxville quadrangle, North Carolina, Tennessee, and South Carolina: U.S. Geological Survey Miscellaneous Geologic Investigations Map I-654, scale 1:250,000.

Hatcher, R.D., Jr., 1978, Tectonics of the western Piedmont and Blue Ridge, southern Appalachians: Review and Speculation: American Journal of Science 278, 276-304.

Hatcher, R.D., Jr., 1981, Thrusts and nappes in the North American Appalachian orogen: The Geological Society of London, Special Publication no. 9, 491-499.

Hatcher, R.D., Jr., 1987, Tectonics of the southern and central Appalachian internides: Annual Reviews of Earth and Planetary Science Letters 5, 337-362.

Hatcher, R.D., Jr., 1989, Tectonic synthesis of the U.S. Appalachians, *in* Hatcher, R.D., Jr., Thomas, W.A., and Viele, G.W., eds., The Appalachian-Ouachita orogen in the United States: Boulder, Colorado, Geological Society of America, The Geology of North America, v. F-2, 233-318.

Hatcher, R.D., Jr., 2000, Facts that delimit Southern Appalachian plate models and tectonic implications: The Geological Society of America, Abstracts with Programs 32, no. 2, p. 25.

Hatcher, R.D., Jr., 2001, Terranes and terrane accretion in the Southern Appalachians; an evolved working hypothesis: The Geological Society of America, Abstracts with Programs 33, no. 2, p. 65.

Keith, Arthur, 1904, Description of the Asheville Quadrangle, North Carolina-Tennessee: U.S. Geological Survey Geology Atlas Folio 116.

King, P.B., Hadley, J.B., Neuman, R.B., and Hamilton, W.B., 1958, Stratigraphy of the Ocoee Series, Great Smoky Mountains, Tennessee and North Carolina: Geological Society of America Bulletin 60, 947-966.

King, P.B. 1964. Geology of the Central Great Smoky Mountains, Tennessee, Geological Survey Professional Paper 349-C, pp.106-112.

King, P.B., Neuman, R.B., and Hadley, J.B., 1968, Geology of the Great Smoky Mountains National Park, Tennessee and North Carolina: U.S. Geological Survey Professional Paper 587, 23 pp., and 1:125,000-scale map.

Liermann, H. P., Isachsen, C., Altenberger, U. and Oberhansli, R., 2002. Behavior of zircon during high-pressure, low-temperature metamorphism: case study from the Internal Unit of the Sesia Zone (Western Italian Alps): European Journal of Mineralogy 14, 61-71.

Manning, C. E. (1998). Fluid composition at the blueschist---eclogite transition in the model system Na_2O - MgO - Al_2O_3 - SiO_2 - H_2O - HCl. Schweizerische Mineralogische und Petrographische Mitteilungen 78, 225-242.

Massey, M.A., and Moecher, D.P., 2005, Deformation and metamorphic history of the Western Blue Ridge–Eastern Blue Ridge terrane boundary, southern Appalachian Orogen, Tectonics 24, TC5010, doi: 10.1029/2004TC001643, 18pp.

Moecher, D. P., Massey, M. A., and Tracy, R.J., 2005, Timing and pattern of metamorphism in the western and central Blue Ridge, TN and NC: Status and outstanding problems. Carolina Geological Society Annual Field Trip Guide Book, 57-66.

Montes, C., 1997. The Greenbrier and Hayesville Faults in Central-Western North Carolina. [Unpublished M.S. Thesis] The University of Tennessee, Knoxville, 109 pp.

Montes, C., and Hatcher, R.D., Jr., 1999. Documenting Late Proterozoic Rifting in the Ocoee Basin, Western Blue Ridge, North Carolina: Southeastern Geology 39, 37-50.

Neuman, R.B., and Nelson, W.H. 1965. Geology of the Western Great Smoky Mountains Tennessee: Geological Survey Professional Paper 349-D, 81 pp.

O'Hara, K., 1990. State of strain in mylonites from the western Blue Ridge province, southern Appalachians: the role of volume loss: Journal of Structural Geology 4, 419-430.

O'Hara, K., and Blackburn, H., 1988. Volume loss model for trace-element enrichments in mylonites: Geology 17, 524-527.

Philippot, P., and Selverstone, J., 1991. Trace-element-rich brines in eclogitic veins: implications for fluid composition and transport during subduction: Contributions to Mineralogy and Petrology 106, 417-430.

Rast, N., and Kohles, K. M., 1986. The origin of the Ocoee Supergroup: American Journal of Science 286, 593-616.

Southworth, S., Schultz, A, and Denenny D., 2006, Geologic Map and Report of the Great Smoky Mountains National Park Region, Tennessee and North Carolina, U.S. Geological Survey Open File Report 2005 - 1225, p.22-24, 71- 73.

Figure References

King, P.B. 1964. Geology of the Central Great Smoky Mountains Tennessee. U.S. Geological Survey Professional Paper 349-C, plate 9 and p.19.

Montes, C., and Hatcher, R.D., Jr., 1999. Documenting Late Proterozoic Rifting in the Ocoee Basin, Western Blue Ridge, North Carolina: Southeastern Geology 39, 37-50.

Passchier, C.W. and Trouw, A.J., 1998. *Microtectonics*. Springer-Verlag Berlin, Heidelburg, New York Publishers, 111 pp.

Southworth, S., Schultz, A, and Denenny D., 2006, Geologic Map of the Great Smoky Mountains National Park Region, Tennessee and North Carolina, U.S. Geological Survey Geologic Map.

Woodward, N., Connelly, J., Walters, R., and Lewis, J. 1991 Tectonic evolution of the Great Smoky Mountains. In Kish, S.A. (ed.), Studies of Precambrian and Paleozoic Stratigraphy in the Western Blue Ridge, Carolina Geological Society Annual Field Conference, pp. 55-68.

VITA

Kristopher M. Clemons

Date of Birth
April 30, 1974; Lexington, KY

Education
Present: M.S. Candidate, Geology, University of Kentucky, Lexington Kentucky.
1996: B.A. in Political Science, Eastern Kentucky University, Richmond, Kentucky.

Research and Teaching Experience
2004 – 2006: Teaching Assistant for Geology for Elementary School Teacher, Introductory Physical Geology, Field Methods II, Field Geology, and Igneous and Metamorphic Petrology.

Graduate Study at the University of Kentucky
Specialization: Petrofabric and Geochemical Analysis
Cognate Area: Structural Geology
Thesis: Kinematic and Petrofabric Analysis of the Greenbrier Discontinuity, Great Smoky Mountains, North Carolina and Tennessee.
Thesis Advisor: David P. Moecher, Associate Professor

Publications
Abstracts of research presented at professional meetings (listed chronologically)

Clemons, Kristopher and Moecher, D.P., 2004. Petrofabric Analysis of the Great Smoky – Snowbird Group Contact, Cove Creek Area, Eastern Great Smoky Mountains, NC., *Geol. Soc. Am. Abs. Progs*. 35, No. 41, pg. 28.

Southworth, Scott, **Clemons, Kristopher**, Schultz, Art, Kunk, Michael J., Aleinikoff, John N., Naeser, Charles, Naeser, Nancy, and Denenny, Danielle, 2005. The Polygenetic Greenbrier fault, Great Smoky Mountains, TN/NC. *Geol. Soc. Am. Abs. Progs*. 37, No. 5, in press.

Clemons, Kristopher and Moecher, D.P, 2005. Kinematic and Petrofabric Analysis of the Greenbrier Discontinuity, Great Smoky Mountains, North Carolina and Tennessee. *Geol. Soc. Am. Abs. Progs*. 37, No. 5, in press.

University, Department, and Professional Service
2004-2005: Department of Geological Sciences Chair Search Committee member
2004-2005: Department of Geological Sciences Graduate Student Representative